THE OHIO STATE UNIVERSITY

A VERY WIDE FREQUENCY BAND PULSED/IF RADAR SYSTEM

D.N. Jones
W.D. Burnside

The Ohio State University

ElectroScience Laboratory

Department of Electrical Engineering
Columbus, Ohio 43212

Technical Report 716148-28
Grant NSG 1613
March 1988

National Aeronautics and Space Administration
Langley Research Center
Hampton, Virginia 23665

NOTICES

When Government drawings, specifications, or other data are used for any purpose other than in connection with a definitely related Government procurement operation, the United States Government thereby incurs no responsibility nor any obligation whatsoever, and the fact that the Government may have formulated, furnished, or in any way supplied the said drawings, specifications, or other data, is not to be regarded by implication or otherwise as in any manner licensing the holder or any other person or corporation, or conveying any rights or permission to manufacture, use, or sell any patented invention that may in any way be related thereto.

TABLE OF CONTENTS

LIST OF FIGURES

CHAPTER I

INTRODUCTION

Constant improvements are being incorporated into the compact range radar cross section measurement facility at The Ohio State University ElectroScience Laboratory Among these improvements is the replacement of a pulsed/RF radar with a more sensitive pulsed/IF radar This new system attempts to minimize the number of components which operate at the transmitted frequency. Thus most of the components in the receiver operate at a single intermediate frequency, so that the hardware may be chosen to have optimal performance at this frequency.

This report develops useful analytic techniques which will help to optimize the performance of individual components as well as the entire radar system. Chapter II contains useful information on the behavior of signal and noise power levels in pulsed radar circuits. The ideas developed in this chapter will make the remaining discussion more straightforward to understand.

In Chapter III the old pulsed/RF system is analyzed so that experience may be gained in applying the concepts of Chapter II. In addition the shortcomings of the old system become apparent and solutions to these problems are discussed. Some subtle problems involving LO and RF leakage within the down converter are closely analyzed, and their elimination is explained. The final purpose of this

analysis is to determine the dynamic range of the system. This is done by systematic record keeping of signal and noise powers for all components and by determining which components are most likely to saturate.

Chapter IV develops techniques which greatly simplify the analysis of the effects of transmit and receive pulse width on the clutter level detected by the receiver. This method does not rely on timing diagrams which can often be confusing. Instead, pulse delays are transformed into target locations within the chamber, so that the relative return levels may be easily determined. The analysis of clutter levels caused by return signals which enter the receiver through the backlobe of the feed antenna is also easily accomplished with this method. Two specific timing schemes are analyzed with respect to clutter, and the one with the lower clutter level is used in the new pulsed/IF system.

The new pulsed/IF system is analyzed in Chapter V using the methods developed in the preceding chapters. By minimizing the number of components which operate at RF, the cost of expensive microwave hardware is kept to a minimum. A comparison between the old and new Ka-band system hardware illustrates the advantage of reduced redundancy within the receiver. In the new system, no switching or amplification is done at Ka-band, while the old system relies on a very expensive Ka-band amplifier and three Ka-band switches. In the new system, the Ka-band signals are converted to an IF where switching and amplification occur. Since the same receiver components are used by the 2-18 GHz system, performance of the receiver is very predictable, and if problems develop, troubleshooting is relatively straightforward.

By using a single frequency (1800 MHz) receiver its components are chosen to have optimal performance at this frequency. The receiver features a low noise amplifier with a noise figure of about .9 dB. This type of performance is not available in a wide band microwave amplifier. Other components such as isolators are also designed to have their best performance at 1800 MHz. They replace wide band isolators which have unpredictable behavior at different frequencies.

The experimental results of Chapter VI show that the radar system has a sensitivity essentially equal to that calculated in Chapter V, and it is a significant improvement over the old one. Sphere tests show that the system is accurate, and with the added sensitivity, a 1/8" diameter sphere may be easily measured even at Ka-band.

The information contained in this report is intended to give the radar designer confidence in producing a reliable system which operates at peak performance.

CHAPTER II

A PULSED/CW RADAR USING AN IF RECEIVE GATE

Time domain analysis of radar targets is helpful in determining which physical features on a target cause the most significant scattering. As with any linear system, the impulse response of a target may be approximated by measuring the scattered field's amplitude and phase over a broad band of frequencies. As the frequency of operation increases, resolution in the time domain improves. In order to apply these techniques to RCS measurements, they must be performed in the far zone of the transmitting antenna so that the incident field at the target is essentially a plane wave. Radar systems of this type have the disadvantage of requiring a large amount of space as illustrated in Figure 2.1, and they are not practical in areas where the weather may be adverse.

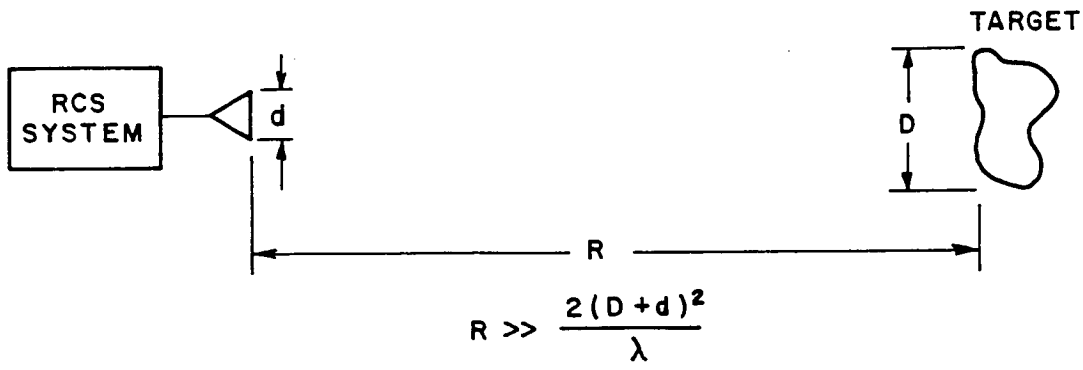

Figure 2.1. Elementary RCS system where the target is in the far-zone of the antenna.

A solution is to use a parabolic reflector with a transmitter and receiver located at its focus as shown in Figure 2.2. By operating at higher frequencies with proportionally smaller targets, far zone scattering may be simulated in a relatively small volume of space. Enclosing this range within a building permits these measurements to be made without regard to weather conditions. Unfortunately, placing the range inside a chamber introduces other scatterers which interfere with the intended target's scattered field. Methods have been developed which minimize these effects. These effects include scattering from the chamber walls as well as the transmit/receive antenna and target pedestal. The first method for removing these effects is subtraction by the "nulling" process. This is done by setting up a signal in the

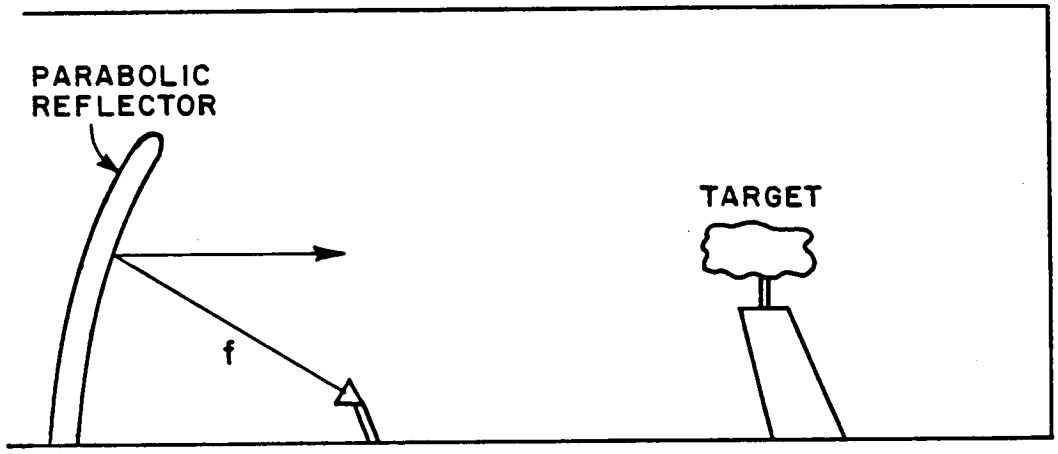

Figure 2.2. An elementary compact range RCS system.

receiver's feed line which is equal in magnitude and opposite in phase to the return from the chamber when no target is present. The target is then placed in the chamber and measured. This method works well except that the tuner, which sets up the nulling signal, must be adjusted for each measurement frequency. This time consuming process results in two disadvantages. First, it makes it impossible to perform time domain work since many frequencies must be measured before a meaningful inverse Fourier transform may be performed. Second, temperature variations cause physical changes within the chamber, which will affect the magnitude and phase of the clutter signal thus reducing the effectiveness of the null with time.

Another type of subtraction can be performed on a computer as illustrated in Figure 2.3(b). A measurement is made with the target and this data is stored in a computer. The target is then removed, and another measurement is made. Finally, the computer subtracts this background information from the target data. This method has the disadvantage of requiring that the receiver's maximum permissable signal input be greater than the largest return from clutter. The return from a target with a small radar cross section may be so small that an accurate measurement would not be possible because the receiver's noise floor is being approached. In this case, the sensitivity of the system is dictated by the presence of clutter. This is not a desirable situation.

A solution to the clutter problem is to gate the transmitter and receiver as shown in Figure 2.4. By pulsing the transmitter quickly so

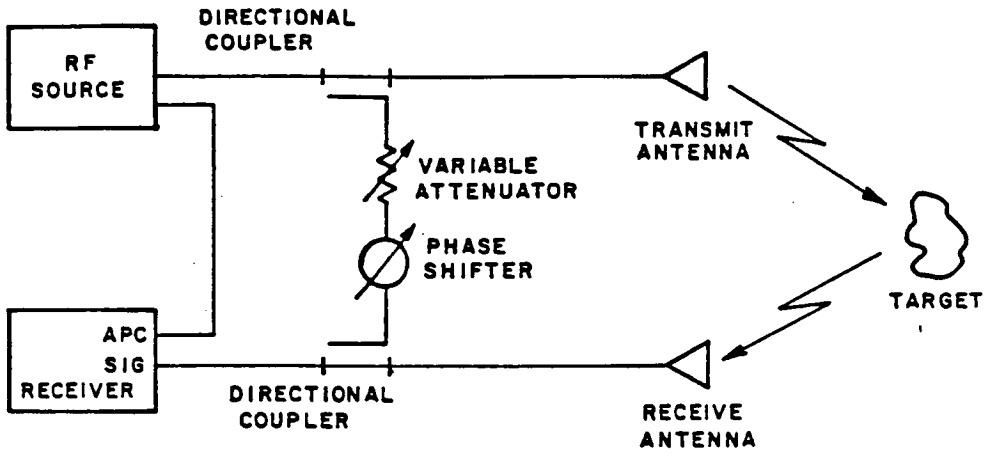

(a) ELECTRICAL NULLING SYSTEM

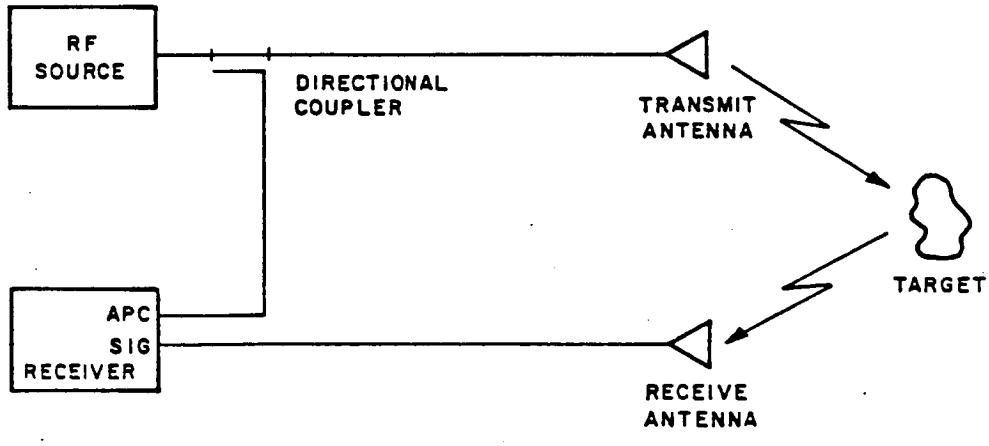

(b) COMPUTER SUBTRACTION SYSTEM

Figure 2.3. Block diagram of basic CW RCS measurement systems.

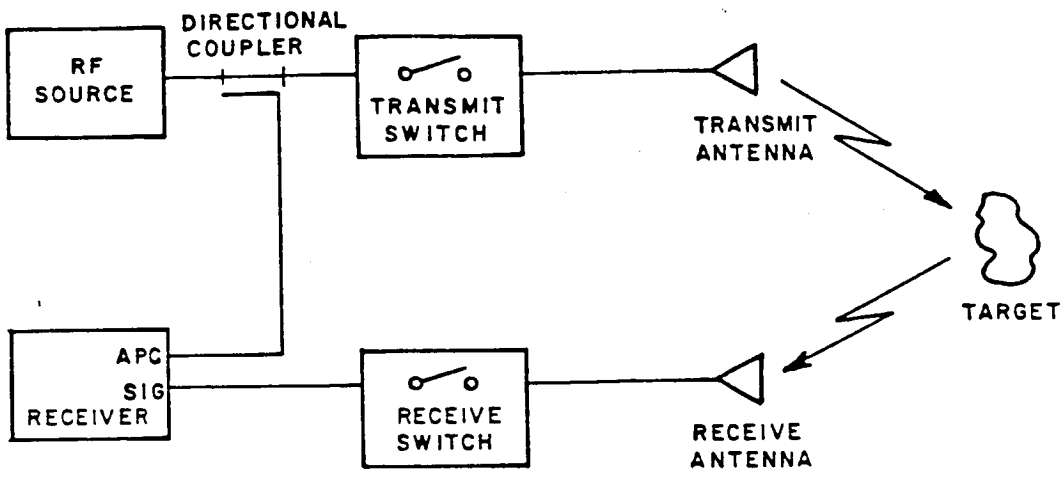

Figure 2.4. Block diagram of basic pulsed/CW RCS measurement system.

that enough different parts of the range will be illuminated at different times. The receiver will detect a pulsed scattered field from each scatterer; targets which are far from the reflector will produce a response at the receiver later than those which are closer. By gating the receiver one or more of these scattered pulses may be selected, and the others rejected. Thus by shifting the position of the receive gate in time with respect to the transmitter gate, different parts of the range may be examined. By carefully choosing the receiver gate position, it is possible to observe returns only from the target area and to gate out clutter. Figure 2.5 indicates the relative timing of the larger returns in a compact range.

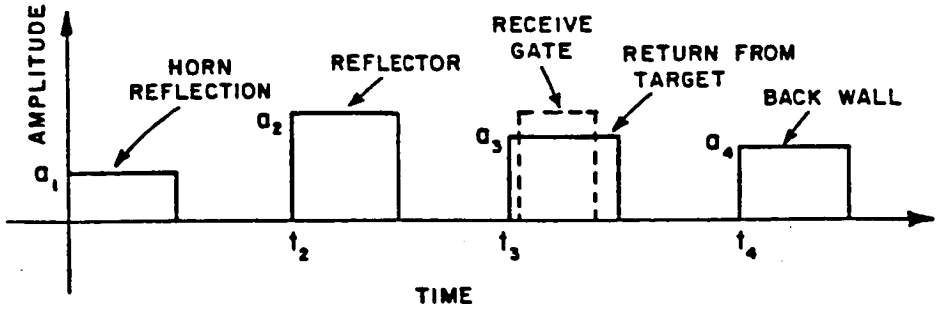

Figure 2.5. Scattered pulse from the compact range.

The size of the region of observation about the target is governed by the duty cycles of both the transmitter and receiver.

The block diagram shown in Figure 2.4 indicates that the switching in the receiver is done at the transmitted frequency. This type of system is referred to as a pulsed/RF radar. After the received signal passes through the switch it is downconverted to an IF where the actual amplitude and phase measurement takes place. When a receiver downconverts a received signal and then gates the IF signal as shown in Figure 2.6, this is referred to as a pulsed/IF system.

The pulsed/IF system is more cost-effective than the pulsed/RF system because most of the receiver components operate at only one pulsed frequency. Thus unpredictable effects between components are eliminated because they always operate under the same conditions. It is much easier to perform a detailed laboratory analysis at one frequency than over a large spectrum of frequencies. Receiver components may be chosen which have optimal performance under these conditions.

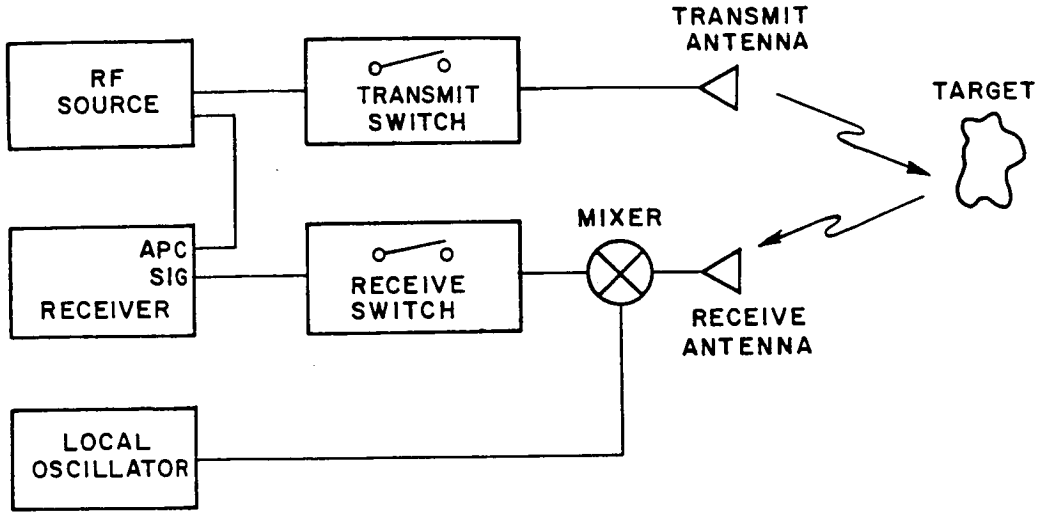

Figure 2.6. Simplified diagram of a pulsed/IF RCS measurement system.

Returning to the timing situation, Figure 2.5 shows the returns from the target as well as unwanted returns from clutter. Mathematically, these terms can be expressed by

$$R(t) = a_1 p_\tau(t-t_2) + a_2 p_\tau(t-t_2) + \ldots a_N p_\tau(t-t_N) \tag{2.1}$$

where

$$p_\tau(t-t_k) = \begin{cases} 1 & t_k+nT<t<t_k+nT+\tau \\ 0 & \text{otherwise} \end{cases} \tag{2.2}$$

τ = transmitted pulse width

T = pulse period

a_k = amplitude of the k^{th} return pulse, and

t_k = propagation delay of the k^{th} pulse.

Within the receiver this signal is gated or equivalently multiplied by a unit amplitude pulse $p_\theta(t-t_r)$ where

θ = receiver pulse width, and

t_r = delay of the receive pulse.

The resulting IF signal is

$$p_\theta(t-t_r)[a_1 p_\tau(t-t_1) + a_2 p_\tau(t-t_2) + \ldots a_N(t-t_2)] \ . \tag{2.3}$$

Assuming the k^{th} pulse is the scatter from the target and that the receiver delay has been properly adjusted to maximize the receiver output, then one finds that

$$p_\theta(t-t_r)R(t) = a_k p_\theta(t-t_r)p_\tau(t-t_k) \ . \tag{2.4}$$

All of the other scatter terms in R(t) are eliminated. This means that clutter is not present in the target scattering information.

To this point nothing has been said about obtaining a CW signal from a pulsed waveform. A pulse train, f(t), with duty cycle, d, and pulse width τ is shown in Figure 2.7. This periodic function may be written as a Fourier series such that

$$f(t) = \sum_{n=-\infty}^{\infty} F_n \, e^{jn\omega_o t} \tag{2.5}$$

where

$$\omega_o = 2\pi f_o = 2\pi/T \tag{2.6}$$

and T = pulse period.

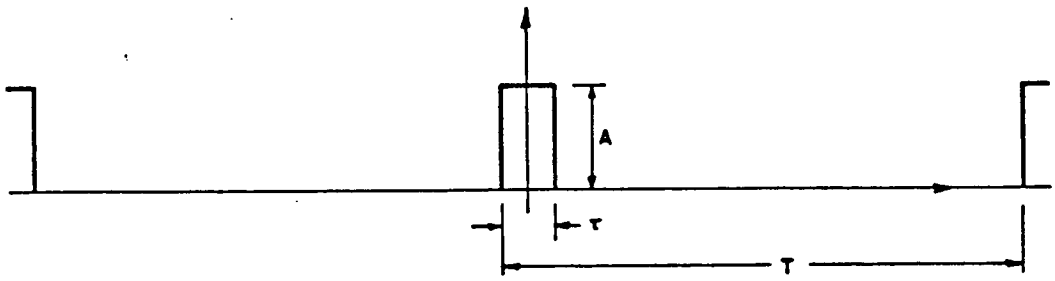

Figure 2.7. Pulse train with amplitude A and duty cycle τ/T.

The function $e^{jn\omega_o t}$ are orthogonal over the interval $-T/2 \leq t \leq T/2$ for any integer n. Multiplying both sides of f(t) by $e^{-jm\omega_o t}$ and integrating over the interval gives the following:

$$\int_{-T/2}^{T/2} e^{-jm\omega_o t} f(t)dt = \sum_{n=-\infty}^{\infty} \int_{-T/2}^{T/2} F_n e^{j(n-m)\omega_o t} dt = \begin{cases} F_m T & n=m, \text{ or} \\ 0 & \text{otherwise} \end{cases} \tag{2.7}$$

where

$$F_m = \frac{1}{T} \int_{-T/2}^{T/2} e^{-jm\omega_o t} f(t)dt \ . \tag{2.8}$$

For our particular f(t), the above integral is given by

$$F_n = 1/T \int_{-\tau/2}^{\tau/2} e^{-jn\omega_o t} \, dt = \frac{2}{n\omega_o T} \sin(n\omega_o \tau/2) \tag{2.9}$$

recall that $\omega_o = \frac{2\pi}{T}$ or (2.10)

$$F_n = \frac{1}{n\pi} \sin\left(\frac{n\pi\tau}{T}\right) \ . \tag{2.11}$$

The duty cycle of the pulse is the pulse width divided by the pulse period such that

$$d = \frac{\tau}{T} . \tag{2.12}$$

It then follows that

$$F_n = \frac{1}{n\pi} \sin(n\pi d) = d\left(\frac{\sin(n\pi d)}{n\pi d}\right) \tag{2.13}$$

or

$$F_n = d \operatorname{sinc}(n\pi d) \qquad n = 0, \pm 1, \pm 2 \ldots \tag{2.14}$$

where

$$\operatorname{sinc} \chi = \frac{\sin\chi}{\chi} . \tag{2.15}$$

This operation was performed on f(t) which is the envelope of the pulsed signal. The actual frequency components which correspond to F_n are

$$f_c + nf_o \qquad n = 0, \pm 1, \pm 2 \ldots \tag{2.16}$$

where f_c = the intermediate frequency of the receiver, and

$f_o = \frac{1}{T}$ = the pulse frequency.

Our system utilizes a pulse frequency of 5 MHz (T = 200 nsec.) and an IF frequency of 1800 MHz, so frequency harmonics are present at 1800 ±5 n MHz, where n is an integer. By selecting a bandpass filter with a bandwidth which is sufficiently narrow, only a few harmonics around 1800 MHz will be passed. The center component corresponds to the transmitter frequency offset by the local oscillator frequency. Essentially, the bandpass filter converts the pulsed/IF signal to a CW/IF signal which may be passed directly to a CW receiver for processing in the normal manner.

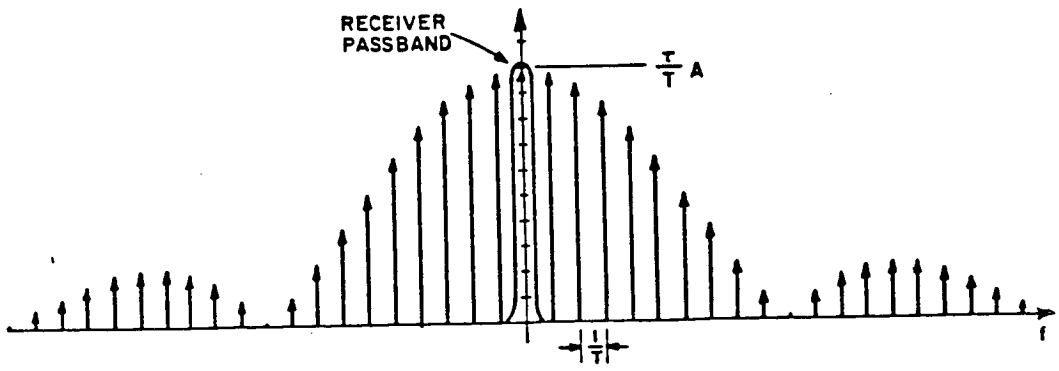

Figure 2.8. IF spectrum and CW receiver passband.

The time-averaged power contained in the pulse (see Figure 2.7) is

$$P_{ave} = \frac{1}{T}\int_0^T f^2(t)dt = \frac{1}{T}\int_0^{\tau} A^2 dt = A^2\,\frac{\tau}{T} = A^2 d \qquad (2.17)$$

which corresponds to a duty cycle loss such that

$$\frac{P_{ave}}{P_{cw}} = \frac{A^2 d}{A^2} = d, \text{ or} \qquad (2.18)$$

$$\text{signal loss in dB} = 10 \log(d) \qquad (2.19)$$

Referring to Figure 2.8, it can be seen that when a CW signal of amplitude A is input to a switch with duty cycle $d = \tau/T$, the corresponding center frequency has an amplitude of Ad. The relative power in the receiver passband is given by the following:

$$\frac{P_{PB}}{P_{cw}} = \frac{A^2|F_0|^2}{A^2} = \frac{(Ad)^2}{A^2} = d^2, \text{ or} \qquad (2.20)$$

$$\text{signal loss in dB} = 20 \log(d)\ . \qquad (2.21)$$

This is the loss associated with pulsing a CW signal and then extracting the corresponding component from the pulsed signal. Appendix A contains

more information on the subject of calculating signal loss

If a noise source with noise power (p_N) over a bandwidth (B) were input to a switch with duty cycle (d), the time-averaged output would be reduced by the switch duty cycle as follows:

$$\text{noise pulse loss in dB} = 10\log(d) \; . \tag{2.22}$$

For the remainder of this report, the bandwidth of interest with respect to noise will be the bandwidth of the CW receiver This will simplify calculations as the noise level is determined through each part of the system.

To summarize the last two paragraphs (see Figure 2.9), the result of gating a CW signal may be viewed in two steps. First, the time-averaged pulse power is reduced by the duty cycle factor. This corresponds to the power contained in all of the Fourier components. Second, filtering out the modulating harmonics results in a corresponding CW signal whose power is reduced again by the duty cycle factor from the pulsed power level. Thus, the total reduction in signal sensitivity is related to the square of the duty cycle. The time-averaged noise power after gating is proportional to the switch duty cycle. It is hoped that the preceeding discussion will make the signal and noise calculations of the following chapters easier to follow. Once these principles are understood, the analysis and design of a quality pulsed RCS system should be straightforward.

The advantage of a pulsed RCS measurement system is that the returns from various clutter terms can be eliminated such that, even

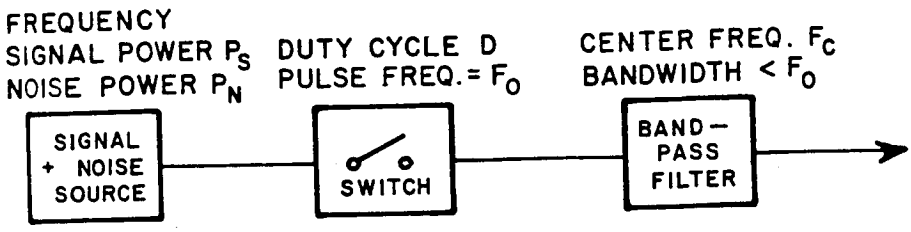

	SIGNAL LOSS	NOISE LOSS
SWITCH	10log(d)	10log(d)
FILTER	10log(d)	--------
TOTAL	20log(d)	10log(d)

Figure 2.9. Signal and noise loss through a switch.

with some signal/noise loss, the signal/clutter performance of the system is significantly improved. Note that gain may now be added to amplify the reduced target signal without saturating the receiver because of clutter. The particular advantage of a pulsed/IF system is that the receiver may be optimally designed to operate at only one frequency, thus reducing frequency-sensitive mismatch problems between components.

In the next chapter, more components will be added to the system to improve performance. A careful analysis of our previous system will be given, and potential problems will be discussed.

CHAPTER III

PULSED/RF RADAR SIGNAL AND NOISE ANALYSIS

In the previous chapter, some basic concepts in pulsed radar are developed. In this chapter, these ideas are used to study our previous pulsed/RF radar system. This is done to aid the reader in understanding how the new pulsed/IF system evolved from the old one. This chapter develops methods for the analysis of any radar system, which are necessary to determine the limitations imposed by the various components within the system.

A. THE 2-18 GHz SYSTEM

Our old pulsed/RF radar system is shown in Figure 3.1. The transmitter, receiver, and down converter are housed in separate enclosures. The task of the transmitter is to pulse the CW signal coming from synthesized source (W.J.#1). The pulsed signal is then transmitted to a hybrid and radiated by the antenna. The hybrid permits the use of one antenna for both transmittion and reception. Originally, the system used two antennas, but the feed support was changed to reduce its scattering. A one feed horn system was adopted, and a hybrid was the only device with which 2-18 GHz could be used without significantly altering the system. Unfortunately, this results in a 6 dB signal loss as will be shown later.

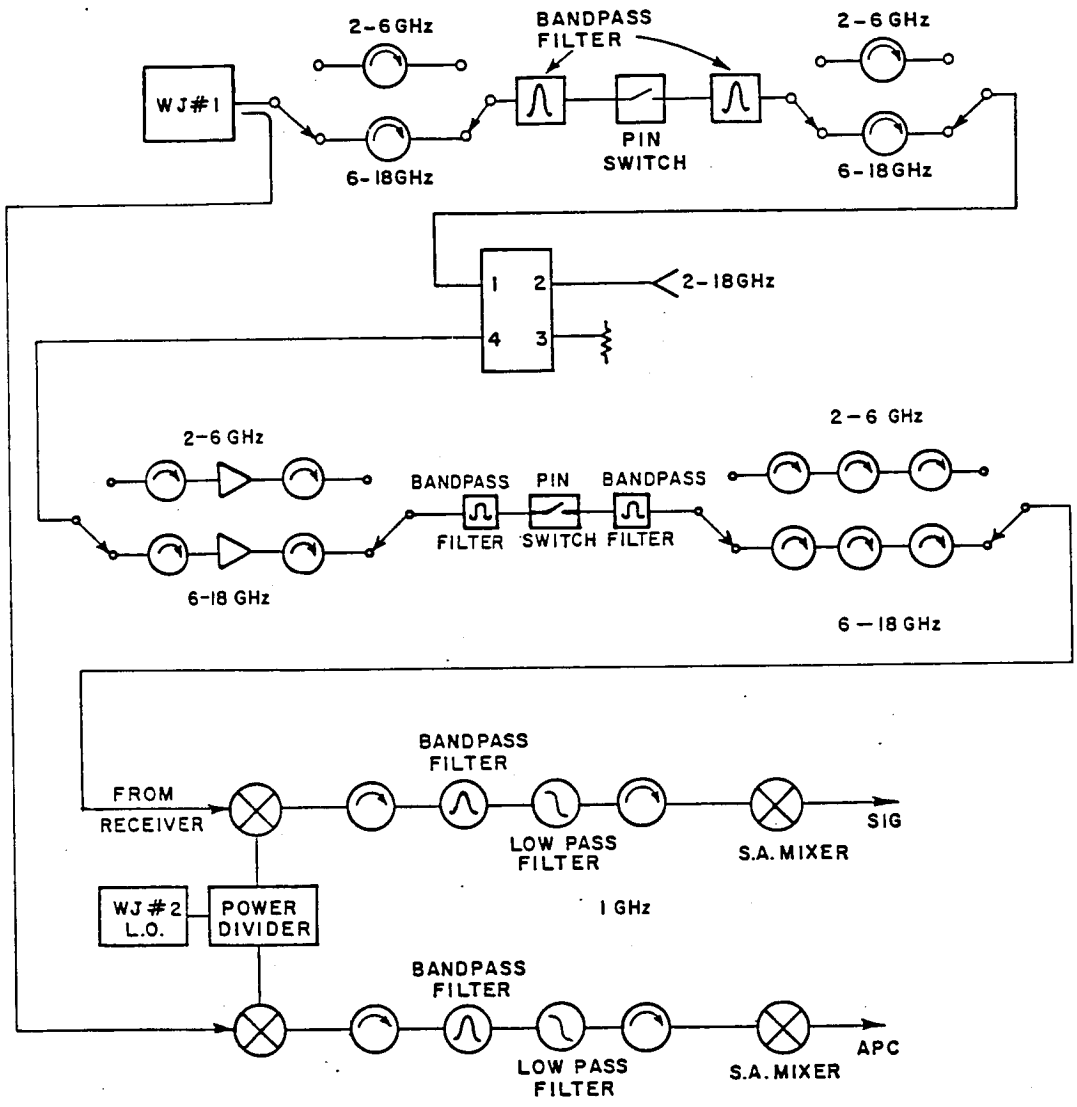

Figure 3.1. Pulsed/RF radar system.

As previously mentioned the most significant aspect of the pulsed/RF receiver is that gating and amplification take place at the transmitted frequency. In the transmitter and receiver, a total of eight coaxial cable switches are used to switch between an amplifier and isolators which operate in the 2-6 GHz band and those which operate over the 6-18 GHz band. These switches are electrically controlled and generally give good performance. However, they are prone to periodically becoming hung up or "stuck" in one particular position which seems to be a characteristic simply of the brand used. When this happens, the system appears to be inoperative in one band, and it can be a time consuming process to determine which switch is not responding. Often the problem disappears as quickly as it appears. It is therefore desirable to keep the number of these switches to a minimum.

The received signal then propagates to the down converter where it is immediately mixed with a signal coming from the local oscillator (W.J.#2). The pulsed signal is converted to a CW signal after the modulating components are removed by the bandpass filter. A reference channel is generated by directly mixing W.J.#1 with W.J.#2 and filtering in a similar process.

This summarizes the basic operation of the pulsed/RF radar system. In the following sections, signal and noise levels are calculated and a more in-depth discussion of its operation is given.

A.1. The Transmitter

The transmitter is drawn again in Figure 3.2 for clarity and operates in a straightforward manner. Its function is to modulate a CW signal coming from the source synthesizer (W.J.#1). The hardware located around the switch removes the undesirable effects of pulsing. The filter attenuates the large low frequency transients produced by the switch as will be discussed in Chapter V. The first set of isolators removes any signals which are reflected by the switch when it opens. This reduces the possibility of power being reflected back into the synthesizer. The second set of isolators absorb power reflected from the hybrid or antenna. The isolators also absorb power which has been scattered by the target/clutter within the chamber, received by the

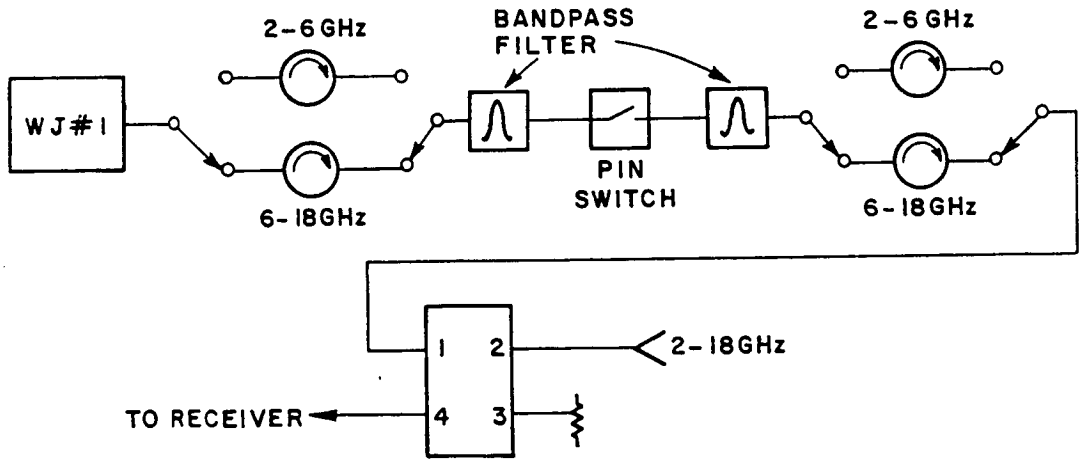

Figure 3.2. The transmitter.

antenna, and coupled into port 1 from port 2. The hybrid itself operates by coupling the input power equally into ports 2 and 3. The signal into the antenna is therefore down by 3 dB. The power which is received by the antenna from the room is coupled equally between ports 1 and 4. Unfortunately, the received signal is reduced by another 3 dB for a total of 6 dB of signal loss by using the hybrid.

Figure 3.3 shows typical signal levels through the transmitter. Noise levels are not computed here since the noise associated with the transmitter is gated out by the switches in the receiver. Note that the noise associated with the scattered signal is dominated by the amplifier noise in the receiver. In general, the signal powers are calculated for the Fourier component whose frequency corresponds to the input frequency.

In this particular case, it is assumed the transmitted pulse has a period of 200 nsec (5 MHz) and a pulse duration of 30 nsec. Thus, one obtains

	2-6 GHz	**6-18 GHz**
Input Power	+20.0 dBm	+17.0 dBm
Isolator	- .8 dB	- .8 dB
Bandpass Filter	- .5 dB	- .5 dB
Switch (insertion loss)	- 3.5 dB	- 3.5 dB
Switch (duty-cycle loss)	-16.48 dB	-16.48 dB
Bandpass Filter	- .5 dB	- .5 dB
Isolator	- .8 dB	- .8 dB
Hybrid	- 3.0 dB	- 3.0 dB
Scattering (0 dB_{sm} target)	-60.0 dB (4 GHz)	-69.6 dB
Hybrid	- 3.0 dB	- 3.0 dB
HYBRID OUTPUT	-68.6 dBm	-81.2 dBm

Figure 3.3. Signal levels for the 2-6 GHz and 6-18 GHz transmitter bands.

$$\text{Duty-Cycle loss} = 20 \log (d) = 20 \log \left(\frac{30 \text{ nsec}}{200 \text{ nsec}}\right) = -16.48 \text{ dB}.$$

In computing the power loss due to scattering from the target, the following equation and parameters have been used:

$$\text{SCATTERING LOSS} = 10 \log \left(\frac{G^2 \lambda^2 \sigma}{(4\pi)^3 R^4}\right) \tag{3.1}$$

where

G = gain of the horn = 9 dB

R = focal length of the reflector = 12 ft.

σ = target size = 1 m^2

For mid-band frequencies of 4 GHz and 12 GHz the scattering losses are -60.0 dB and -69.6 dB, respectively. These two calculations are the only theoretical calculations required; the remainder of the values have been measured using laboratory equipment. The signal from the hybrid as calculated in Figure 3.3 is then input to the receiver. The receiver signal and noise levels are calculated in the next section.

A.2. The Receiver

Figure 3.4 shows the receiver with its RF switch and amplifiers. As with the transmitter, the filters and isolators in the receiver are used to reduce the presence of undesirable effects. The isolators located before the amplifiers absorb energy reflected from the amplifier inputs. The cable between the hybrid and the receiver is rather long, and a pulse which is reflected from the amplifier may bounce within the cable a sufficient number of times to enter the gate of the receiver. If this pulse were created by clutter, the receiver would always detect

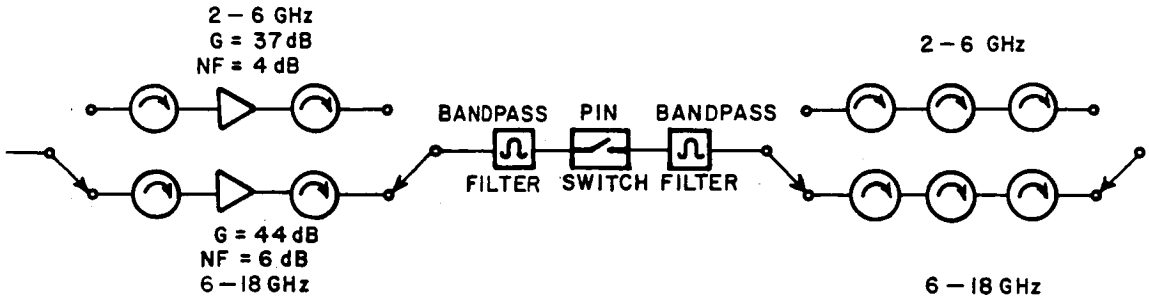

Figure 3.4. The receiver.

a signal even if no target were present. It is always desirable to keep cable lengths short for this reason. The isolators located after the amplifiers absorb reflected energy from the bandpass filter and switch. The need for the three isolators placed at the output of the receiver will become clear in the next section on the down converter.

Figure 3.5 shows typical calculations for the signal and noise power within the receiver. The calculations were carried out assuming a receive gate of 20 nseconds adjusted to receive the maximum signal from the target so that 10 nsec of the target pulse is gated out by the receiver. The effective signal loss due to receive gating is given by

$$20 \log \left(\frac{20 \text{ nsec}}{30 \text{ nsec}}\right) = -3.52 \text{ dB} .$$

Noise power has been calculated using a bandwidth of 55 Hz, the bandwidth of the CW receiver, and the duty-cycle loss in noise power has

	2-6 GHz		6-18 Ghz	
	Signal	Noise	Signal	Noise
Input	-68.6 dBm		-81.2 dBm	
Isolator	- .8 dB		- .8 dB	
Amplifier	+37.0 dB	-118.0 dBm	+44.0 dBm	-108.0 dBm
Isolator	- .8 dB	- .8 dB	- .8 dB	- .8 dB
Bandpass Filter	- .5 dB	- .5 dB	- .5 dB	- .5 dB
Switch (Insertion Loss)	- 3.5 dB	- 3.5 dB	- 3.5 dB	- 3.5 dB
Switch (Duty-Cycle Loss)	- 3.52 dB	- 10.0 dB	- 3.52 dB	- 10.0 dB
Bandpass Filter	- .5 dB	- .5 dB	- .5 dB	- .5 dB
3 Isolators	- 2.4 dB	- 2.4 dB	- 2.4 dB	- 2.4 dB
RECEIVER OUTPUT	-43.6 dBm	-135.7 dBm	-49.2 dBm	-125.7 dBm

Figure 3.5. Receiver signal and noise power.

been calculated according to the methods given in Chapter II. In the next section, the down converter is described.

A.3. The Down Converter

Originally the pulsed/RF system was designed to be operated with no down converter. The output of the above receiver was fed directly to the mixer of a CW receiver as shown in Figure 3.6, and the receiver would detect the Fourier component in the pulse train which corresponded to the original transmitted frequency. The local oscillator within the CW receiver would remain in this case, 45 MHz away from the RF carrier frequency. Some of the signal from the CW receiver's LO passes through the mixer back toward the switch. The switch reflects this signal and modulates it with a signal of period 200 nsec. This signal then is mixed with the original LO signal, and a baseband signal is produced at

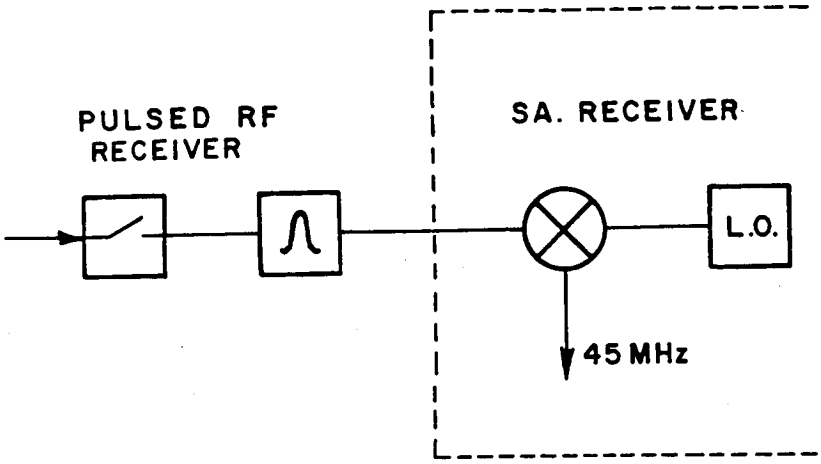

Figure 3.6. Pulsed receiver switch and CW receiver mixer.

the mixer output. Since the signal is periodic, a harmonic is present at 5 n MHz where n=0,1,2..., which includes 45 MHz, the IF of the CW receiver [1]. This means that a signal is present independent of the RF frequency, even if no target signal were present. For this reason several isolators were added to the output of the pulse system to absorb any LO signal which could be reflected back toward the CW receiver.

With the introduction of the down converter shown in Figure 3.7, this problem was effectively eliminated. The down converter utilizes a local oscillator source (W.J.#2) which mixes the incoming pulsed target signal down to a carrier frequency of 1 GHz. Then, the bandpass filter removes most of the modulating components from the 1 GHz signal, and the lowpass filter ensures that no harmonics of 1 GHz pass to the CW receiver. The second isolator provides a good matched input to the CW receiver's mixer. Any LO signal which gets past this isolator will be strongly attenuated by the bandpass filter. It may appear that in solving the problem with the SA mixer, the same problem may be present

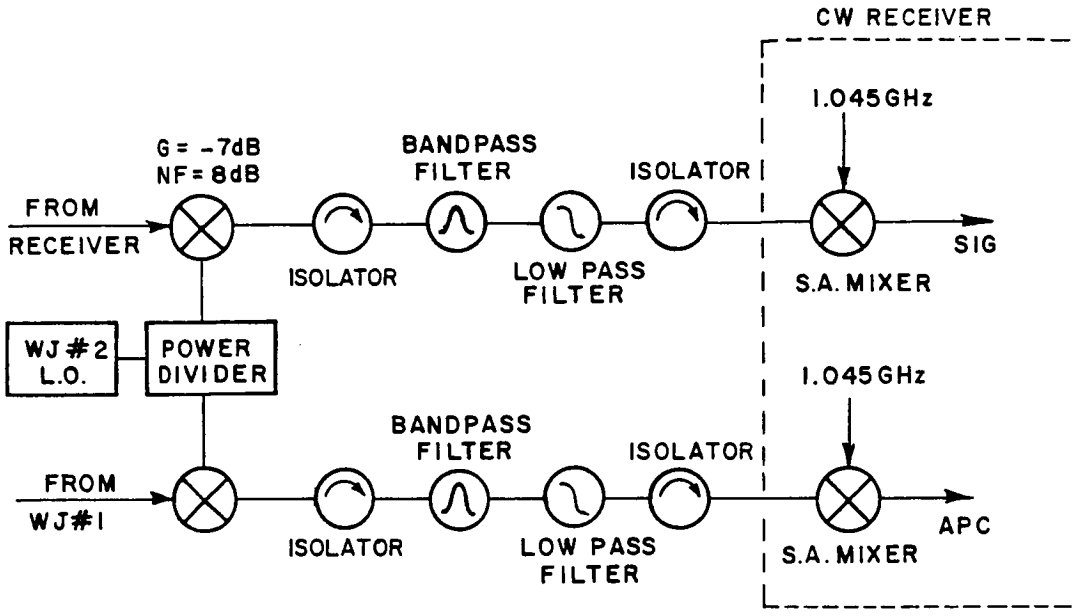

Figure 3.7. The down converter.

with the first mixer. It is true that the LO signal from W.J.#2 may be modulated by the switch, but the signal which has components at 5n MHz (n=0,1,2...) is not likely to have a strong component at 1 GHz (n=200). In addition, the system is often run from 2002.5 MHz to 18002.5 MHz in 10 MHz steps, so the down converter actually runs at 1002.5 MHz which is close enough to 1000 MHz to pass through the bandpass filter. The LO of the CW receiver is adjusted to 1047.5 MHz, and a 45 MHz signal is produced. Since the bandwidth of the receiver is 55 Hz any signal which may be present at 47.5 MHz is eliminated. The problem of LO modulation has now been effectively eliminated.

Figure 3.8 shows calculations for signal and noise powers within the down converter. The noise generated within the mixer has been ignored since it is about 15 dB below the input noise power. The

	2-6 GHz		6-18 Ghz	
	Signal	Noise	Signal	Noise
Input	-43.6 dBm	-135.7 dBm	-49.2 dBm	-125.7 dBm
Mixer	- 7.0 dB	- 4.0 dB	- 7.0 dB	- 4.0 dB
Isolator	- .4 dB	- .4 dB	- .4 dB	- .4 dB
Bandpass Filter	- .8 dB	- .8 dB	- .8 dB	- .8 dB
Lowpass Filter	- .3 dB	- .3 dB	- .3 dB	- .3 dB
Isolator	- .4 dB	- .4 dB	- .4 dB	- .4 dB
DOWN CONVERTER OUTPUT	-52.5 dBm	-141.6 dBm	-58.1 dBm	-131.6 dBm

Figure 3.8. Down converter signal and noise power.

conversion loss of the mixer is 7 dB, but it should be noted that noise is present at both the signal frequency and its image frequency. Therefore, the noise power is doubled, or the apparent noise conversion loss is 3 dB less than the actual conversion loss, or 4 dB.

Figure 3.9 shows the signal input range to the CW receiver. Comparing these numbers with the results in Figure 3.8, it is apparent that the receiver has a much higher noise floor than that of the pulse system. Another amplifier could be added to the pulse receiver to raise the noise floor and make the system much more sensitive to small targets. It appears that at least a 10 dB amplifier could be added, and by using low noise amplifiers even more sensitivity could be obtained.

MAXIMUM SIGNAL INPUT TO S.A. MIXER	-30 dBm
NOISE FLOOR WITH 55 Hz RECEIVER BANDWIDTH	-122 dBm

Figure 3.9. Scientific Atlanta model 1780 receiver dynamic range.

Figure 3.10 shows that the 2-6 GHz amplifier shown in Figure 3.4 reaches a 1 dB gain compression point with an output of +20 dBm, while that of the 6-18 GHz amplifier is +14 dBm. The 1 dB gain compression point is reached as the amplifier begins to saturate with increasing input power. In comparing these values with those in Figure 3.5 one must recall that the power values calculated here have been for the Fourier component which corresponds to

2-6 GHz OUTPUT: +20 dBm

6-18 GHz OUTPUT: +14 dBm

Figure 3.10. Amplifier output for 1 dB gain compression.

the transmitter frequency. The duty cycle loss should be removed from these calculations so that the unswitched power level may be determined. This is important because it is the instantaneous power within the pulse which must be compared to the 1 dB gain compression figures quoted above. This power will be referred to as peak power for the remainder of this report. Referring to Figure 3.5, the power at the output of the 2-6 GHz amplifier is as follows:

INPUT	-68 6 dBm
ISOLATOR	- .8 dB
AMPLIFIER	+37.0 dB
DUTY CYCLE	+16.48 dB
	-15.9 dBm

The 16.48 dB duty cycle figure is the same number which was originally subtracted in Figure 3.3. The corresponding output for the 6-18 GHz band amplifier is -21.5 dBm. Comparing these numbers with those of Figure 3.10 indicates that for a 0 dBsm target the output of the 2-6 GHz amplifier is 36 dB below its 1 dB gain compression point while the output of the 6-18 GHz amplifier is 35.5 dB below its corresponding 1 dB gain compression point.

The input signal required to compress the gain of the down converter mixer is 0 dBm. As with the amplifiers, this mixer's input must be compared to the peak power of the pulse. Referring back to Figure 3.8 and adding 20 dB (10% duty cycle) to the signals present at the mixer's input shows that within the 2-6 GHz band, the peak power is -23.6 dBm, and -29.2 dBm within the 6-18 GHz band.

Referring to Figures 3.8 and 3.9, the signal input to the SA mixer for a 0 dBsm target is 12.5 dB below maximum input within the 2-6 GHz band, and 18.1 dB for the 6-18 GHz band. In this case, only 10 dB was added to the power levels in Figure 2.8 since most of the Fourier components have been removed by the bandpass filter in the down converter. Only the first sidebands around 1 GHz are significant so the signal behaves like an AM modulated signal where the modulating frequency is 5 MHz.

Summarizing this information, Figure 3.11 shows that in the presence of very large target returns, the SA receiver is the first component to reach its maximum signal input, closely followed by the mixer in the down converter, and finally followed by the RF amplifiers.

	2-6 GHz	6-18 GHz
AMPLIFIER	36 dBsm	35.5 dBsm
MIXER IN DOWN CONVERTER:	+23.6 dBsm	+29.2 dBsm
SA MIXER:	+12.5 dBsm	+18.1 dBsm

Figure 3.11. Radar cross section levels which cause component saturation.

This information is very important because it shows which components are under the most stress in the presence of large signals. In the next section, a similar process will be performed on our old Ka-band radar system.

B. THE KA-BAND SYSTEM

Figure 3.13 shows the old pulsed/RF Ka-band radar system. Its operation is similar to that of the 2-18 GHz radar previously analyzed. The boxes marked "X2" are frequency doublers which produce the Ka-band frequencies. The switch, amplifier, doubler and isolator shown near the top of the figure comprise the transmitter section. The doubler and all components which precede it are actually part of synthesizer #1, but they have been shown as being discrete to help illustrate the frequency generating mechanism. Note that a directional coupler is used in conjunction with a single antenna. Switching and amplification are done within the receiver followed by the down converter which operates at 1 GHz. The down converter is slightly different in that an amplifier and

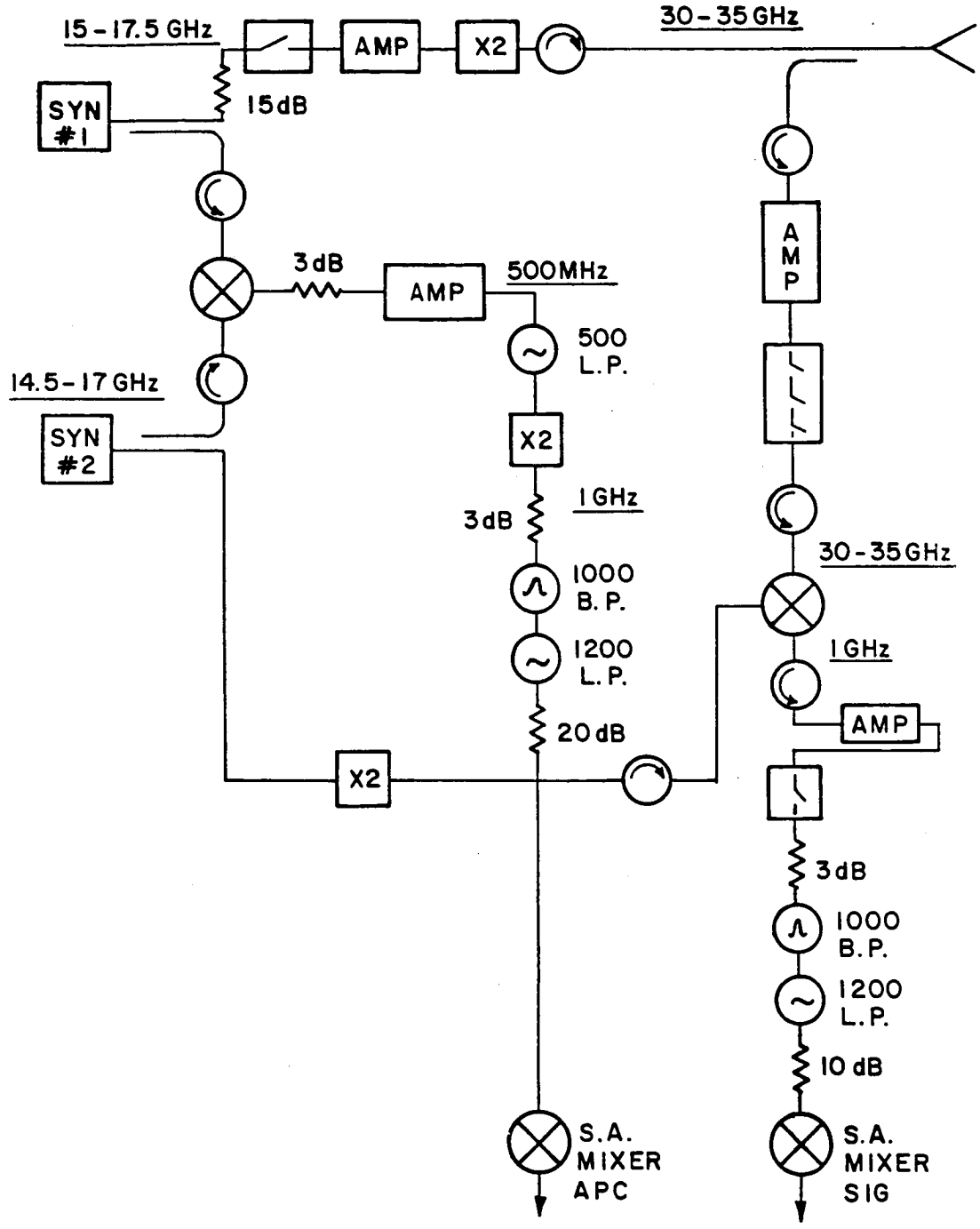

Figure 3.12. The Ka-band pulsed/RF radar system.

switch have been added. The system amplifier helps boost the weak signal coming from the RF receive section, and the switch improves the isolation of the Ka-band switches. The local oscillator frequency is 500 MHz below that of the transmit frequency because doubling both source frequencies results in the difference frequency also being doubled. It is for this reason that a doubler is required in the reference channel.

B.1. The Transmitter

The signal and noise levels for the transmitter are shown in Figure 3.13. Scattering is calculated here with an antenna gain of 15 dB. As previously mentioned, the frequency doubler and all components which precede it are internal to the first synthesizer, so their characteristics are of interest only to the extent of their influence on signal and noise levels. The signal level quoted for the amplifier is the usual Fourier component of a 30 nsec pulse. The noise is calculated for an amplifier with a 30 dB gain and a noise figure of 12 dB over a bandwidth of 55 Hz. Since the amplifier is placed after the switch, its noise is present in the transmitter at all times. In computing the scattering loss for noise, a figure of 20 dB has been used because this is the estimated return due to the antenna mismatch. Thus, noise is present at the input to the receiver at all times. If the amplifier were located before the switch, then noise would only be associated with the signal pulse, and the signal and noise reflected at the antenna

	Signal	Noise
Amplifier Output	- 4.5 dBm	-114.7 dBm
Doubler	- 10.0 dB	- 10.0 dB
Isolator	- 1.0 dB	- 1.0 dB
Directional Coupler	- 3.0 dB	- 3.0 dB
Scattering (0 dBsm target)	- 66.2 dB (32.5 GHz)	- 20.0 dB
Directional Coupler	- 3.0 dB	- 3.0 dB
DIRECTIONAL COUPLER OUTPUT	- 87.7 dBm	-151.7 dBm

Figure 3.13. Signal and noise levels for the Ka-band transmitter.

would be gated by the receiver. The noise scattered by the target would be down by an additional 45 dB and would be lost in the receiver's noise. Unlike the 2-18 GHz system, the transmitter's noise in the Ka-band system is comparable to the receiver's noise, so it cannot be neglected.

B.2. The Receiver

The two types of noise calculated in Figure 3.14 refer to noise generated within the transmitter and receiver, respectively. Both noise levels are carried to the output of the receiver where they are added. The switch is assumed to be operating with a 20 nsec gate width. As with the 2-18 GHz system the receive gate is assumed to be aligned with the target pulse to maximize power, which results in a loss of 3.52 dB from converting a 30 nsec pulse to a 20 nsec gate.

	Signal	Noise		
		Transmitter	Receiver	Total
Input Power	- 87.7 dBm	-151.7 dBm		
Isolator	- 1.0 dB	- 1.0 dB		
Amplifier	+ 41.5 dB	+ 41.5 dB	-107.7 dBm	
Switch (Insertion Loss)	- 7.0 dB	- 7.0 dB	- 7.0 dB	
Switch (Duty-Cycle Loss)	- 3.52 dB	- 10.0 dB	- 10.0 dB	
Isolator	- 1.0 dB	- 1.0 dB	- 1.0 dB	
TOTAL	- 58.7 dBm	-129.2 dBm	-125.7 dBm	-124.1 dBm

Figure 3.14. Signal and noise levels for the Ka-band receiver.

B.3. The Down Converter

The mixer in the down converter (Figure 3.15) has a conversion loss of 5 dB and an apparent noise conversion loss of 2 dB with the noise contribution from the image frequency. The amplifier has a relatively low noise figure of 1.8 dB, so its noise contribution may be neglected. The switch is assumed to be adjusted such that it does not gate out any part of the target pulse, so its only effect on the signal is to add insertion loss. Its purpose is to stop any signal which may leak through the Ka-band switches when they are in their open state. The same bandpass and low pass filters used in the other down converter are used in this system also.

	Signal	Noise
Input	- 58.7 dBm	-124.1 dBm
Mixer	- 5.0 dB	- 2.0 dB
Isolator	- .4 dB	- .4 dB
Amplifier	+ 41.0 dB	+ 41.0 dB
Switch (Insertion Loss)	- 3.5 dB	- 3.5 dB
Attenuator	- 3.0 dB	- 3.0 dB
Bandpass Filter	- .8 dB	- .8 dB
Lowpass Filter	- .3 dB	- .3 dB
Attenuator	- 10.0 dB	- 10.0 dB
OUTPUT	- 40.7 dBm	-103.1 dBm

Figure 3.15. Signal and noise levels for the Ka-band down converter.

Referring to Figure 3.15, it is noticed that having an additional amplifier in the down converter has raised the noise level of the pulse system above that of the CW receiver (-122 dBm). This results in a maximization in the sensitivity of the system. Further improvement could be realized if the transmitter power were increased, and if amplifiers with lower noise were used.

For large signal inputs, it is useful to determine which components reach saturation first as the target size is increased. Figure 3.16 shows the input power required for a 1 dB gain compression for the Ka-band amplifier, mixer and 1 GHz amplifier. A 0 dBsm target will produce: a -72.2 dBm peak signal at the input to the Ka-band amplifier, a -38.7 dBm signal at the input to the mixer, and a -44.1 dBm signal at the input to the 1 GHz amplifier. These peak power numbers indicate that the SA receiver will saturate well before the above three components (see Figure 3.17). Since the SA receiver has a maximum input

Ka-band Amplifier	-31 dBm
Mixer	0 dBm
1 GHz Amplifier	-28 dBm

Figure 3.16. Input required for a 1 dB gain compression.

Ka-band Amplifier	+41.2 dBsm
Mixer	+38.7 dBsm
1 GHz Amplifier	+16.1 dBsm
SA Receiver	+ 0.7 dBsm

Figure 3.17. Radar cross sections which cause component saturation for the Ka-band system.

	Max Target Size (dBsm)	Min Target Size (dBsm)
2-6 GHz	12.5	-69.5
6-18 GHz	18.1	-63.9
Ka-band	0.7	-62.4

Figure 3.18. Maximum target size and target size which produces a signal equal to the system noise floor.

of -30 dBm, Figure 3.15 indicates that the largest target which may be measured by this system is +0.7 dBsm. Figure 3.18 shows the largest targets measurable by this system as well as the target size which produces a signal equal to the noise floor of the system. For 2-18 GHz the noise floor is -122 dBm caused by the SA receiver while that of the Ka-band is -103.1 dBm.

This completes the theoretical analysis of our old 2-18 GHz and Ka-band systems. The signal and noise power calculations performed in this chapter have illustrated the application of the concepts developed in Chapter II. It has been found that the noise level of the 2-18 GHz system is well below that of the SA receiver. This would indicate that an additional amplifier may be added to the pulsed system to raise its noise level to that of the SA receiver without raising the apparent overall noise level of the system. This would permit the measurement of targets with a smaller radar cross section. The Ka-band system has an amplifier in the down converter which has raised the noise of the pulsed system above that of the SA receiver. According to Figure 3.15 the signal to noise ratio for a 0 dBsm target is only slightly less than that for the 2-18 GHz system. This is the case even though the transmitter's power is much lower on the Ka-band system as a result of the relatively low output of the frequency doublers.

In Chapter V, our new pulsed/IF radar system will be introduced and analyzed. It will include additional amplification in the receiver and have a minimal amount of hardware in the receiver which operates at the transmitter's frequency. Redundancy will be reduced by using the same

IF receiver for all bands which will greatly reduce the cost of the Ka-band hardware as well as any new frequency bands which may be added in the future.

CHAPTER IV

THE EFFECTS OF PULSE WIDTH ON CLUTTER LEVEL

In Chapter III, it is suggested that more amplification should be added to the new radar design. Another consideration is the level of clutter measured by the old system relative to its noise floor. Clutter is most easily defined by describing what it is not; it is not the radar's measured response of the target to an incident plane wave, nor is it a random response of the radar. When a target is measured, its response is stored in a computer for later calibration. The same measurement is made again, but the target is removed from the target zone. This is referred to as a background measurement, and it is subtracted by the computer from the target measurement as part of the calibration process. The phasor components of the measured target signal are pictured in Figure 4.1. It is desirable to perform a phasor subtraction between the measured target signal and a background measurement with precisely the same clutter phasor. Unfortunately, instabilities within the radar system limit the ability to make a background measurement with an identical clutter phasor. The ability of the system to subtract is determined by subtracting two consecutive background measurements. A subtracted level of about 50 dB below the original clutter level is generally considered to be very good.

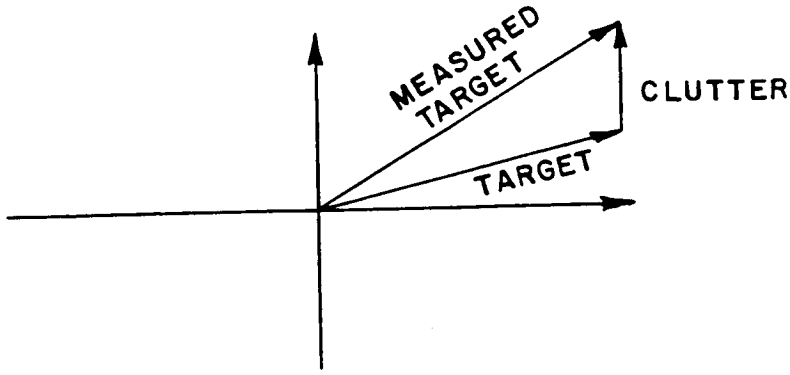

Figure 4.1. Phasor components of the measured target signal.

Note that Figure 4.1 does not include a small random phasor to account for noise in the system and other time varying changes in response. When so much clutter is present that its total return is greater than 50 dB above the noise floor of the system, subtraction of two successive background measurements is very difficult to maintain. In the old system of Chapter III, clutter levels are somewhat less than 50 dB above the noise floor, so subtraction adequately removes the clutter. If amplification is to be added to a new system, something must be done to reduce the clutter which presently enters the time gate of the receiver; otherwise, the returns from small targets which are above the noise floor will be lost in the clutter.

In order to understand how pulse widths in the transmitter and receiver affect clutter levels, it is necessary to construct timing diagrams which represent the pulsed returns from various scatterers within the particular chamber. Figure 4.2 is a sketch of the range along with a source of potential interference, discontinuities in the microwave absorber caused by recessed ceiling lights. Note that X_1 and

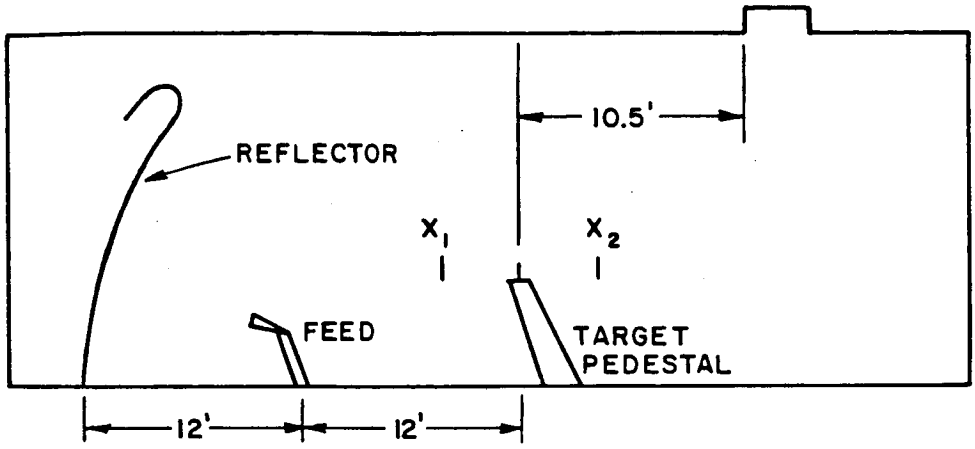

Figure 4.2. The compact range.

X_2 represent the boundaries of the intended target zone and are equal to the one way distance travelled by a pulse between the feed horn and the corresponding target zone boundary. The time for the pulse to travel to each boundary is given by

$$\tau_1 = \frac{X_1}{C} \tag{4.1}$$

and

$$\tau_2 = \frac{X_2}{C} \, . \tag{4.2}$$

The lights appear to be located about 10.5 ft. (10.5 nsec) behind the center of the target zone. Actually, several scattering centers are associated with the lights, but the one closest to the target zone is sufficient for this discussion.

Figure 4.3(a) shows the return pulses from the target zone boundaries, X_1 and X_2, assuming t=0 corresponds to the leading edge of

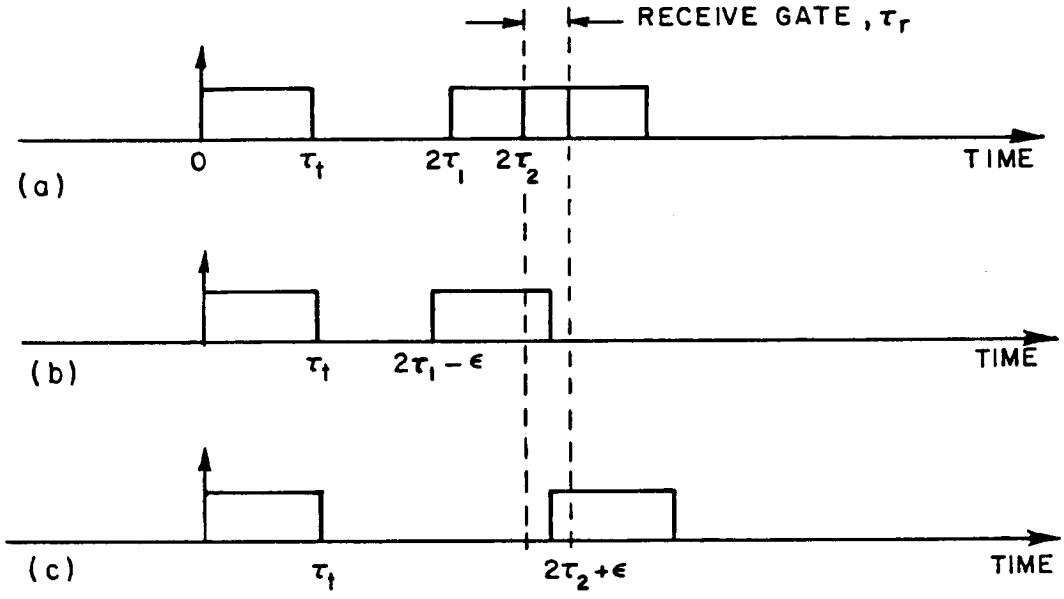

Figure 4.3. Timing diagrams for thin targets located:

(a) at the boundary of the target zone
(b) in front of the target zone
(c) in back of the target zone

the pulse transmitted into the chamber. The vertical scale is an arbitrary amplitude scale, and τ_t is the pulse width of the transmitter. If the receive gate is adjusted to pass signals from $2\tau_2$ to $2\tau_1 + \tau_t$, then targets between X_1 and X_2 will have pulse returns which are fully sampled by the receiver. There are positions just outside of the target area that will cause returns which enter the gate of the receiver, but they will not be fully sampled by the receiver. Figure 4.3(b) shows the return from a target located just in front of X_1, while Figure 4.3(c) shows one just behind X_2. It is evident that these pulses are starting to fall outside the gate of the receiver, and the receiver cannot accurately measure their amplitude. The receiver has a pulse width of τ_r (Figure 4.3(a)) which is given by

$$\tau_r = (2\tau_1 + \tau_t) - 2\tau_2 \tag{4.3}$$

$$= 2(\tau_1 - \tau_2) + \tau_t \tag{4.4}$$

where

$$\tau_2 - \tau_1 = \frac{1}{C}(X_2 - X_1) \, . \tag{4.5}$$

Recall that $X_2 - X_1$ is the size of the target zone, so let

$$D_t = X_2 - X_1 \tag{4.6}$$

then

$$D_t = \frac{C}{2}(\tau_t - \tau_r) \, . \tag{4.7}$$

A similar expression can be derived for the size of the region from which a return may enter the receive gate. The earliest observable

pulse arrives at $2\tau_1 - \tau_r$, and the latest arrives at $2\tau_2 + \tau_r$. Since these are two way travel times, the actual size of this zone corresponds to half of the difference between them. The size of this region of sensitivity is defined as D_s:

$$\frac{2D_s}{C} = (2\tau_2 + \tau_r) - (2\tau_1 - \tau_r) \tag{4.8}$$

or

$$D_s = \frac{C}{2}(\tau_t + \tau_r) \ . \tag{4.9}$$

These are useful expressions for D_t and D_s. Note that $C \simeq 1$ for length in feet and time in nsec. Also, note that D_s and D_t become equal as $\tau_r \to 0$.

A potential problem is the sensitivity of the feed horn in its back lobe. Signals which have been scattered back toward the reflector may enter the receiver through the rear of the horn. Since these signals do not have to propagate as far, it appears as though the target zone has moved behind the original target zone by a distance equal to half the reduction in propagation distance. Thus the same timing diagrams may be used except the position of the receive gate has been delayed by a time corresponding to the difference in propagation distances. This problem and how it is affected by the gate width will be discussed in the following two sections.

A. 30/20 Timing Scheme

In Chapter III, a 30 nsec transmit gate and 20 nsec receive gate are assumed to be used when calculating signal and noise powers. For τ_t=30 nsec and τ_r=20 nsec, the size of the target zone, D_t, is ~5 feet,

while the sensitivity zone, D_s, is ~25 feet. Figure 4.4(a) shows the general case for a sketch of apparent pulse width versus position about the center of the target zone. The equation for this line is

$$\tau_r'(x) = \begin{matrix}\text{apparent} \\ \text{pulse} \\ \text{width}\end{matrix} = \begin{cases} \left(\frac{2X + D_s}{D_s - D_t}\right)\tau_r & \frac{-D_s}{2} < X < \frac{-D_t}{2} \\ \tau_r & \frac{-D_t}{2} < X < \frac{D_t}{2}, \text{ and} \\ \left(\frac{D_s - 2X}{D_s - D_t}\right)\tau_r & \frac{D_t}{2} < X < \frac{D_s}{2}. \end{cases} \tag{4.10}$$

The response for a target in the sensitivity zone relative to its response at the center of the target zone is:

$$20\log\left(\frac{\tau_r'(X)}{\tau_r}\right). \tag{4.11}$$

The loss associated with scatterers outside the target zone is identical to a duty cycle loss, and it results from not fully sampling the returns from these positions.

Figure 4.4(b) is a sketch of the actual condition for the case under consideration. Referring to Figure 4.2, the feed horn is 12 feet in front of the target zone center; while, the lights are 10.5 feet beyond it. The relative scattering losses due to position for the feed horn and lights are -26 dB and -14 dB, respectively.

The interference due to the feed horn back lobe is easily analyzed by shifting the target zone center back (away from the reflector) 12 feet. This corresponds to half of the 24 ft. the signal no longer must

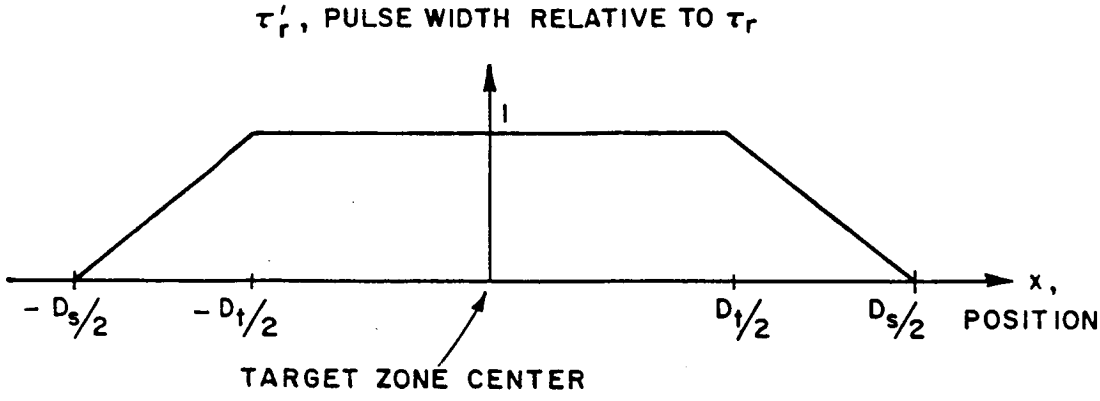

(a) general case

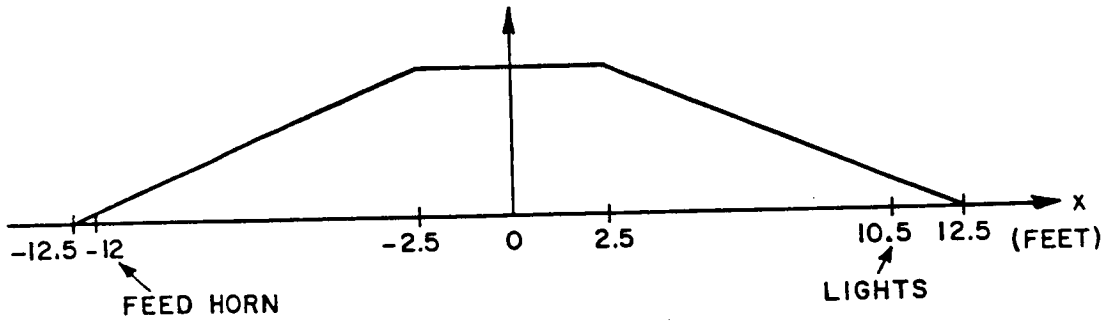

(b) 30/20 case

Figure 4.4. Target and sensitivity zones.

travel between the horn, the reflector and back to the horn. The result is shown in Figure 4.5. The vertical scale in Figure 4.5 accurately indicates the relative pulse width; however, the amplitude of those pulses is reduced by the front to back ratio of the feed antenna. Three sources of interference are present: target, lights and backwall. Fortunately, the target and backwall are in rather insensitive areas, so their contributions are not significant. The lights are, however, in a sensitive location, within the apparent target zone.

When the backlobe case is combined with the standard one, the actual response detected by the receiver will be a superposition of Figures 4.4(b) and 4.5 where the scatterers in Figure 4.5 appear to be 12 feet in front of their actual location. This is the case because the receiver is unable to determine whether a pulse propagates along the standard path and is scattered within the sensitivity zone, or whether the pulse propagates via the backlobe path and scattered by objects located 12 feet behind the original sensitivity zone. In both cases the total propagation path length is the same. Figure 4.6 shows the result with the vertical axis drawn only for reference since the main lobe of the feed horn is more sensitive than the back lobe, as previously mentioned.

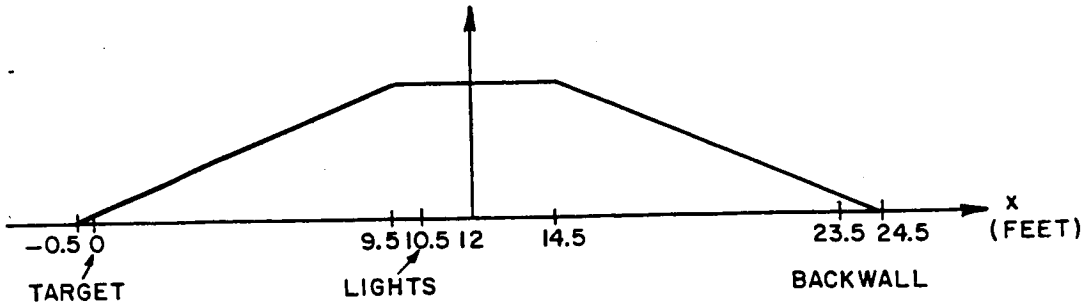

Figure 4.5. Leakage through the feed horn back lobe.

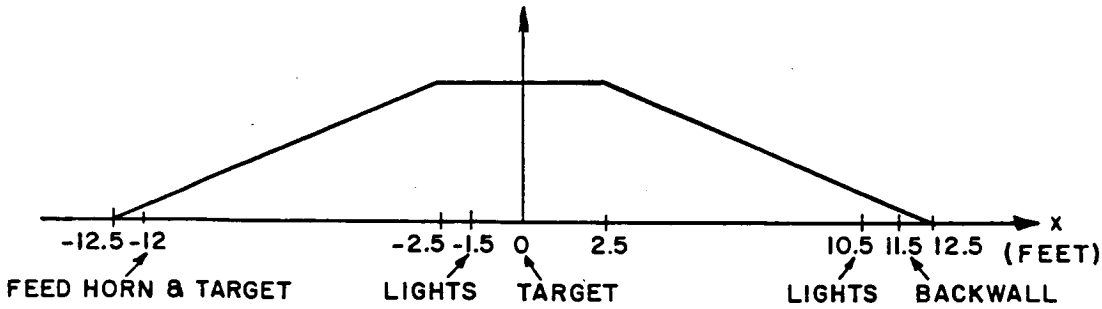

Figure 4.6. Superposition of Figures 4.4(b) and 4.5.

B. 20/10 Timing Scheme

It is a straightforward matter to apply the concepts developed thus far to a new case, a 20 nsec transmit pulse width and 10 nsec receive pulse width. The size of the target zone, D_t, is 5 feet as before, and the size of the sensitivity zone, D_s, is 15 feet. Figure 4.7 shows the sensitivity zone for this case. Clearly, the lights and the feed horn are effectively gated in this case. The next case to consider is the back lobe leakage problem, and Figure 4.8 shows this case. Once again, with a smaller sensitivity zone, some clutter is eliminated, namely the target and backwall, but the lights remain and must be reduced or eliminated by another method. Figure 4.9 shows the total response, and it contains much less clutter than Figure 4.6.

In conclusion, some very useful techniques have been developed in this chapter for analyzing the regions of sensitivity for the receiver. It is evident that the receive pulse width should be as narrow as possible, so that the receiver is only sensitive to objects in the target zone. In this case, the size of the target zone would essentially be governed by the size of the transmit pulse. Unfortunately, duty cycle loss and PIN switch speed set a lower limit on the receive pulse width.

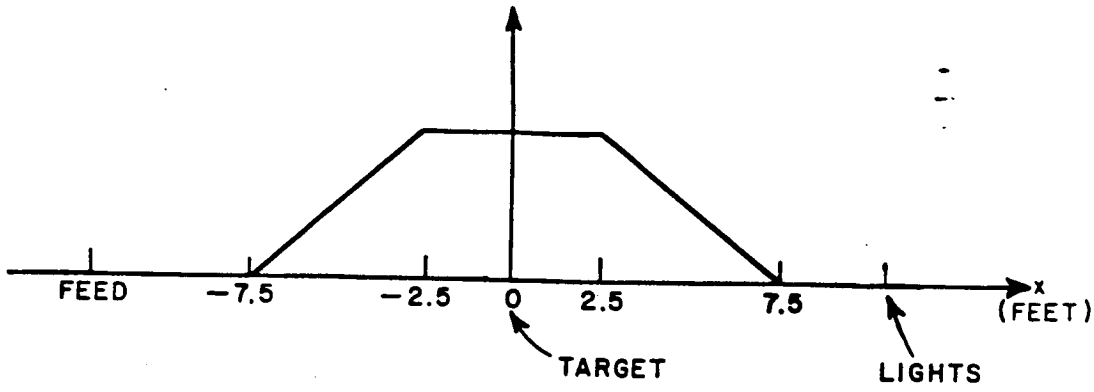

Figure 4.7. Sensitivity zone for the 20/10 case.

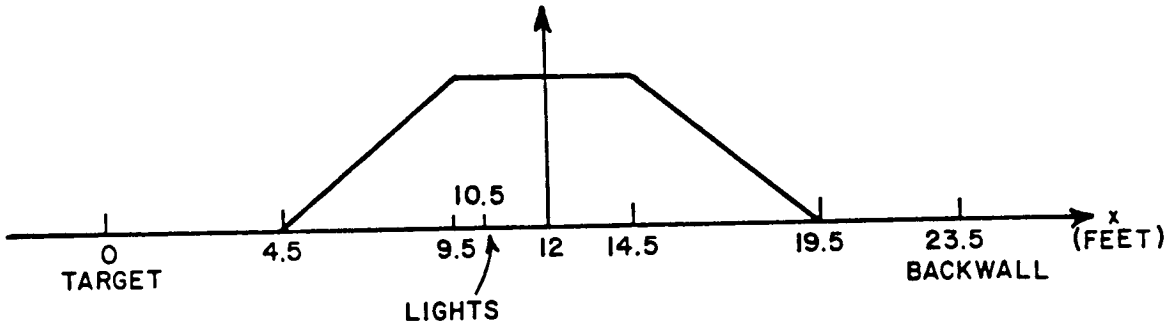

Figure 4.8. Sensitivity zone for back lobe leakage.

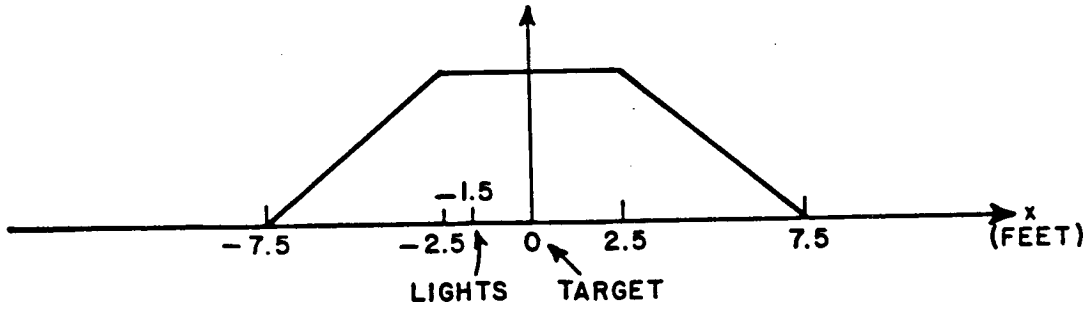

Figure 4.9. Superposition of Figures 4.7 and 4.8.

CHAPTER V

PULSED/IF RADAR SIGNAL AND NOISE ANALYSIS

In the first two chapters, basic concepts were developed, and our old pulsed/RF radar system was analyzed. That system has several shortcomings including an insufficient amount of sensitivity as well as the inability to add additional frequency bands without adding a significant amount of hardware. The new pulsed/IF system is designed here to address these shortcomings.

In the first few sections of this chapter, the pulsed/IF system is analyzed in the same way that the pulsed/RF radar system was analyzed in Chapter III. Plots of several individual components are included to indicate typical performance. It should be kept in mind that the calculated signal and noise power may vary significantly with frequency as indicated by some of the insertion loss plots. In the following sections, an in-depth discussion will be presented on the potential problems with this system along with their solutions. For the remainder of this report the pulsed/RF radar system will be referred to as the "old" system, and the pulsed/IF system will be referred to as the "new" one.

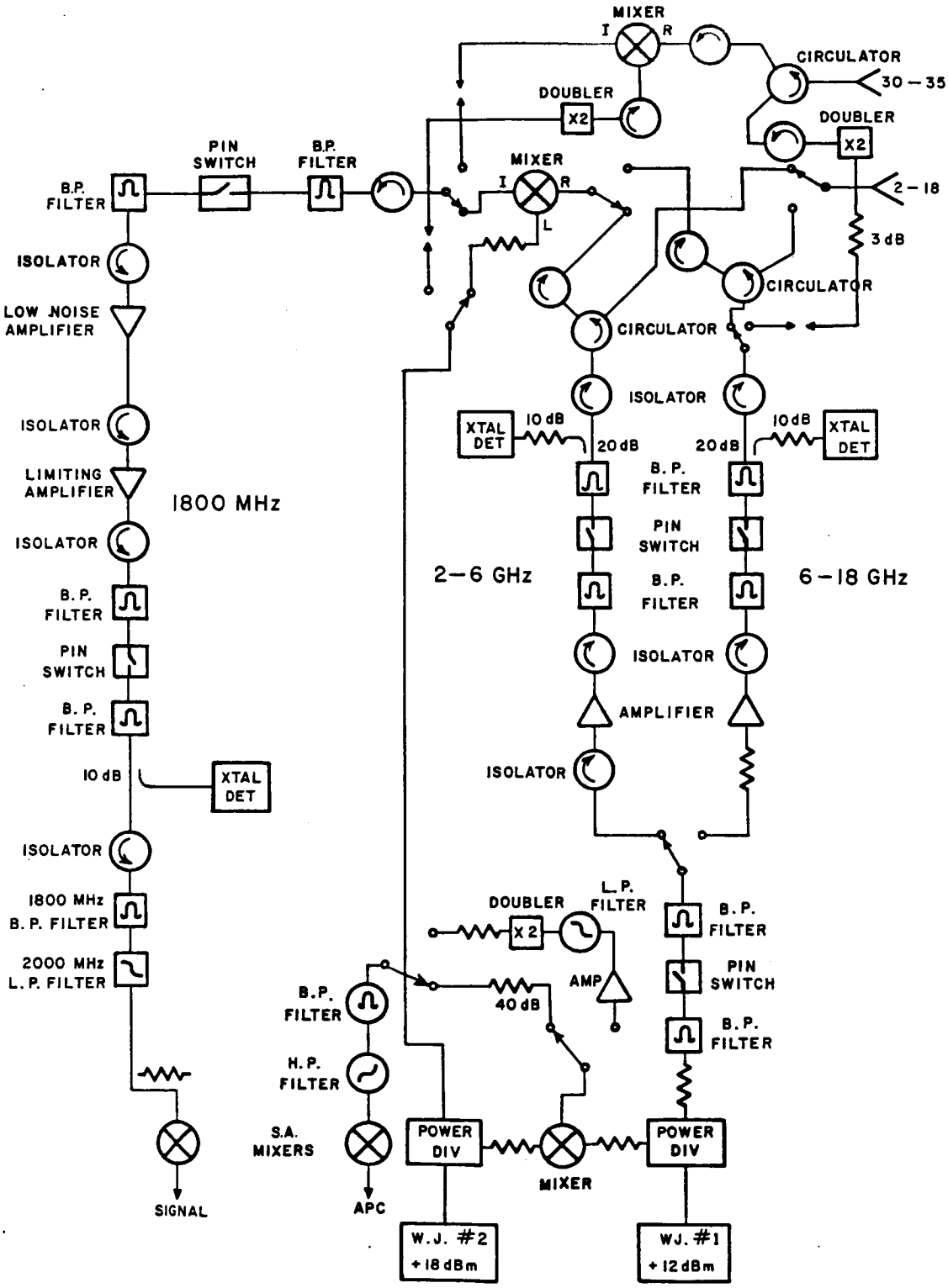

Figure 5.1. The new pulsed/IF radar system.

A. THE NEW SYSTEM

The new system is illustrated in Figure 5.1. It is broken down into two subsystems: the transmitter and the receiver. The most apparent difference between the old and new systems is that the receiver and down converter in the old system have been merged into a single receiver in the new system. The receiver down converts the RF signal to a constant IF of 1800 MHz, so that all of the amplification and gating are done at one frequency. Another difference is that the Ka-band hardware uses the 6-18 GHz transmitter to generate 27-36 GHz pulsed signals. The returns are mixed down to 1800 MHz where they are sent to the receiver and processed in the normal manner. Utilizing the transmitter and receiver of the 2-18 GHz system saves the amount of hardware required when adding on more frequencies of operation, and it also simplifies troubleshooting.

B. THE TRANSMITTER

The transmitter's purpose in the new system is the same as that of the old one, that is to pulse the CW signal from the source (WJ#1), and transmit this signal with the feed antenna as shown in Figure 5.2. Transmitter power is calculated in Figure 5.3. Basically, the new system differs from the old one in three ways: first, two PIN switches are used instead of one; second, amplifiers are used to boost the power transmitted; and third, the hybrid has been replaced by two circulators so that 6 dB in signal is no longer lost.

Figure 5.4 shows the result of pulsing a PIN switch at 5 MHz with no RF signal applied. These large transients could possibly damage

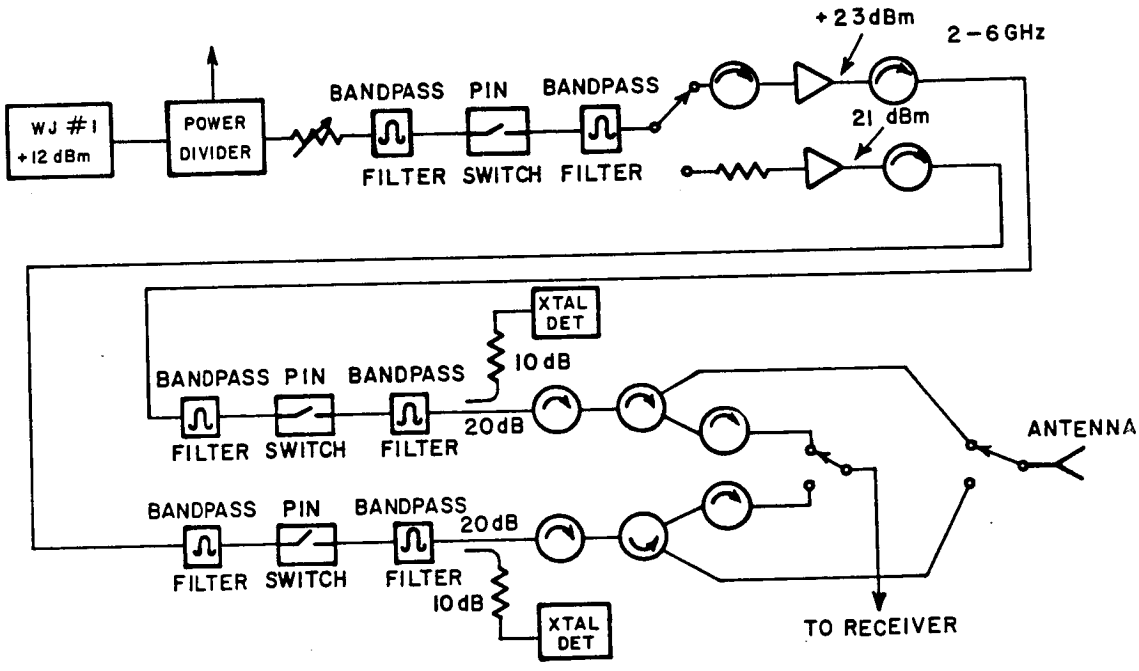

Figure 5.2. Schematic of transmitter.

	2-6 GHz	6-18 GHz
Amplifier output	+ 23.0 dBm	+ 21.0 dBm
Duty cycle loss (20 nsec)	- 20.0 dB	- 20.0 dB
Isolator	- .8 dB	- .8 dB
Bandpass filter	- .5 dB	- .5 dB
Switch (insertion loss)	- 3.5 dB	- 3.5 dB
Bandpass filter	- .5 dB	- .5 dB
Directional coupler	- .3 dB	- 1.2 dB
Isolator	- .8 dB	- .8 dB
Circulator	- .7 dB	- 1.0 dB
Scattering (0 dBsm target)	- 60.0 dB	- 69.6 dB
Circulator	- .7 dB	- 1.0 dB
Isolator	- .8 dB	- .8 dB
Transmitter Output	- 65.6 dBm	- 78.7 dBm

Figure 5.3. Transmitter signal power.

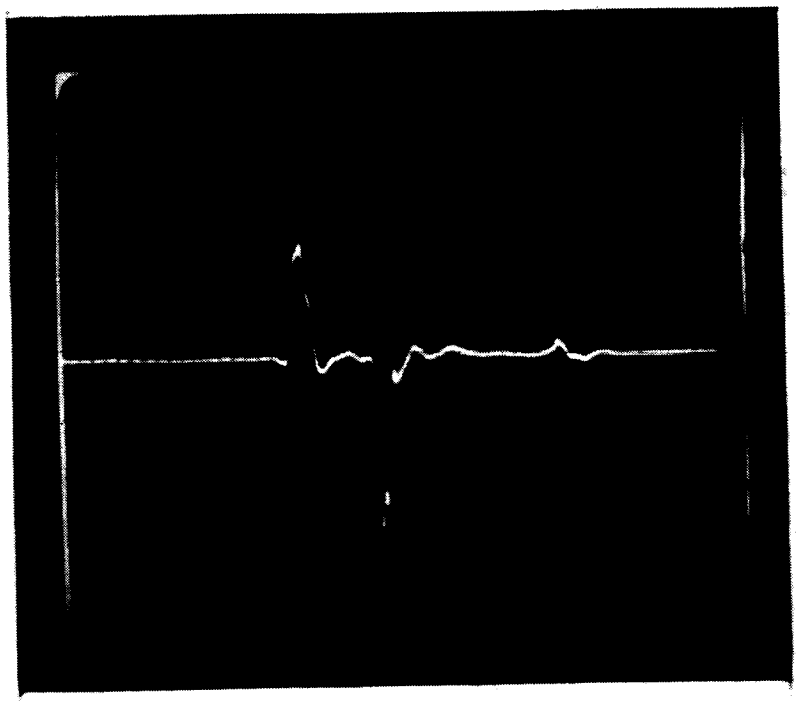

Figure 5.4. Switch transients without filtering and with no RF applied. (.5V/div vertical, 20 nsec/div horizontal)

microwave components. By placing a 1.5-18 GHz bandpass filter on the input and output of the switch, the low frequency transients are effectively eliminated. Since these transients have a period of 200 nsec (F=5 MHz), Fourier components are present at 5 n MHz (n=0,1,2...), so some of these components will be present in the passband of the filter; however, these components are of lower amplitude and will not damage the electronic hardware. Figures 5.5 and 5.6 show plots of the PIN switch loss. These plots are read by noting the position of the arrowhead at the right edge of the graticule; this is the reference line. Its value is given by the "REF" number above the graticule, and the magnitude of each horizontal division is given just below this number. It should be noted the reference line is not always at the top of the graticule. Figures 5.7 and 5.8 show plots of bandpass filter insertion loss for two different filters. The RLC filter is used only where no 6-18 GHz signals are present since the CIR-Q-TEL filters have lower insertion loss near 18 GHz. On the other hand, the RLC filters have a lower cutoff frequency (~1 GHz), so they are better suited for work at IF frequencies, since they will not attenuate any significant Fourier components of the target return which would otherwise "smear" the time domain signal before it is gated by the receiver.

Two PIN switches are used in order to improve the isolation between the transmitter and receiver. With one switch in the open state, some signal will leak through and enter the receiver. This situation is illustrated in Figure 5.9. The leakage is exaggerated to clearly show how this may corrupt the target return. Roughly 140 dB of isolation is

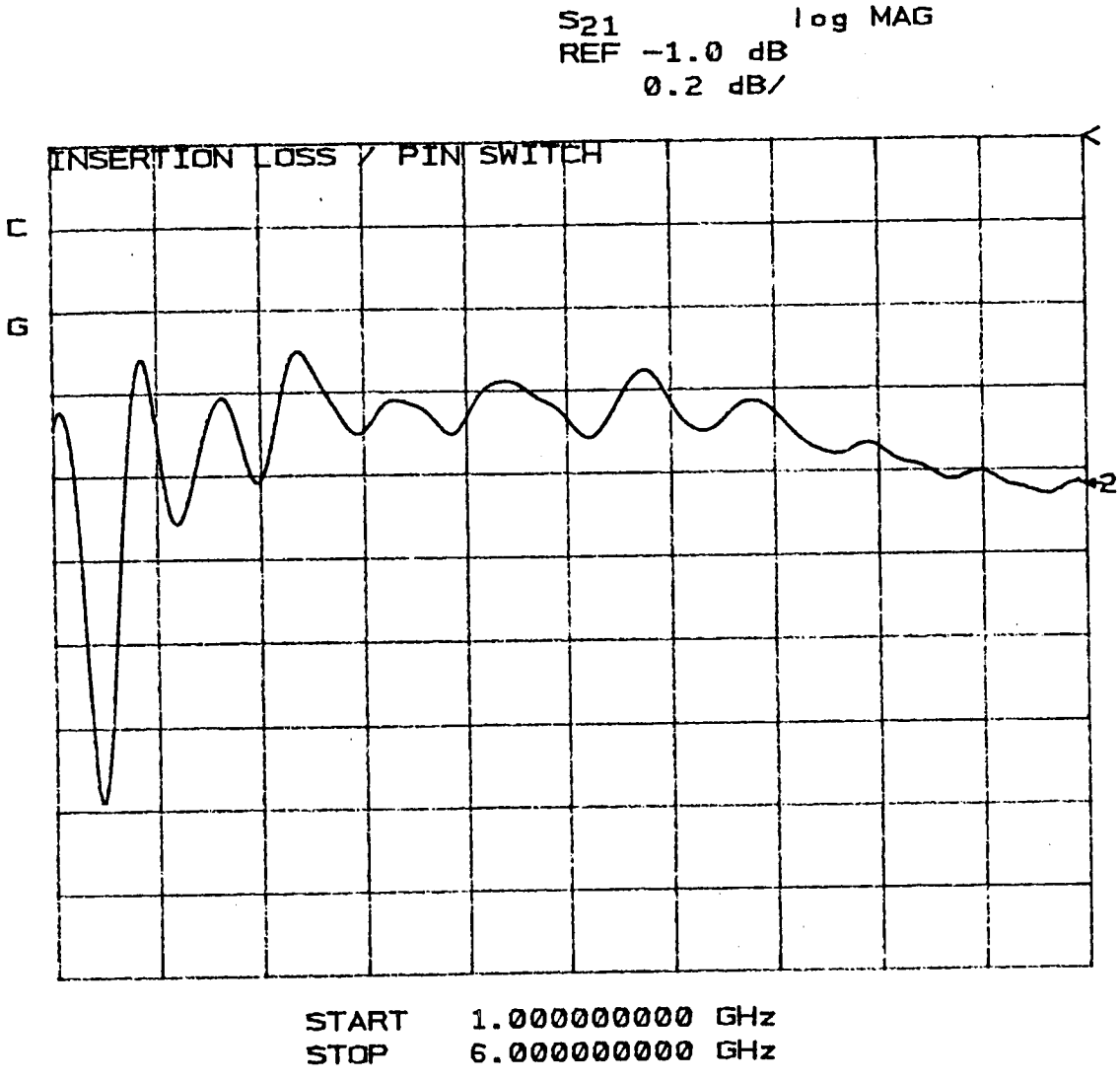

Figure 5.5. PIN switch insertion loss 1 to 6 GHz.

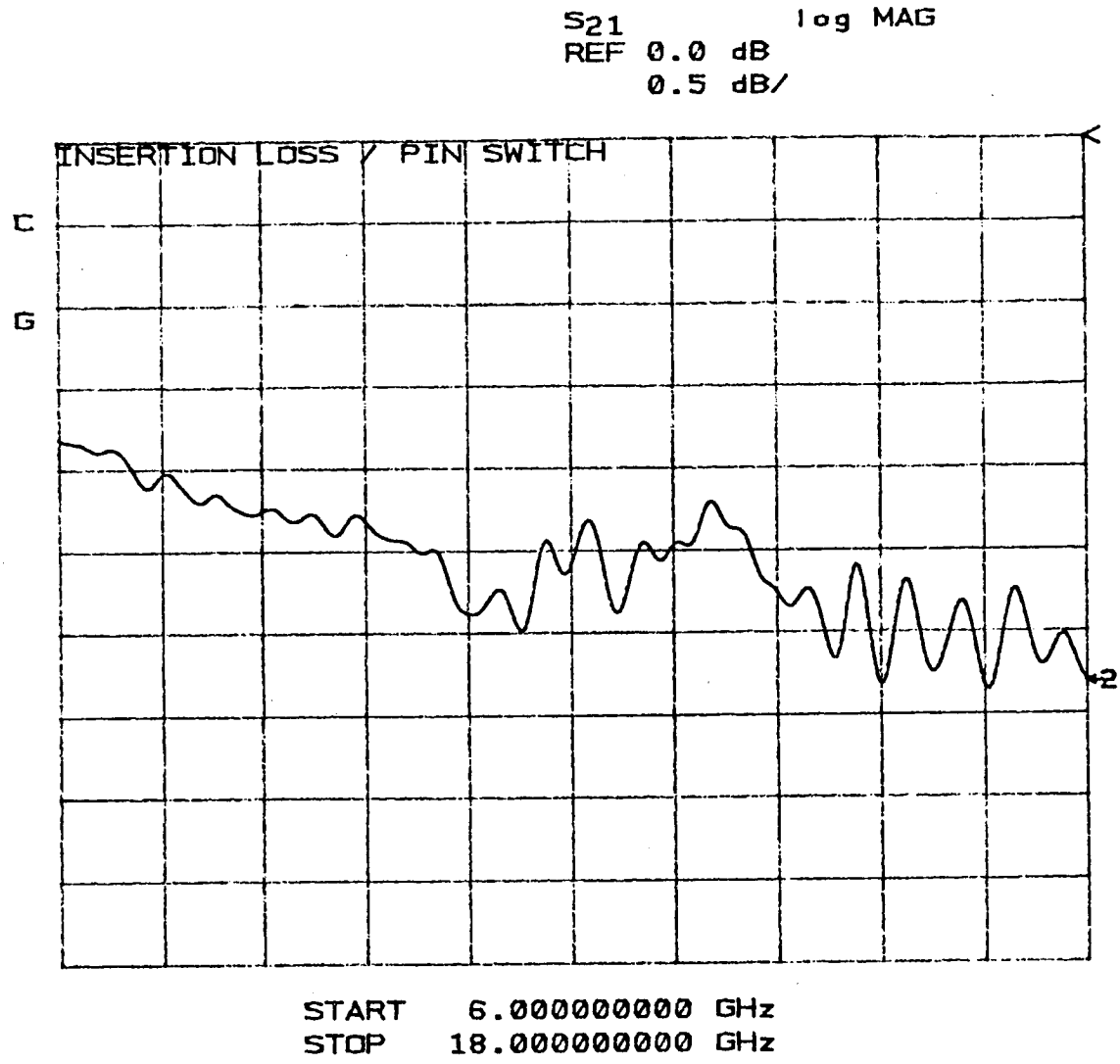

Figure 5.6. PIN switch insertion loss 6-18 GHz.

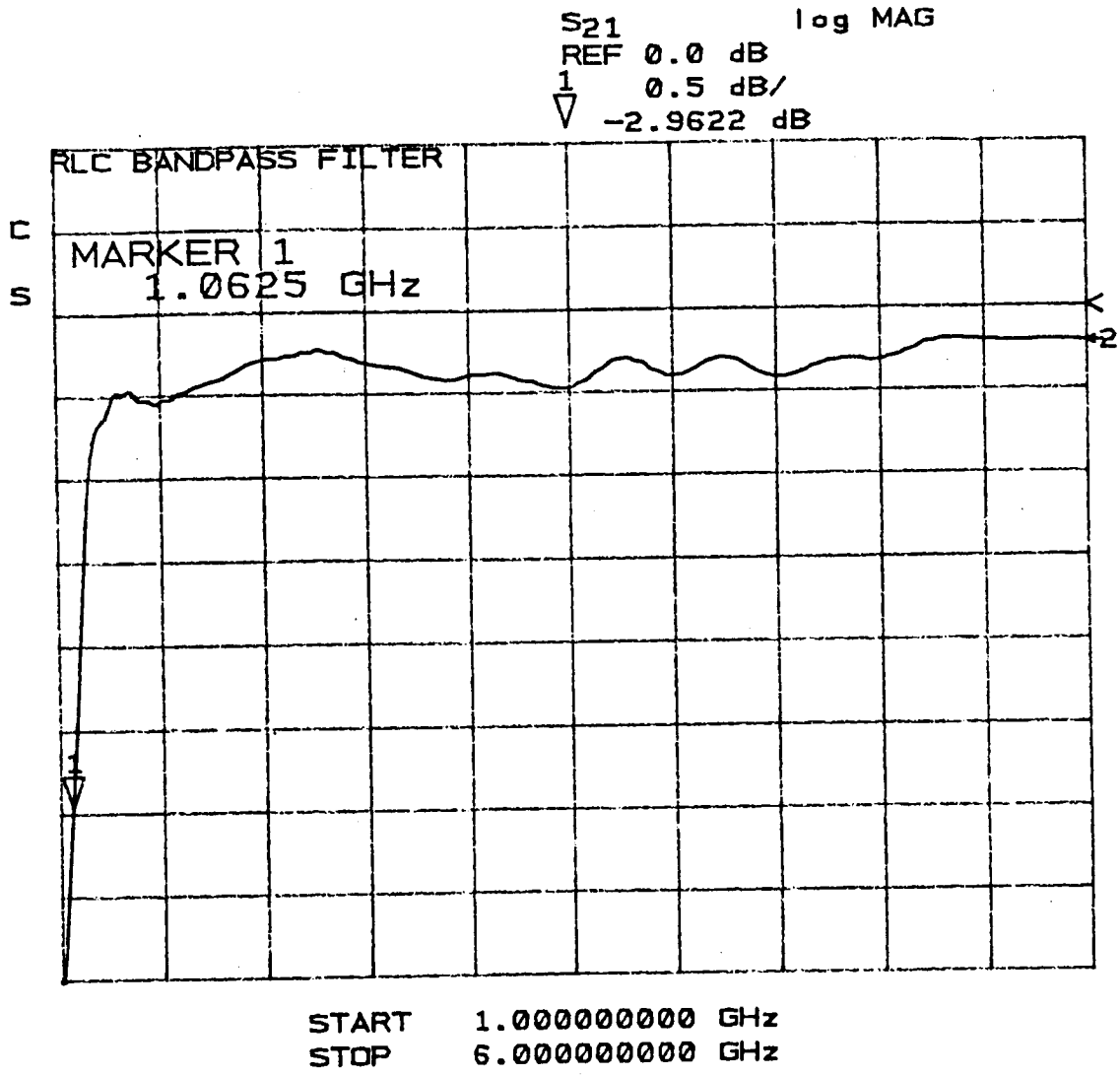

Figure 5.7. Insertion loss of filter which removes PIN switch transients 1-6 GHz.

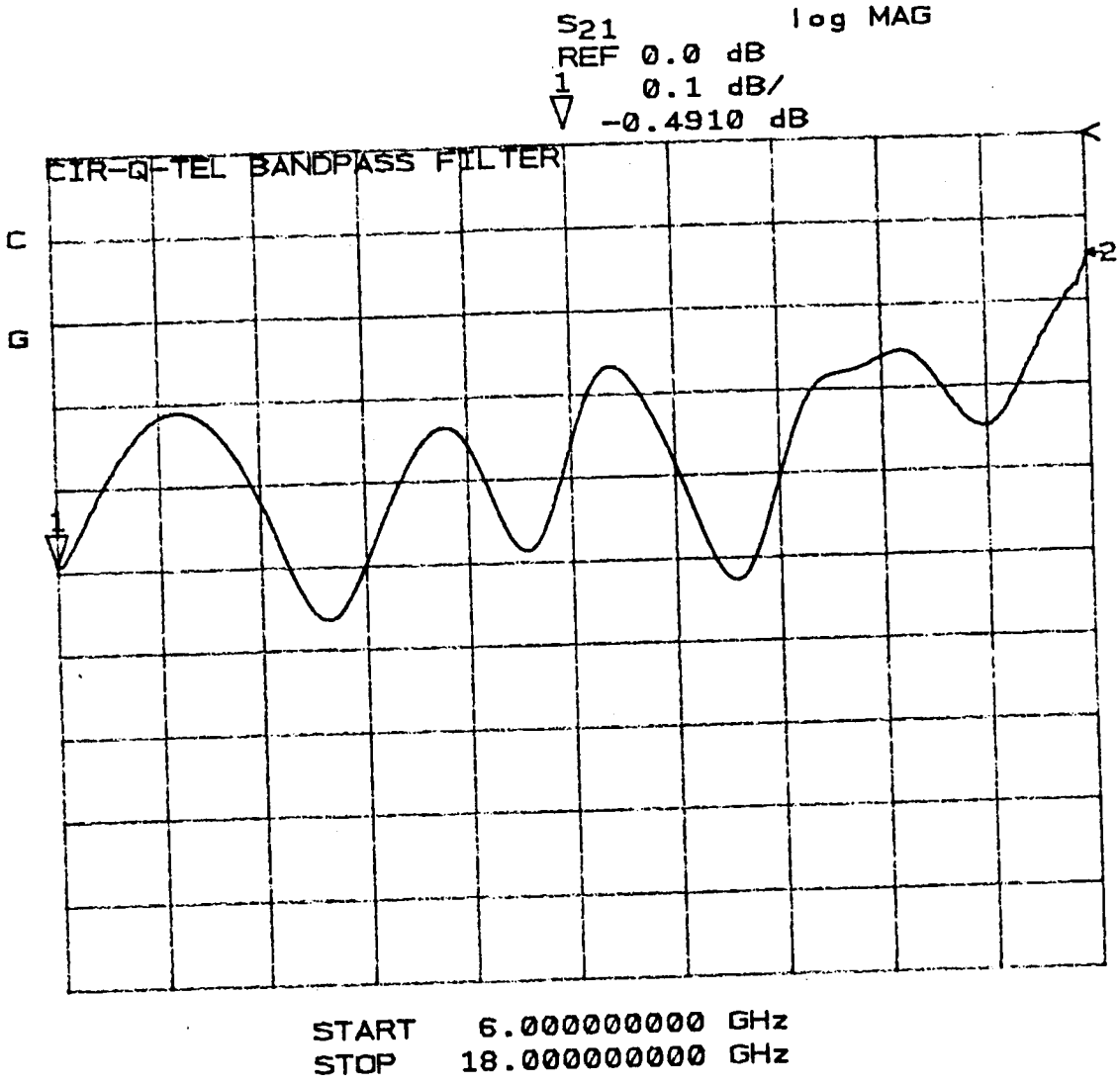

Figure 5.8. Insertion loss of a bandpass filter with lower loss near 18 GHz.

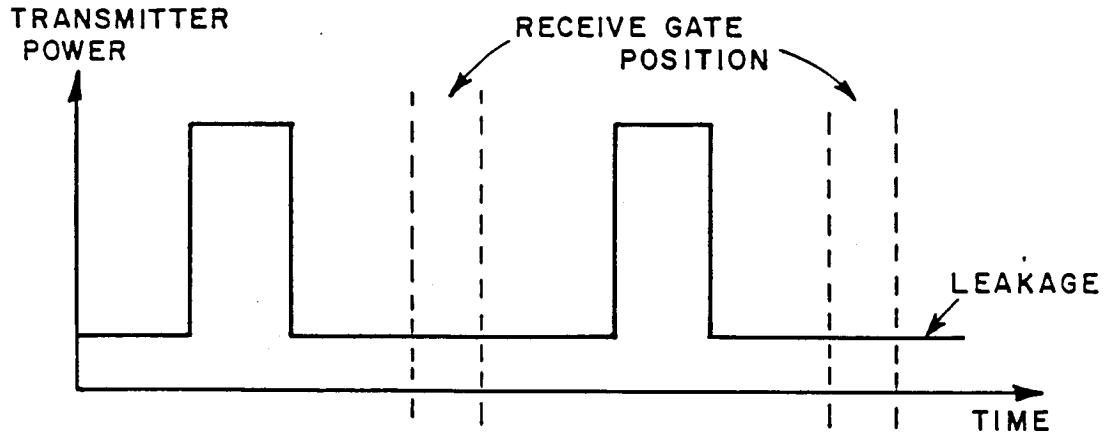

Figure 5.9. Leakage within the transmitter.

needed to keep the leakage below the noise floor of the receiver. Since the PIN switches used have isolation values of 70-130 dB depending on the model, it is evident that two switches are required. One may wonder what would be the best location to place both of these switches within the transmitter. If both switches had been placed before the amplifier, noise from the transmitter amplifiers would have leaked into the receiver as described in Chapter III which is analogous to the situation in Figure 5.9.

If both switches had been placed after the amplifier, an interesting problem would have arisen. Figure 5.10 shows a pulse which has been produced by a single switch located after the 2-6 GHz amplifier. Evidently the switch reacts adversely when it must switch +22 dBm of power. About 15 nsec after the switch closes the oscillations in amplitude cease, and the switch behaves normally. For this reason, one switch is placed before the amplifier to control the

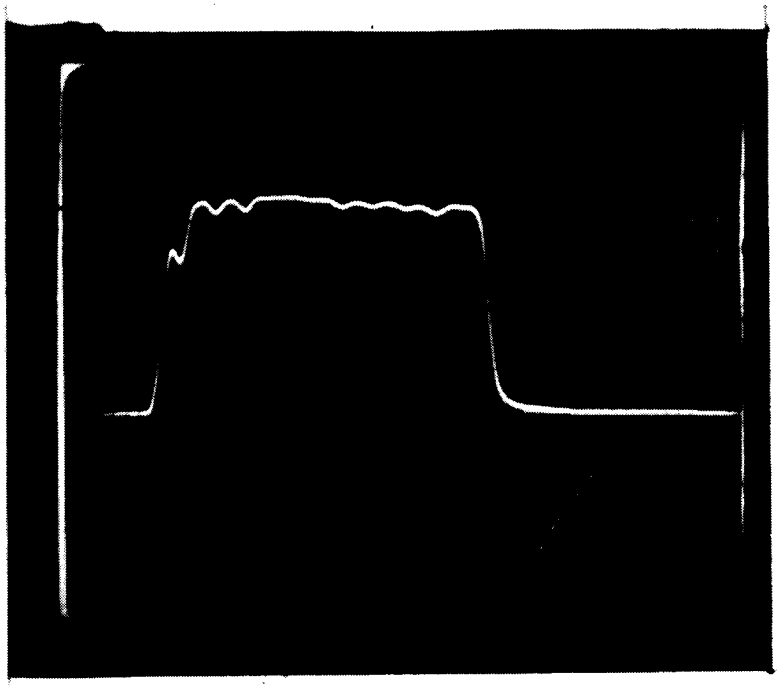

Figure 5.10. One switch after the 2-6 GHz amplifier (10 MV/div vertical, 10 nsec/div horizontal).

pulse width, and a second switch is placed after the amplifier with a wider pulse width which is timed to close ~15 nsec after the pulse from the first switch passes through. This situation is shown in Figure 5.11 for the 2-6 GHz band. The first switch refers to the switch before the amplifier while the second refers to the switch after the amplifier. Figure 5.12 shows the corresponding switching situation for the 6-18 GHz band.

The pulse envelopes shown above may be generated in two different ways. One way is to use a mixer to mix the pulsed/RF signal down to baseband. The test may be done as shown in Figure 5.13. In this case the device under test would be the transmitter circuit between the first bandpass filter and the bandpass filter after the second switch with the

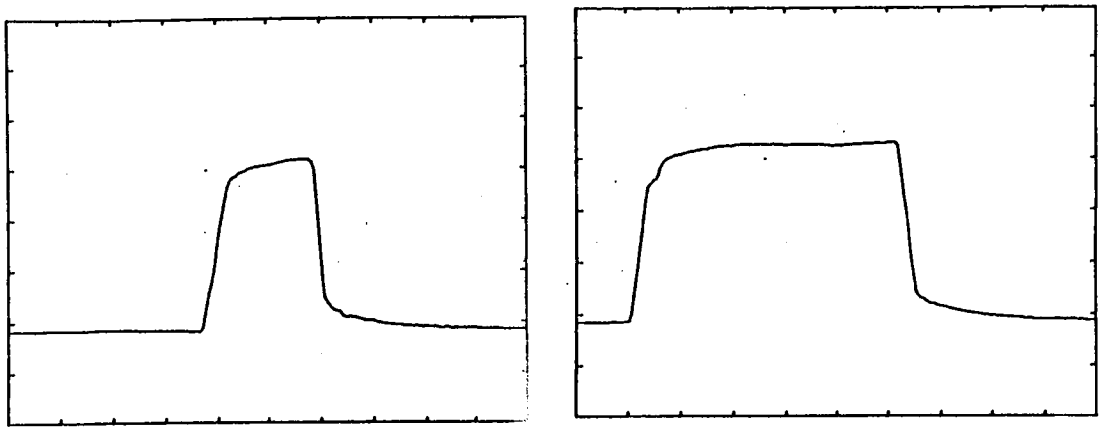

(a) First transmit switch

(b) Second transmit switch

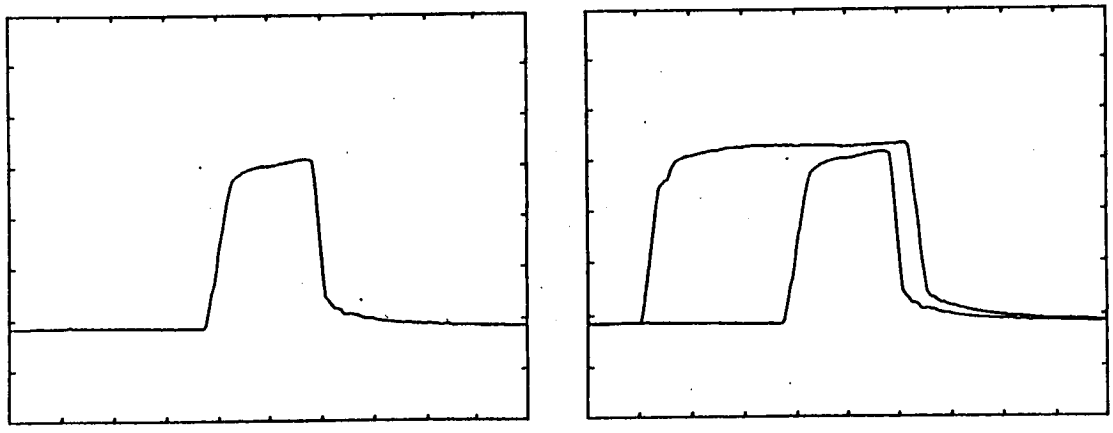

(c) First and second transmit switches.

(d) Relative timing between Figures (b) and (c).

Figure 5.11. Relative timing between switches in the 2-6 GHz band.

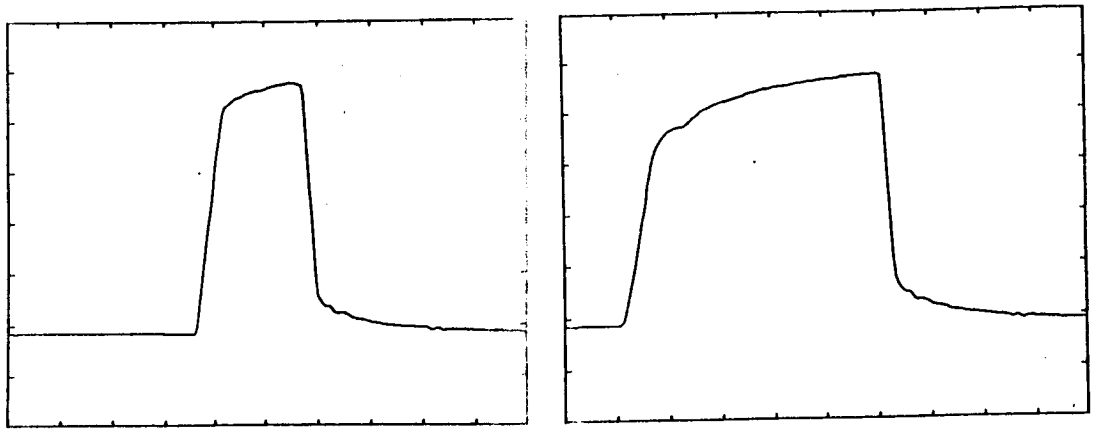

(a) First transmit switch

(b) Second transmit switch

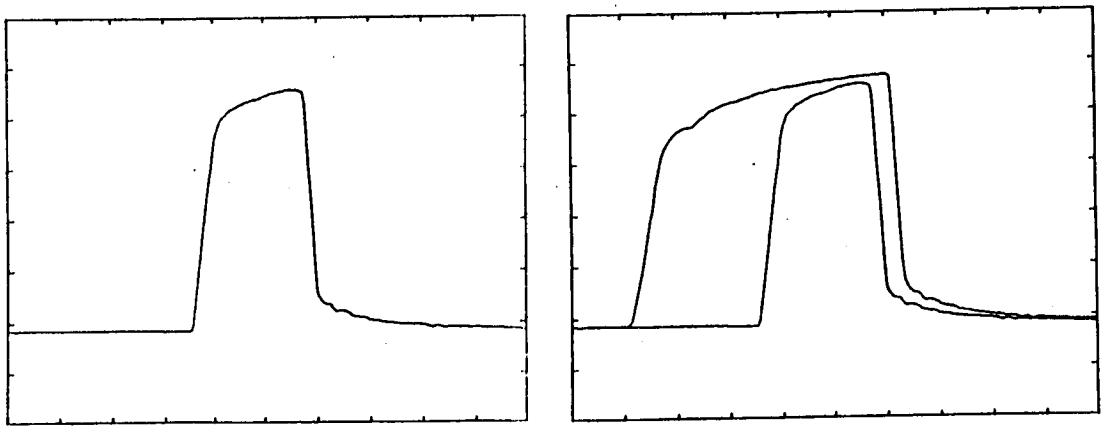

(c) First and second transmit switches.

(d) Relative timing between Figures (c) and (d).

Figure 5.12. Relative timing between switches in the 6-18 GHz band.

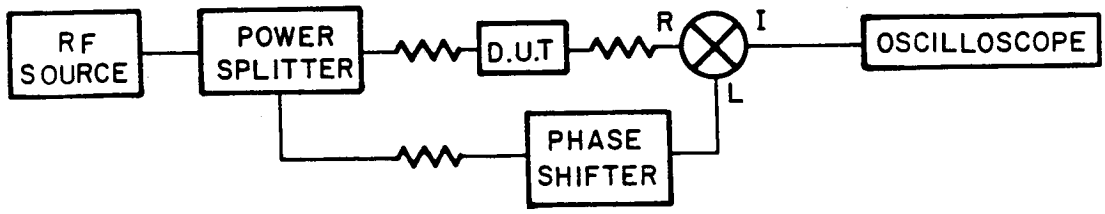

Figure 5.13. Mixer method for observing an RF envelope.

amplifier running at full output. The phase shifter is adjusted to make the two lines between the power splitter and the mixer equal in electrical length so that a maximum output is observed on the oscilloscope. The second method for observing an RF envelope is to simply use a diode detector. Detectors are now available which closely approximate the performance of a mixer, and they have the advantage of permitting the RF source to be swept, while the phase shifter must be adjusted at every frequency in the mixer method. Crystal detectors have been placed on each branch of the transmitter so that only an oscilloscope needs to be added to determine if the transmitter is operating correctly.

Isolators have been placed around the amplifiers to absorb any reflected waves due to impedance mismatches, and one has been placed before the circulator for the same reason. An isolator has also been placed between the circulator and the mixer in the receiver to absorb any LO signal which has leaked into the RF port. Since isolators have a lower VSWR within their specified band of operation than outside, the LO is adjusted to operate 1.8 GHz above the transmit frequency (high-side tuning) in the lower half of the band, e.g., 2-4 GHz, and to operate 1.8 GHz below the transmit frequency (low-side tuning) in the upper half of the band, 4-6 GHz. The same is done in the 6-18 GHz range as well as the 27-36 GHz band. This will minimize the mismatch effects between the mixer and isolator due to LO leakage within the mixer.

Figures 5.14 - 5.23 show typical performance for the components which comprise the transmitter.

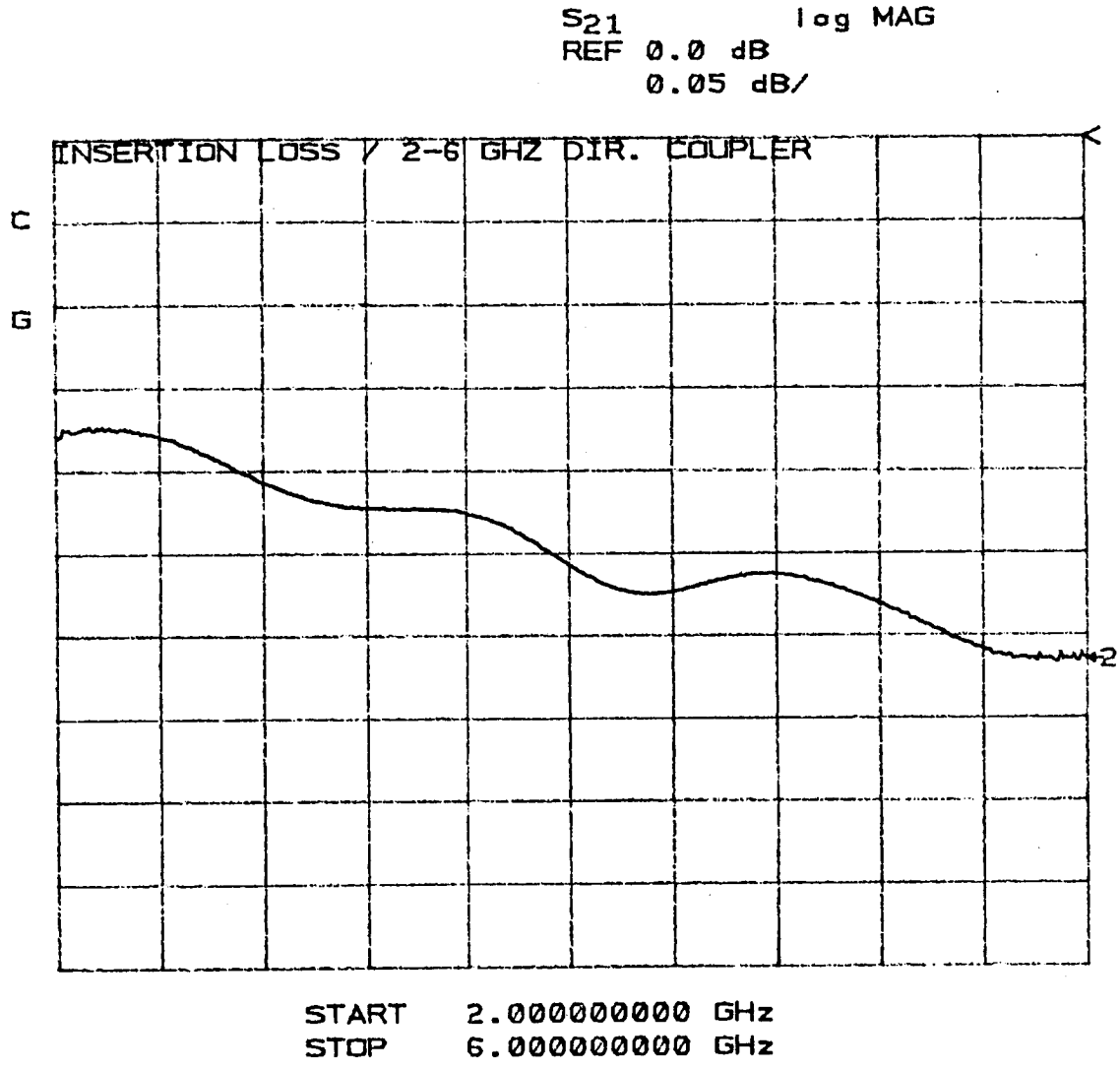

Figure 5.14. Insertion loss of a 2-6 GHz directional coupler.

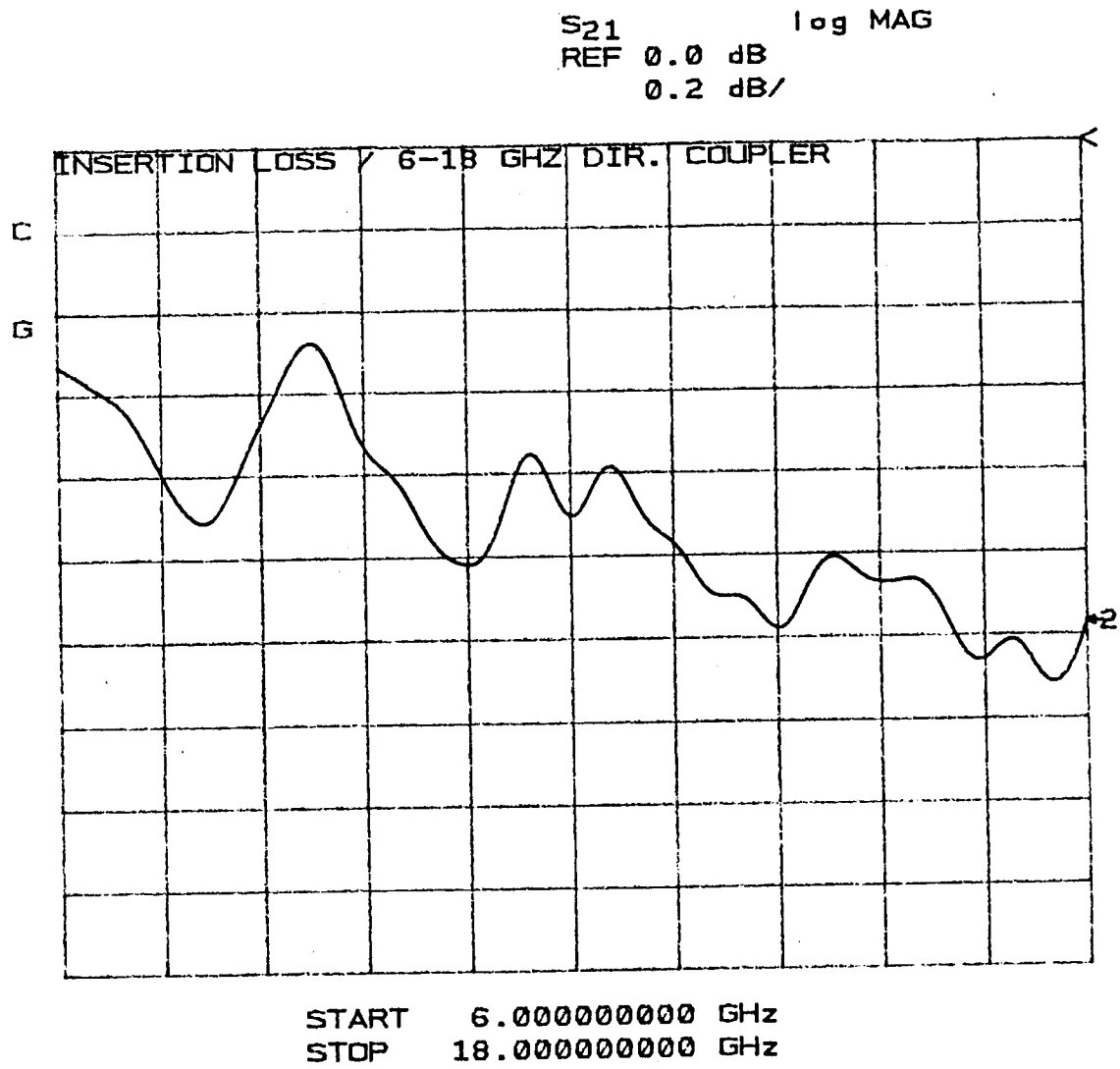

Figure 5.15. Insertion loss of a 6-18 GHz directional coupler.

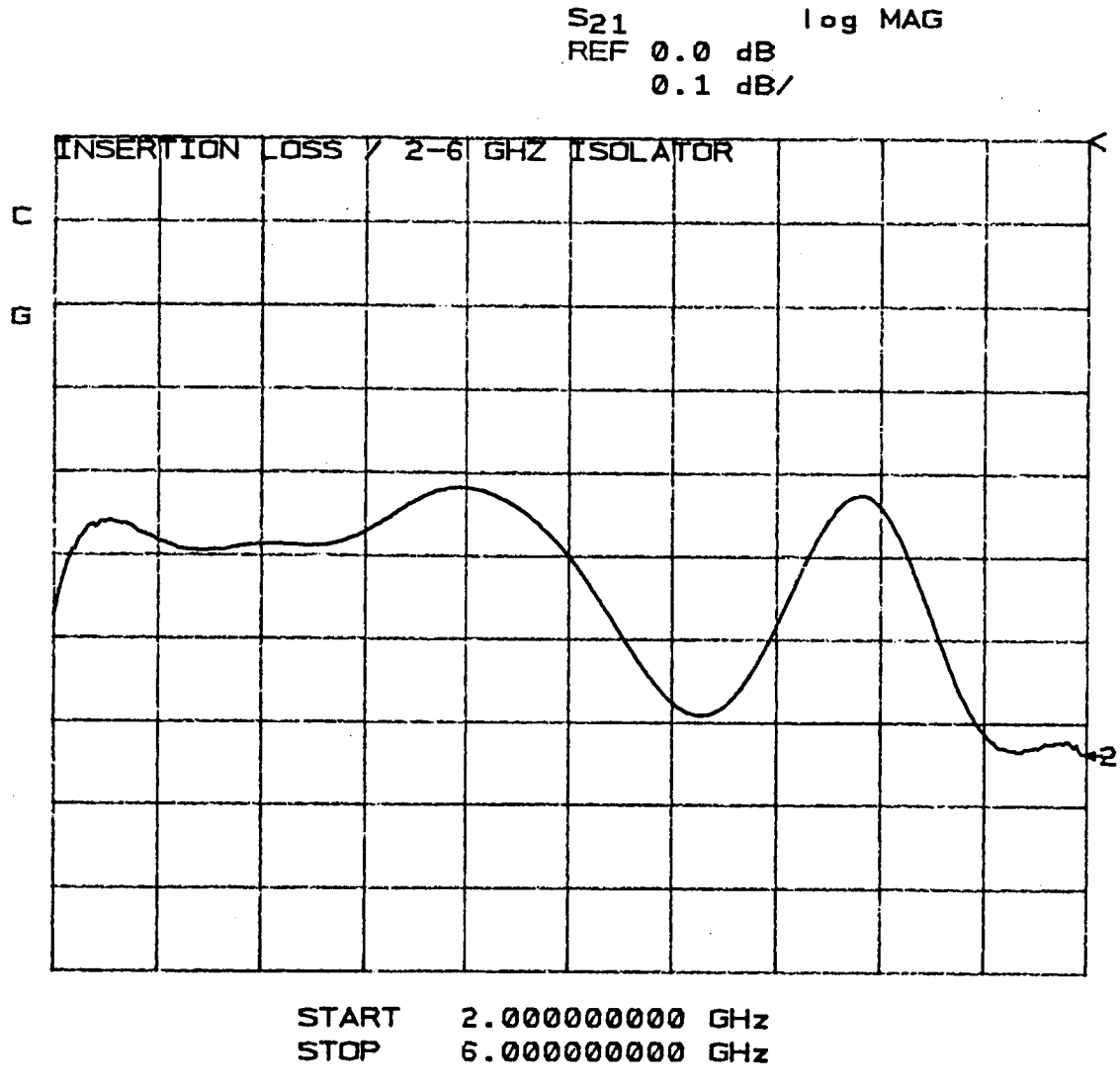

Figure 5.16. Insertion loss of a 2-6 GHz isolator.

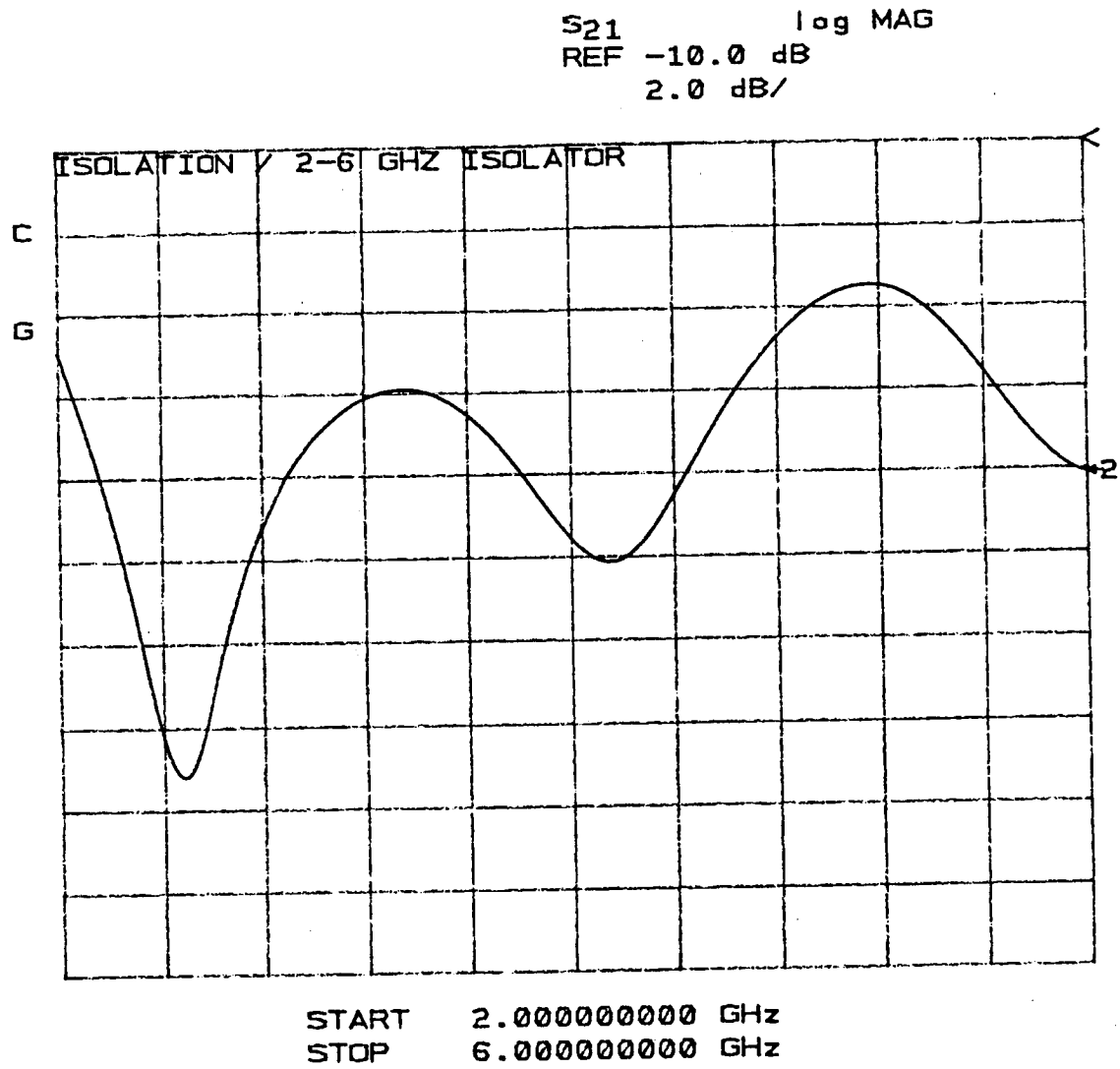

Figure 5.17. Isolation of a 2-6 GHz isolator.

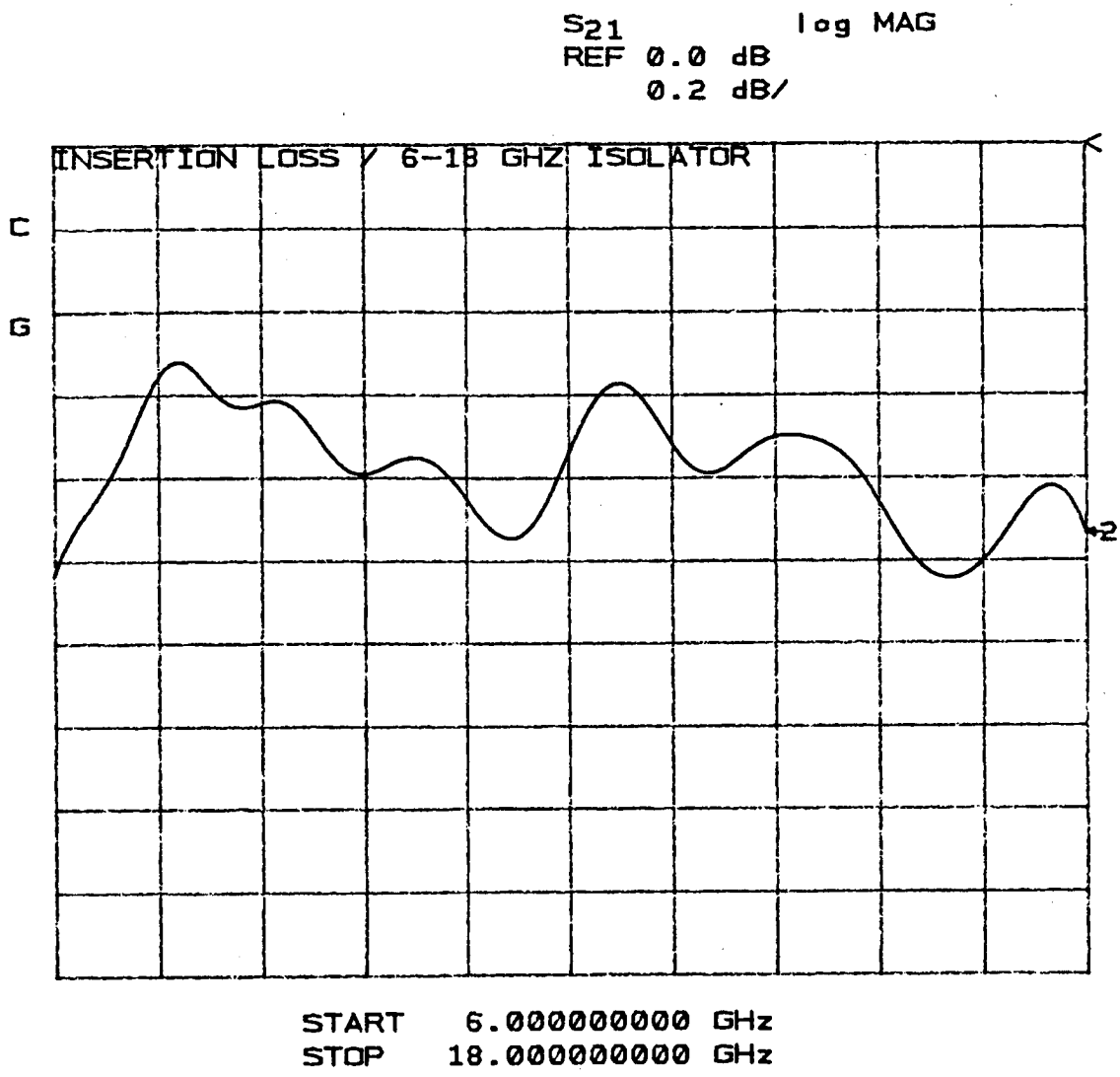

Figure 5.18. Insertion loss of a 6-18 GHz isolator.

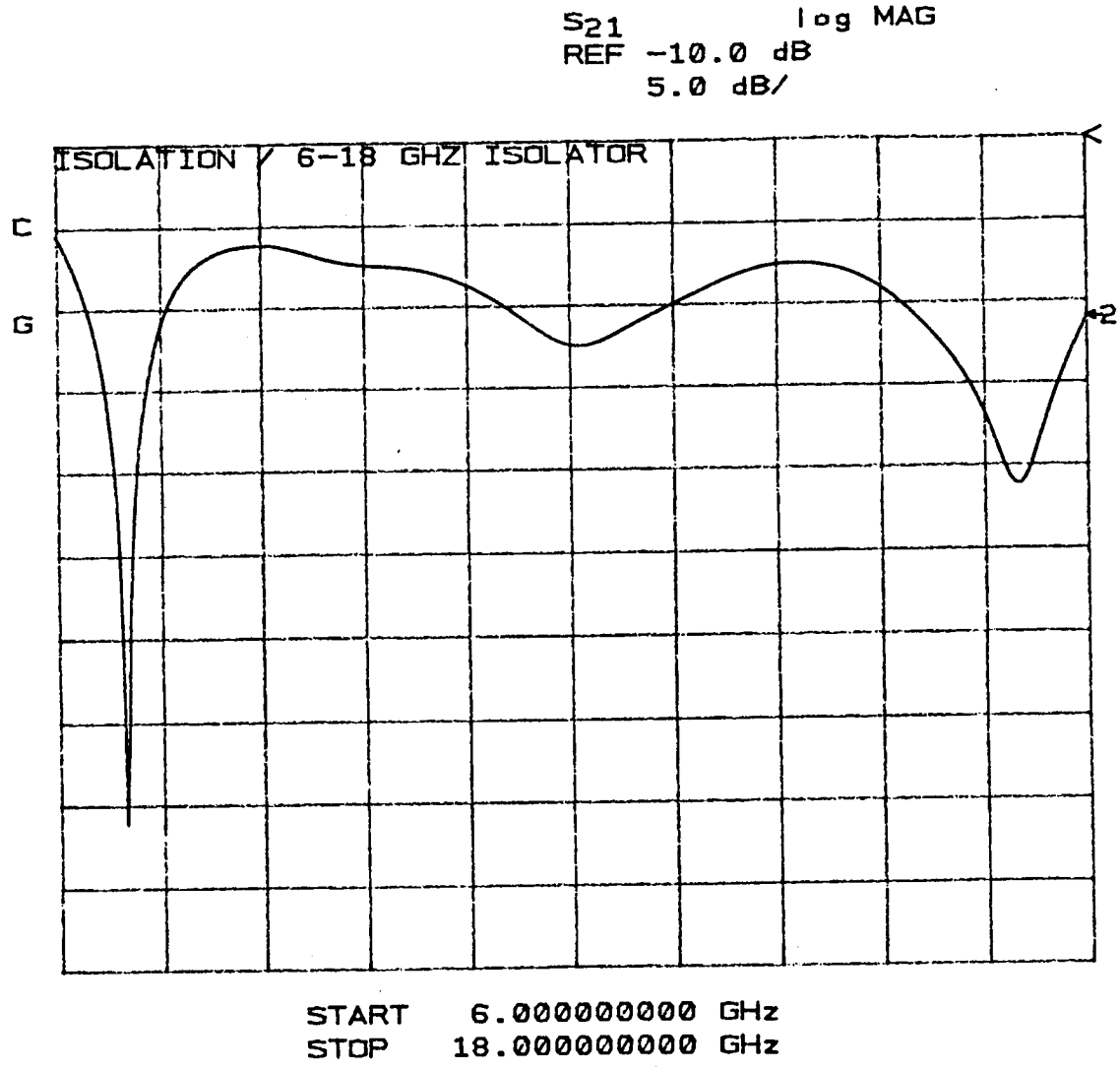

Figure 5.19. Isolation of a 6-18 GHz isolator.

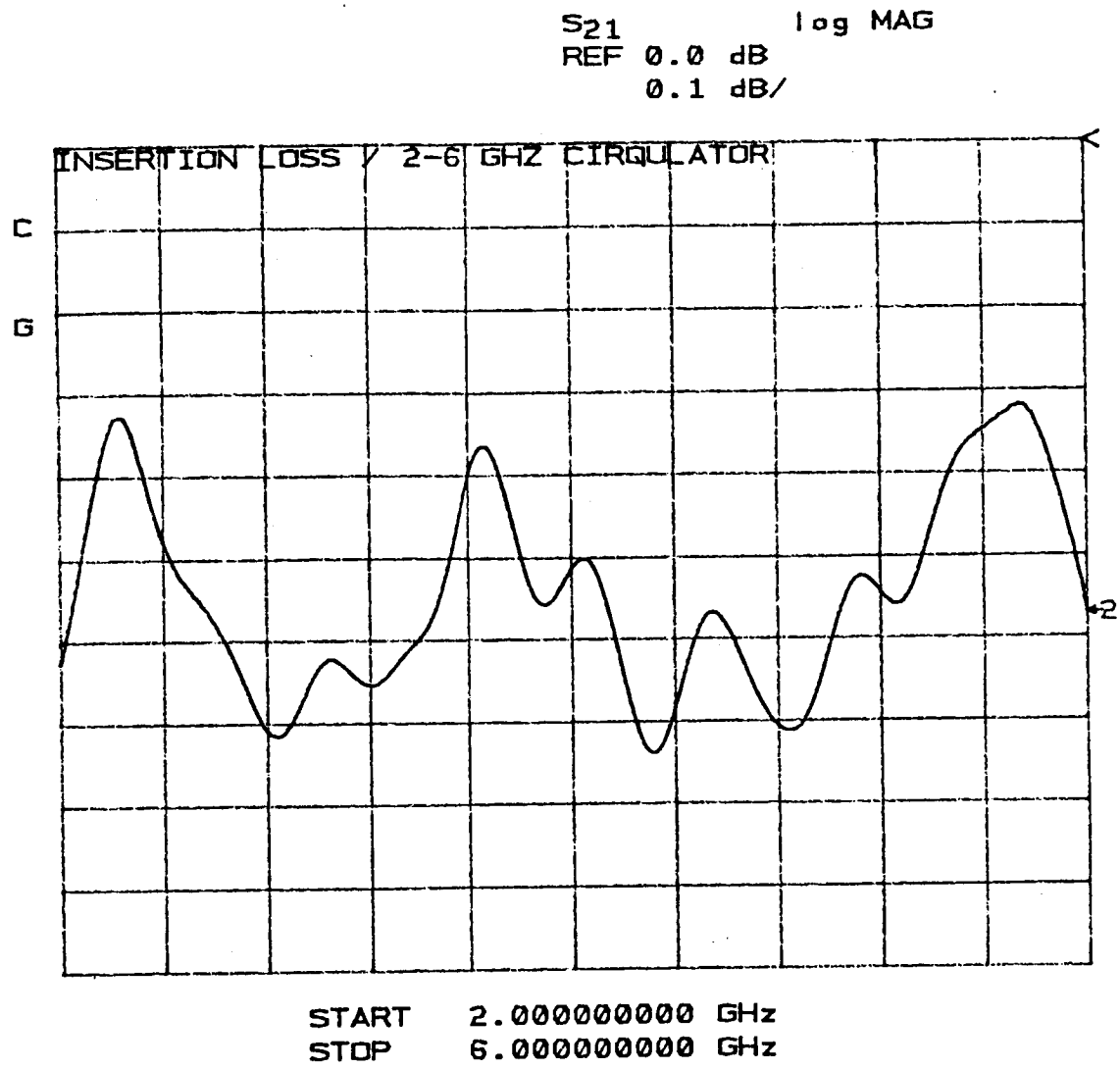

Figure 5.20. Insertion loss of a 2-6 GHz circulator.

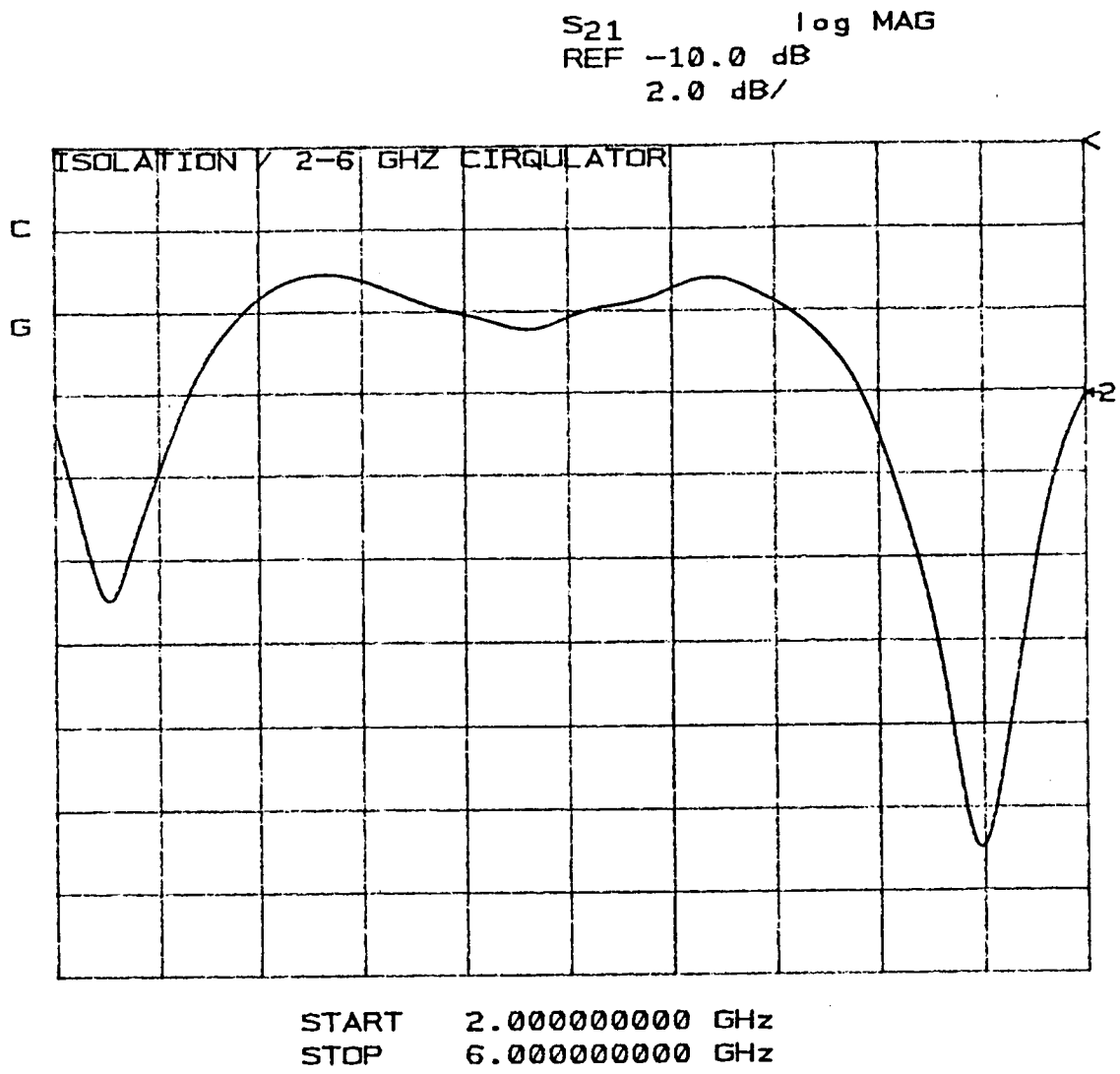

Figure 5.21. Isolation of a 2-6 GHz circulator.

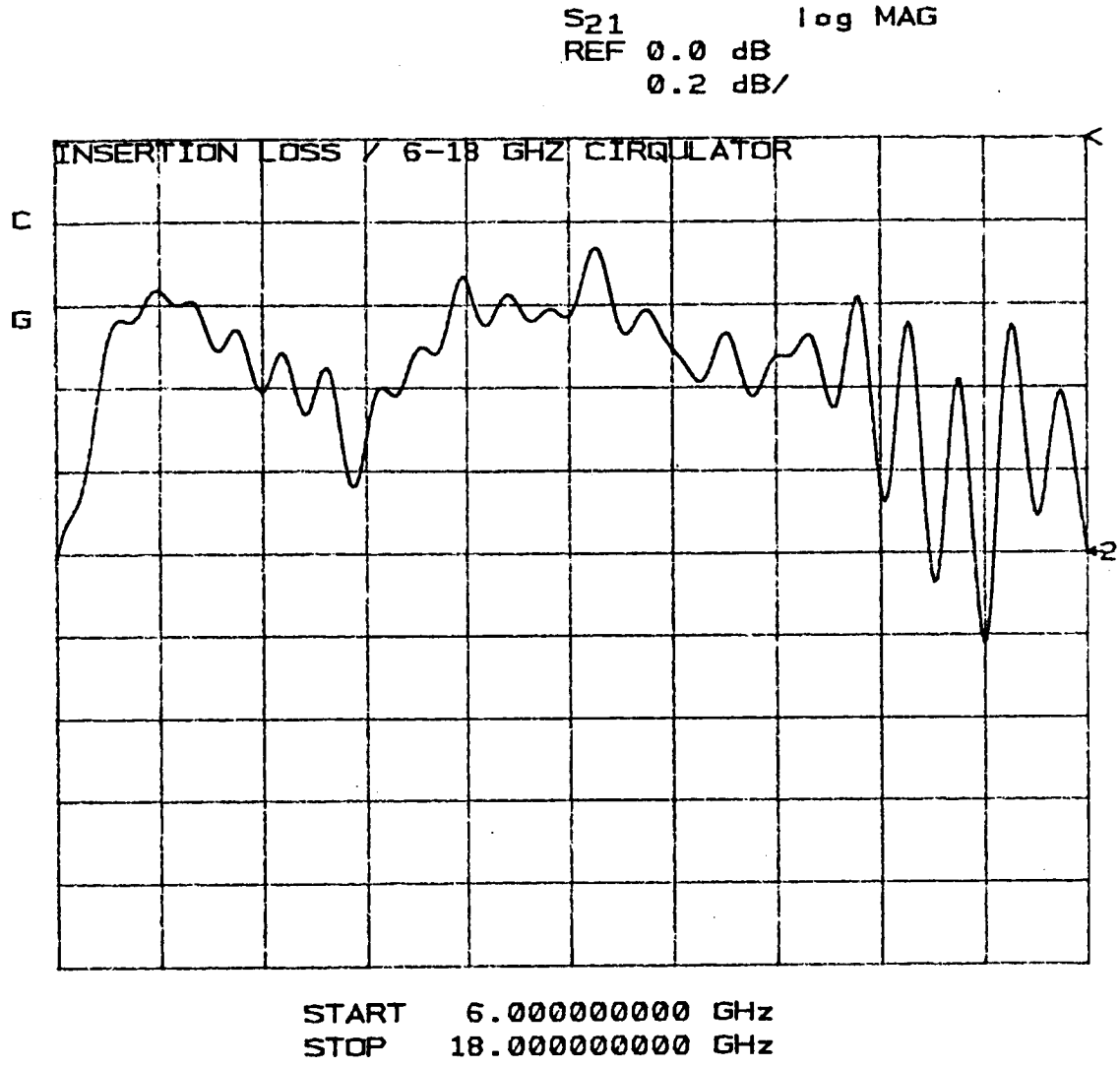

Figure 5.22. Insertion loss of a 6-18 GHz circulator.

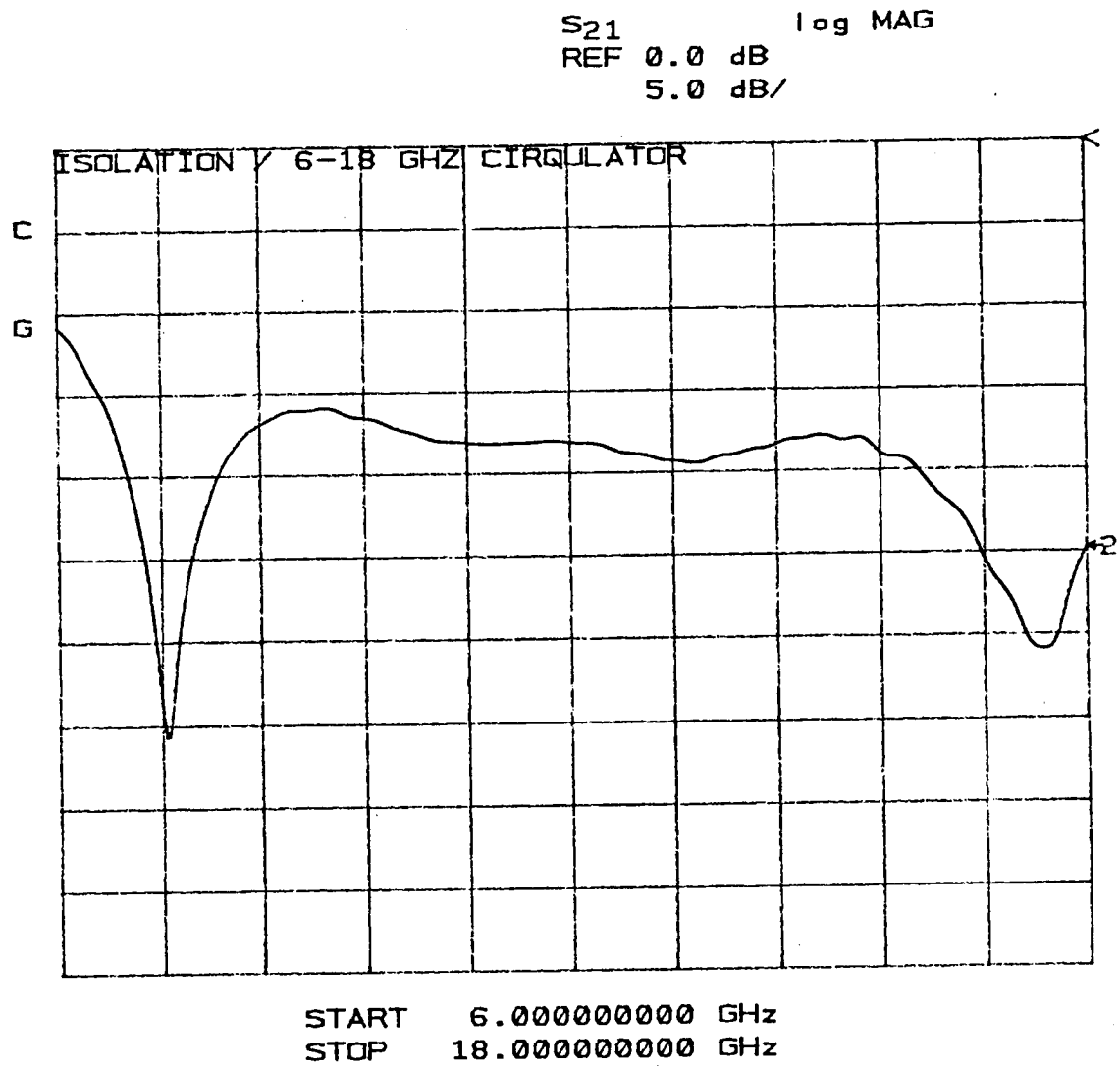

Figure 5.23. Isolation of a 6-18 GHz circulator.

C. THE RECEIVER

The receiver is shown in Figure 5.24; whereas, the signal and noise power calculations for the receiver are shown in Figure 5.25. An advantage of working with a single frequency receiver is that amplifiers with very low noise figures may be used which have relatively narrow bandwidths. It should be noticed in the calculations that the mixer's noise after amplification is roughly equivalent to that of the LNA. The mixer's noise is traced through the system in Figure 5.25 and added to the amplifier's noise at the bottom of the figure. When the noise of the system was actually measured, the noise of the amplifier actually dominated, so it is believed that a noise figure of 8 dB for the mixer is rather pessimistic. The amplifier following the LNA is referred to as a limiting amplifier and has the characteristic of being able to withstand large signal inputs without being damaged. In this case, the gain would merely compress once a given input had been exceeded, and below this input the amplifier is linear. A plot of output power and gain versus input power is shown in Figure 5.26. This type of amplifier characteristic is necessary because large signals may enter the receiver either by placing a large target in the target area or while attempting to adjust the relative timing of the transmit and receive switches.

Referring to Figure 5.1, it should be noticed that a pulse propagating through the transmitter will have some of its energy reflected into the receiver due to an impedance mismatch at the antenna as well as leakage within the circulator. These pulses are only about 15-20 dB below the incident pulse's power level. With 70 dB of gain

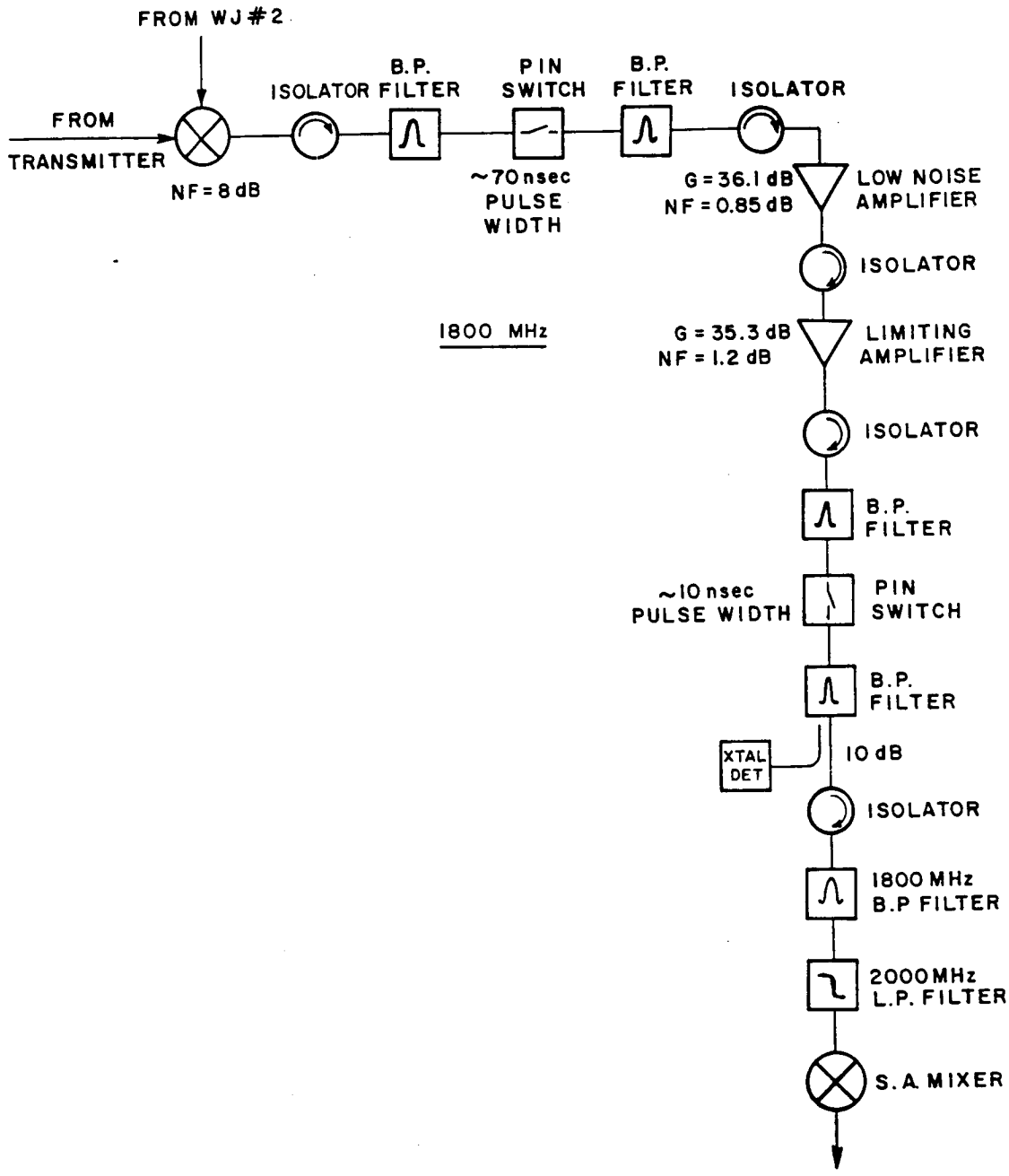

Figure 5.24. Schematic of the pulsed/IF receiver.

	2-6 GHz Signal	6-18 GHz Signal	Mixer Noise	LNA Noise
Receiver input	- 65.6 dBm	- 78.7 dBm		
Mixer	- 8.0 dB	- 8.0 dB	-157.0 dBm	
Isolator	- .3 dB	- .3 dB	- .3 dB	
BP filter	- .3 dB	- .3 dB	- .3 dB	
PIN switch (insertion loss)	- 2.0 dB	- 2.0 dB	- 2.0 dB	
PIN switch (70 nsec) (duty-cycle loss)	----	----	- 4.6 dB	
BP filter	- .3 dB	- .3 dB	- .3 dB	
Isolator	- .3 dB	- .3 dB	- .3 dB	
Low noise amplifier	+ 36.1 dB	+ 36.1 dB	+ 36.1 dB	-127.0 dBm
Isolator	- .3 dB	- .3 dB	- .3 dB	- .3 dB
Limiting Amplifier	+ 35.3 dB	+ 35.3 dB	+ 35.3 dB	+ 35.3 dB
Isolator	- .3 dB	- .3 dB	- .3 dB	- .3 dB
BP filter	- .3 dB	- .3 dB	- .3 dB	- .3 dB
PIN switch (insertion loss)	- 2.0 dB	- 2.0 dB	- 2.0 dB	- 2.0 dB
PIN switch (10 nsec) (duty-cycle loss)	- 6.0 dB	- 6.0 dB	- 8.4 dB	- 13.0 dB
BP filter	- .3 dB	- .3 dB	- .3 dB	- .3 dB
Directional coupler	- .6 dB	- .6 dB	- .6 dB	- .6 dB
Isolator	- .3 dB	- .3 dB	- .3 dB	- .3 dB
1800 MHz BP filter	- 1.4 dB	- 1.4 dB	- 1.4 dB	- 1.4 dB
2000 MHz LP filter	- .3 dB	- .3 dB	- .3 dB	- .3 dB
Output	- 17.2 dBm	- 30.3 dBm	-105.8 dBm	

Figure 5.25. Signal and noise power calculations for the receiver.

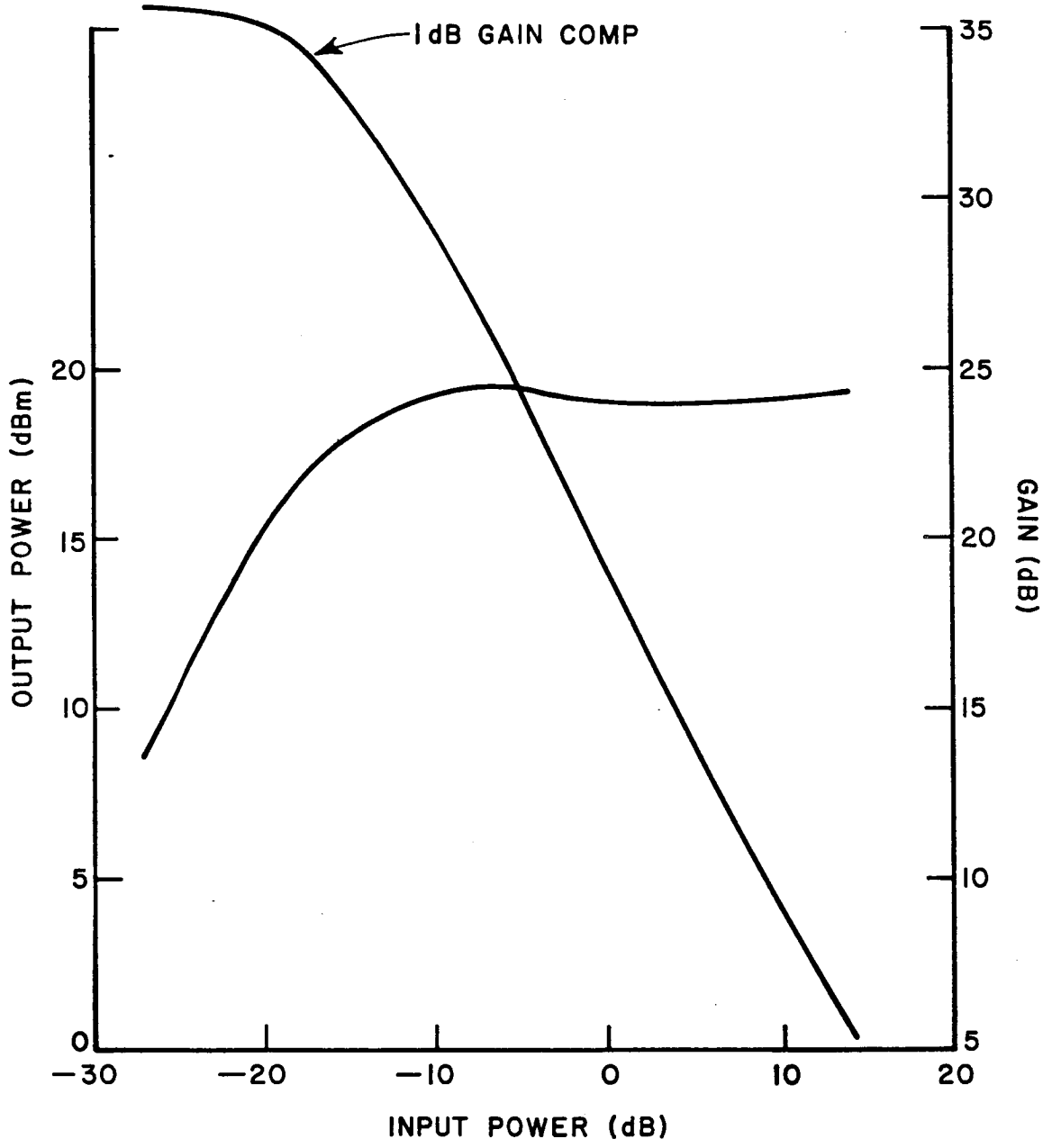

Figure 5.26. Limiting amplifier characteristics at 1800 MHz.

within the receiver and an input of about 0 dBm peak power, the receiver will be heavily saturated. While this signal will not compress the gain of the mixer, that of the low noise amplifier will be compressed by a significant amount, although not enough to damage it. The second amplifier might be permanently damaged by such a large signal if it were not for the use of a limiting amplifier. Unfortunately, the recovery time from saturation for this pair of amplifiers is not short enough to permit an accurate measurement of the target pulse whose leading edge is only about 50 nsec after the trailing edge of the reflected pulse.

A solution to this problem is to place a PIN switch before the low noise amplifier and to time it such that it is open when the reflected pulse enters the receiver and is closed when the target pulse enters. Any reflected energy from the switch will be absorbed by the isolator located immediately after the mixer. A second switch located after the limiting amplifier guarantees good isolation from unwanted signals. Referring to Figure 5.26, the maximum output of the limiting amplifier is +19 dBm, and the minimum signal detectable by the receiver is -122 dBm, so ~140 dB of switch isolation is required. Another problem with using one switch is that some switches "bounce" which can permit passage of unwanted signals. This phenomenon is shown in Figure 5.27. The bounce is very sensitive to pulse width and tends to be prominent in some switches and absent in others. For these reasons, a second switch was added to the receiver, and good results have been obtained with this arrangement. Using two switches in the transmitter also cures any switch bounce problems, which may be viewed as another form of leakage.

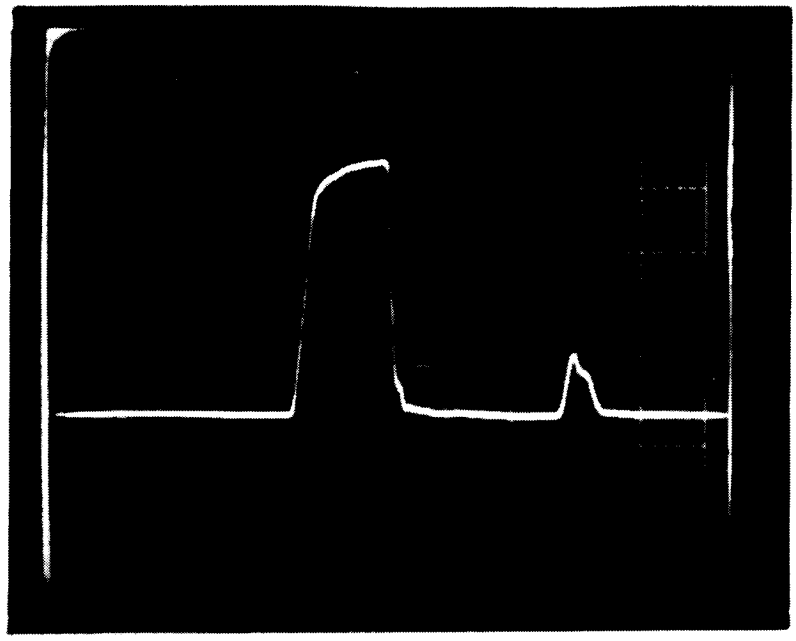

Figure 5.27. PIN switch bounce.
(20 mV/div vertical, 20 nsec/div horizontal)

A bandpass filter with a center of frequency of 1800 MHz is present to select the Fourier component of the pulsed target return with that frequency and to reject any LO signal from the SA mixer. A crystal detector is placed after the second switch so that the switches in the receiver may be easily aligned with the transmitter.

Figures 5.28(a) through (e) show the relative timing between the two switches in the receiver. The transients caused by the closing and opening of the first switch may, after significant amplification, enter the gate of the second switch, so the first switch's pulse width is made sufficiently large to keep this from happening without permitting the

passage of any part of the reflected pulse from the antenna/circulator. The transients shown in Figure 5.28(a) have been measured with no signal input to the receiver; the remainder have been measured with an input signal present. As discussed in Chapter IV, some sensitivity is sacrificed so that clutter may be reduced by narrowing the pulse width of the second switch to 10 nsec. The duty cycle loss associated with this change (-6 dB) is more than offset by the increase in gain over the old system. Figures 5-29 - 5.33 are plots of component behavior for the IF receiver.

With the added sensitivity of the receiver, it is now very important to understand which components approach their maximum input first as the target's cross section increases. Figure 5.34 indicates the maximum input power for the components in the receiver which are power sensitive. The peak power present at each input for a 0 dBsm target is also given as well as the size of target required to make the two values equal.* Note that the SA receiver saturates well before any of the other components, and it does so for relatively small targets. For this reason a 20 dB attenuator is placed at the input to the SA mixer so that a -18 dBsm target may now be measured. This is the approximate RCS for a six inch sphere which is used to calibrate the data, and this attenuation gives good performance for many targets. For larger targets more attenuation may be added as required.

---

* Recall that in finding peak power values, only 10 dB is added to the original SA values since most of the Fourier components have been removed by the bandpass filter.

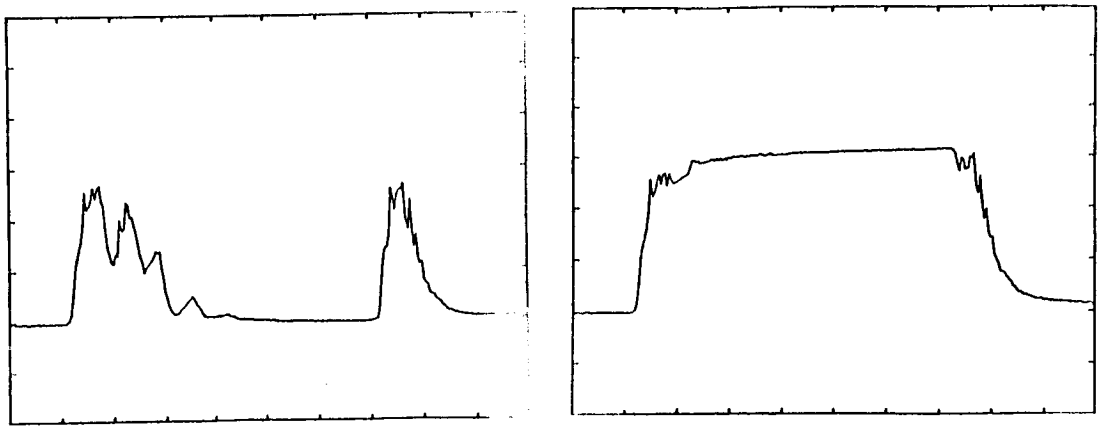

(a) transients of first switch

(b) first switch only

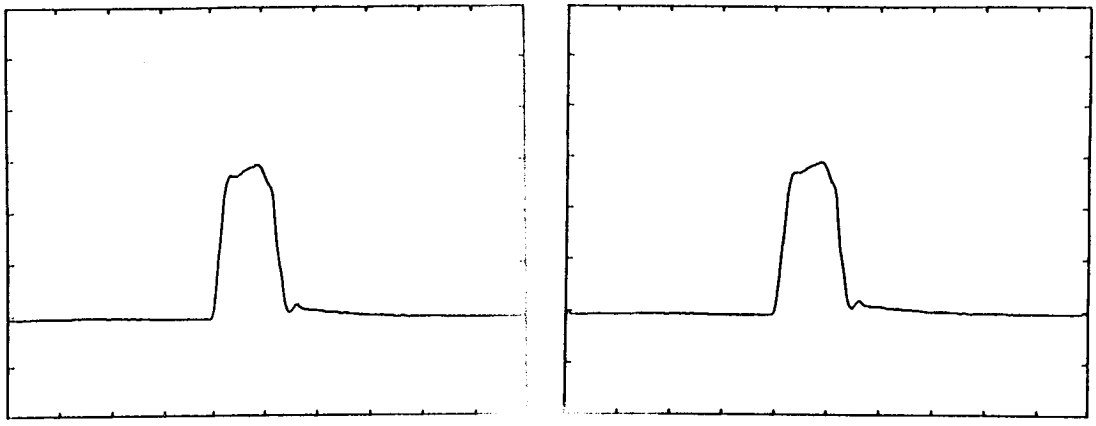

(c) second switch only

(d) first and second switch

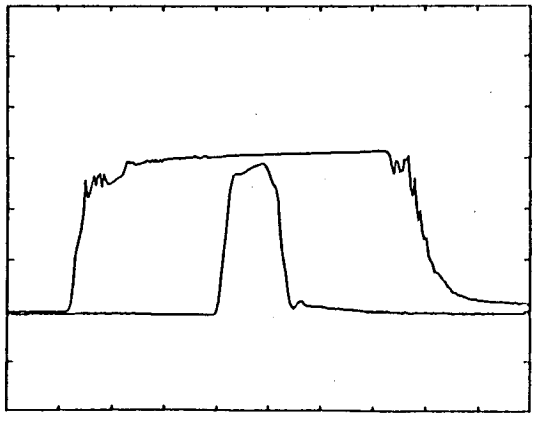

(e) a and d superimposed

Figure 5.28. Relative timing between switches within the receiver.

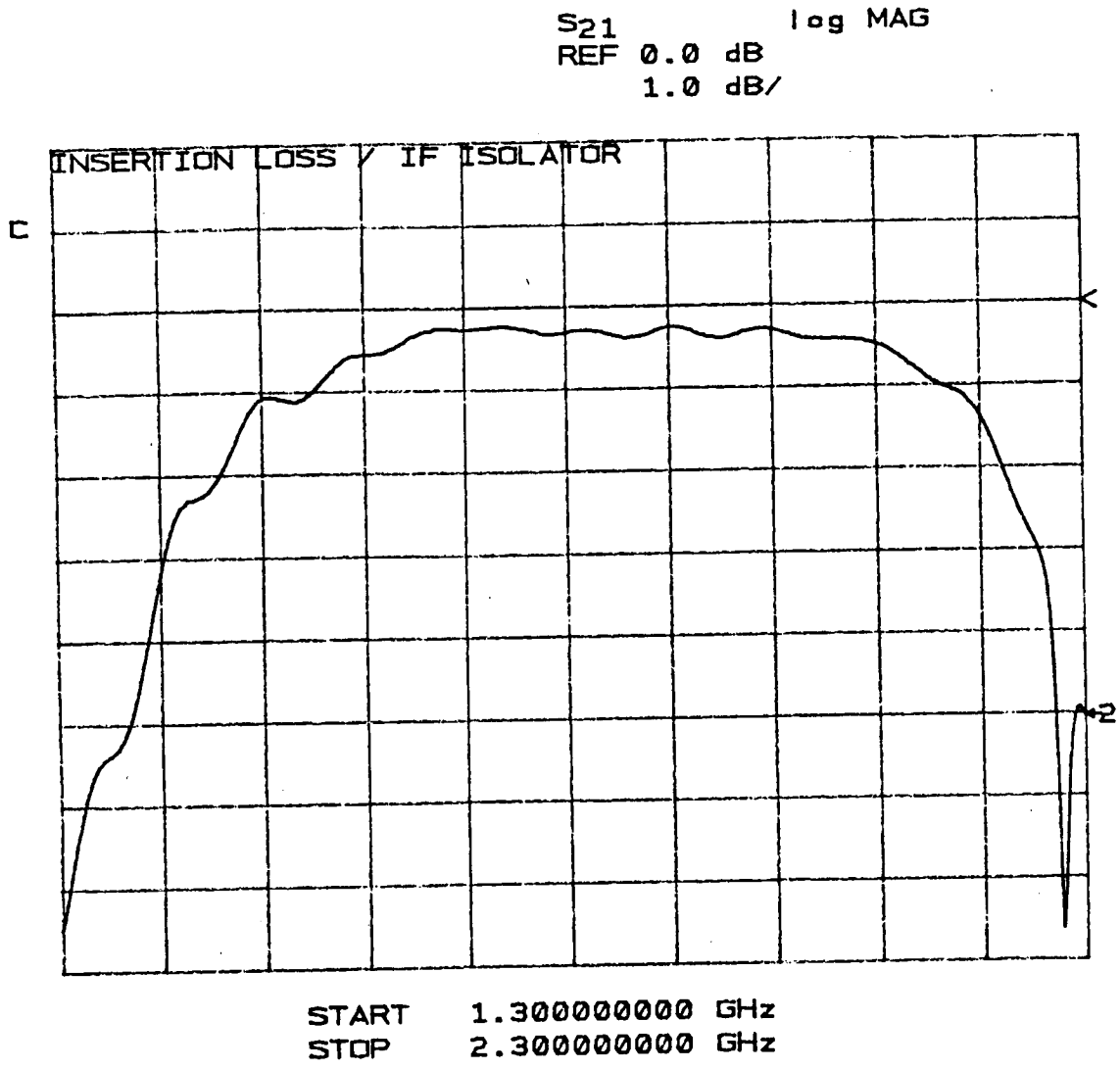

Figure 5.29. Insertion loss of an IF isolator.

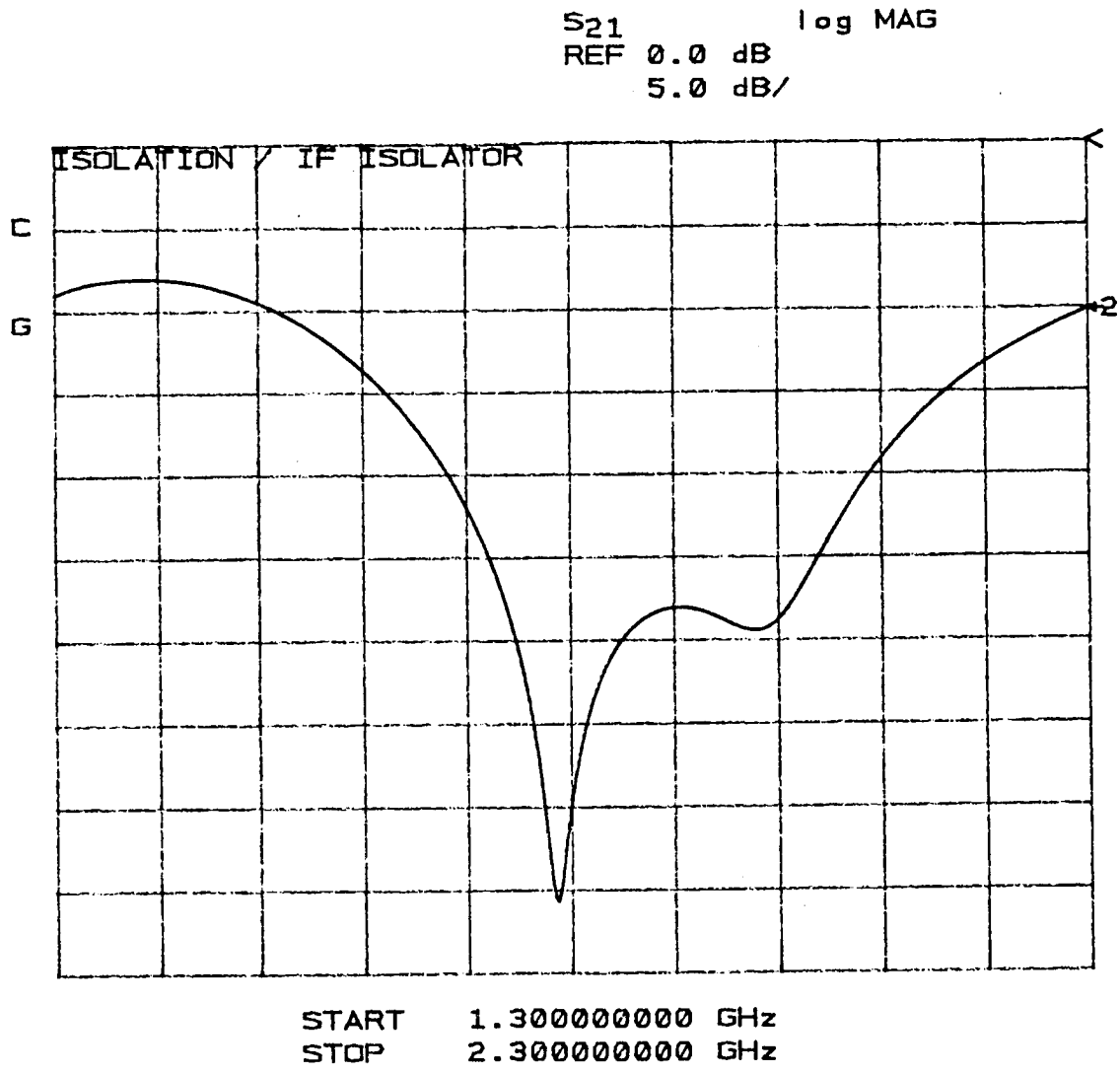

Figure 5.30. Isolation of an IF isolator.

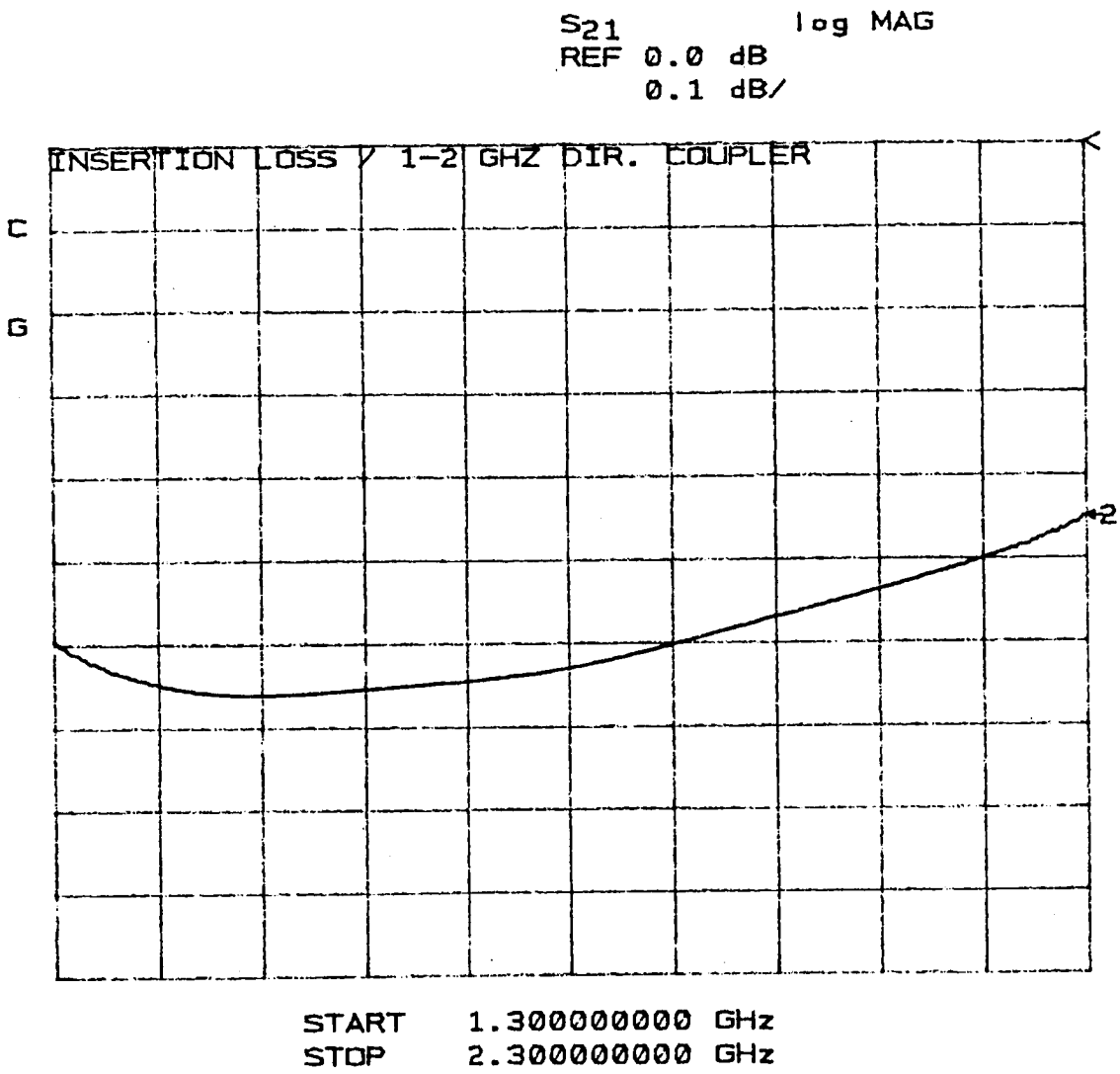

Figure 5.31. Insertion loss of a 1-2 GHz directional coupler.

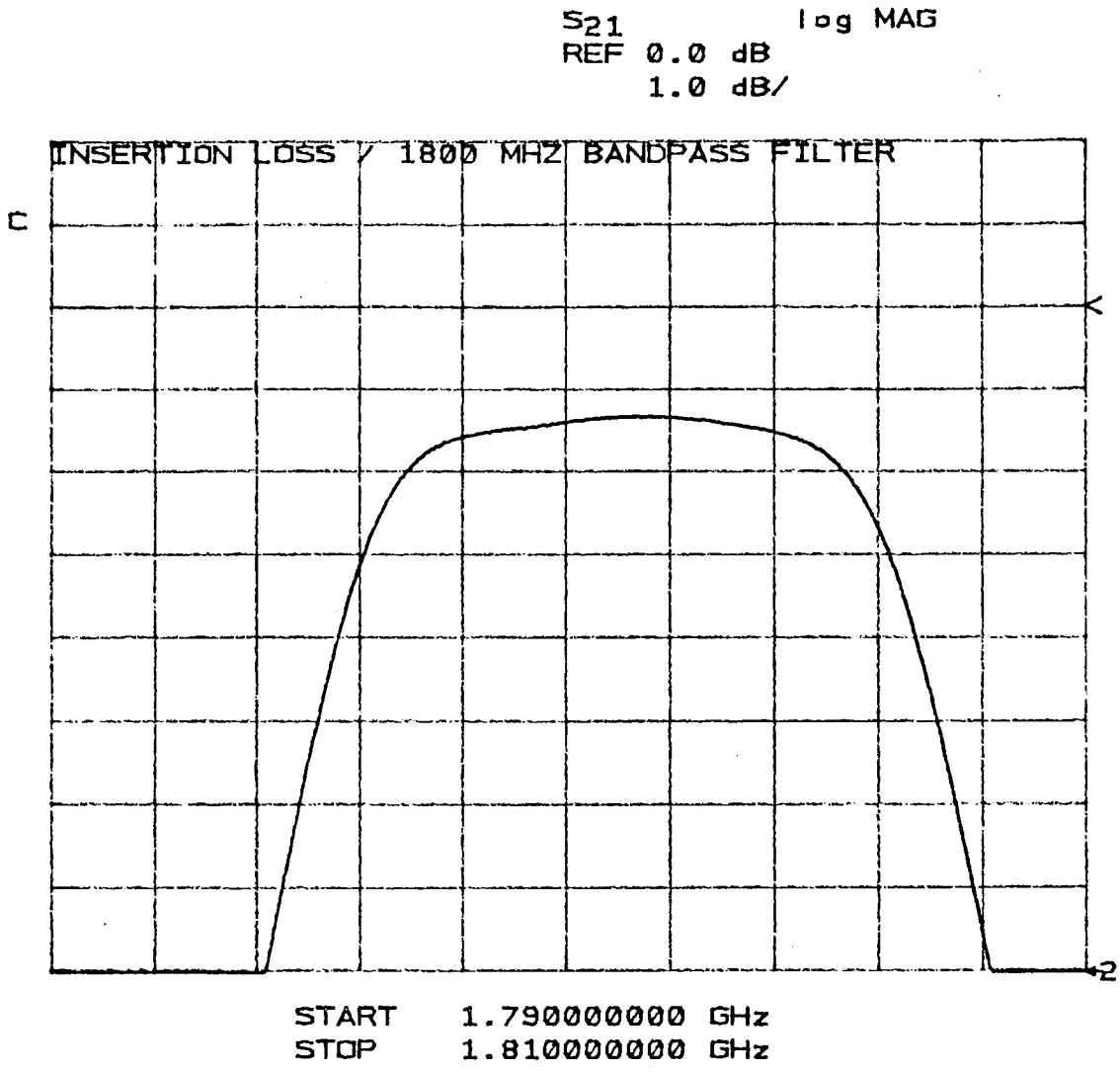

Figure 5.32. Insertion loss of an 1800 MHz bandpass filter.

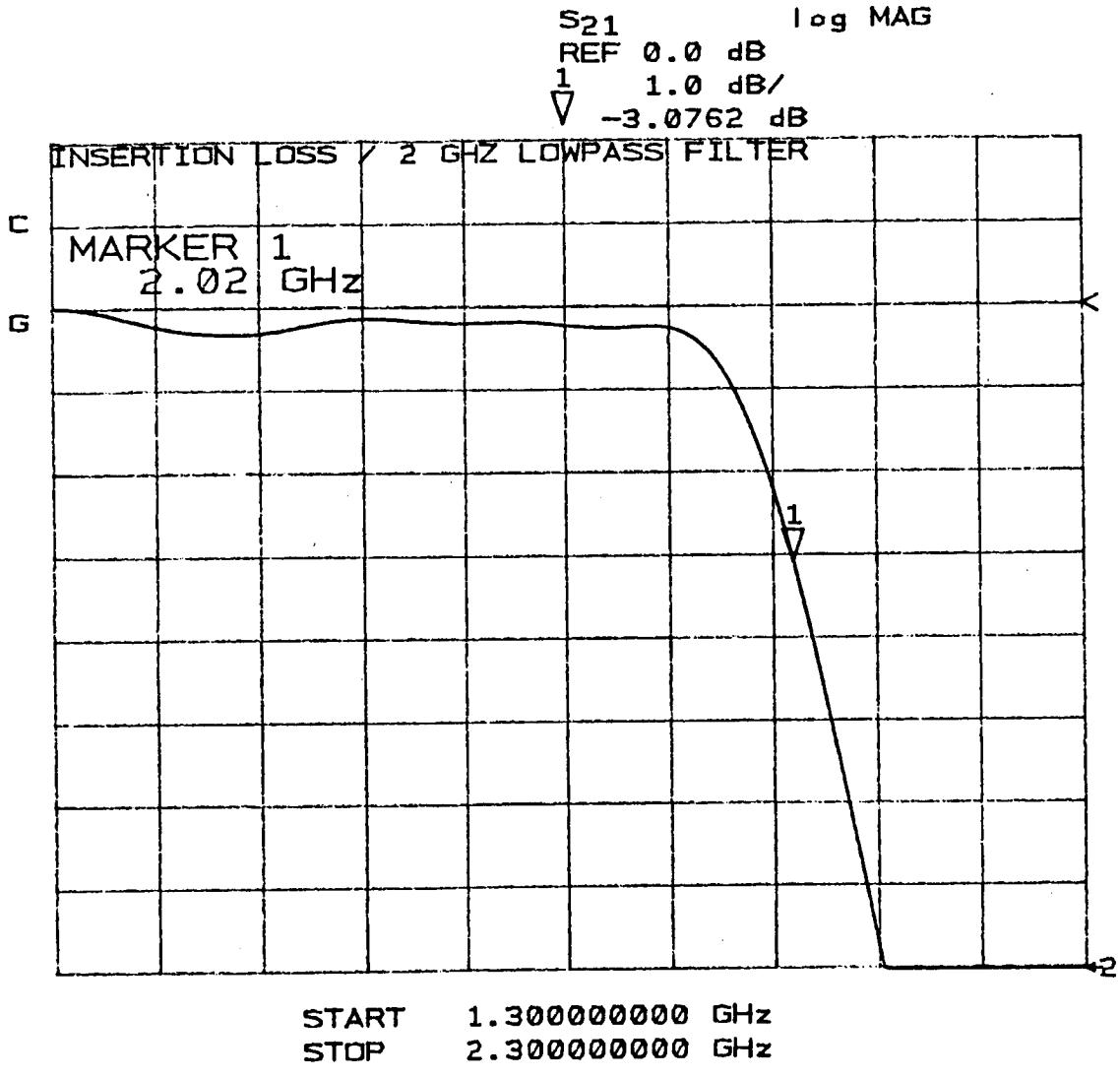

Figure 5.33. Insertion loss of a 2 GHz lowpass filter.

	MAX INPUT (dBm)	Peak Power for 0 dBsm target (dBm)		Max Target Size (dBsm)	
		2-6 GHz	6-18 GHz	2-6 GHz	6-18 GHz
Mixer	0	-45.6	-58.7	45.6	58.7
Low Noise amp	-22	-56.8	-69.9	34.8	47.9
Limiting amp	-18	-21.0	-34.1	3.0	16.1
SA receiver	-30	- 7.2	-20.3	-22.8	- 9.7

Figure 5.34. Maximum target size for 2-18 GHz band.

D. THE KA-BAND SYSTEM

Figures 5.35(a) and (b) show a schematic for the Ka-band system as well as the corresponding signal and noise powers. It is immediately apparent that this system is much simpler than that of the old system. Utilizing a common receiver has eliminated redundancy and substantially reduced costs. Any additional bands which are desired may be added in a similar manner. This system operates in a manner analogous to the 2-18 GHz system with the exception that the mixer, circulator, and isolators operate within the Ka-band. For this reason, the calculations for the IF receiver have been taken from Figure 5.25, and the appropriate duty cycle losses have been considered. As before, the mixer noise and amplifier noise are roughly equal, so their contributions at the output of the receiver are added. The mixer is the only component shown which may become saturated, and this occurs only for very large targets when other components within the IF receiver have already saturated. Figure 5.36 shows the smallest RCS which will saturate the SA receiver. With the addition of a 20 dB attenuator before the SA mixer, the maximum target size is +16.5 dBsm. Figure 5.37 gives a summary of the largest targets measurable as well as those cross sections which result in a return signal power equal to the noise floor of the system. The first column is formed by taking the maximum target sizes in Figures 5.34 and 5.36 and adding 20 dB. The second column is formed by taking the difference between the noise floor (-122 dBm with the 20 dB attenuator) and the 0 dBsm target signal level and adding 20 dB.

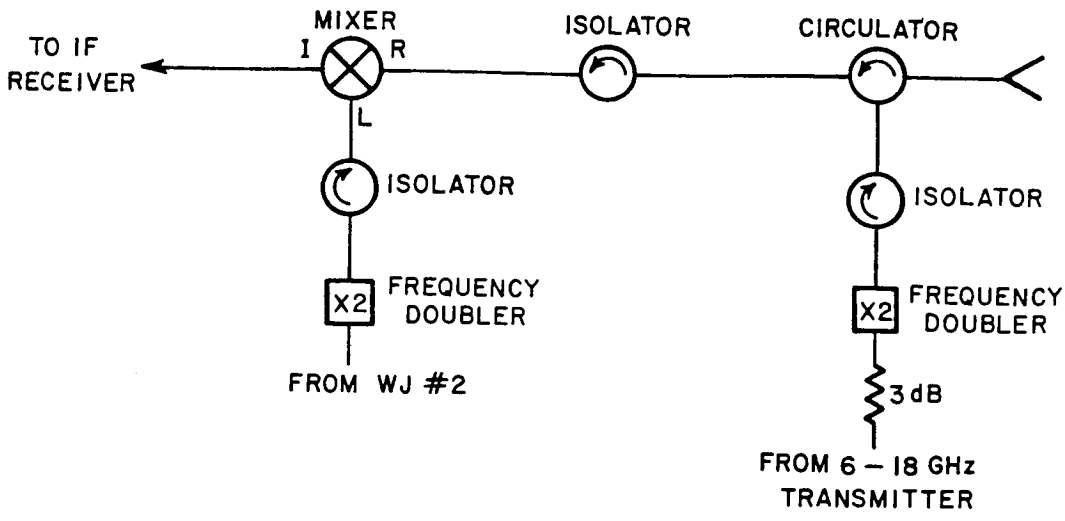

(a) schematic diagram

	Signal	Noise	
		Mixer	Amplifier
Input	- 6.3 dBm		
Attenuator	- 3 dB		
Frequency doubler	-10 dB		
Isolator	- 1 dB		
Circulator	- .2 dB		
Scattering (0 dBsm target)	-66.2 dB		
Circulator	- .2 dB		
Isolator	- 1 dB		
Mixer	- 5 dB	-158 dBm	
IF Receiver	+56.4 dB	+ 49.4 dB	-110.5 dBm
OUTPUT	-36.5 dBm	-106.5 dBm	

(b) signal and noise calculations

Figure 5.35. The Ka-band system.

	Max Input (dBm)	Peak Power for 0 dBsm target (dBm)	Max Target size (dBsm)
SA receiver	-30	-26.5	-3.5

Figure 5.36. Maximum target size for the Ka-band system.

	Max RCS (dBsm)	Min RCS (dBsm)
2-6 GHz	- 2.8	-84.8
6-18 GHz	+10.3	-71.7
Ka-band	+16.5	-65.5

Figure 5.37. Summary of maximum and minimum radar cross sections for the new system with a 20 dB attenuator at the SA receiver input.

Figure 5.37 may be directly compared with Figure 3.19 which shows the coresponding values for the old system. Clearly, sensitivity has been improved for all bands. It should be noticed that the difference between columns one and two (dynamic range) is equal to 82 dB for all bands in Figure 5.37, while in Figure 3.19 the dynamic range for the Ka-band system is only 63.1 dB. This is the case because the noise floor in the old system is dominated by the RF amplifiers and not by the SA receiver. For the other bands 82 dB is the maximum dynamic range, and this is true because the dynamic range of the system must be 10 dB less than the dynamic range of the SA receiver (-30 dBm -(-122 dBm) = 92 dB). The 10 dB reduction results because the peak power input to the SA receiver is 10 dB greater than that of the single Fourier component. For the old Ka-band system its dynamic range is reduced by the difference between its noise floor, -103.1 dBm, and the noise floor of the SA receiver, -122 dBm; therefore, the Ka-band dynamic range is 63.1 dB, (82 dB - (-103.1 dBm - (-122 dBm))). Thus, it is desirable to have the noise level of the pulsed portion of the radar slightly lower than that of the CW receiver so that the full dynamic range of the CW receiver may be utilized. This has been accomplished in the new radar with the use of a 20 dB attenuator on the input of the SA receiver.

It is evident that many factors must be considered when designing a radar system, and it is important to keep careful records of signal and noise levels as well as dynamic range to ensure that the radar and its components are operating at peak efficiency. Following the steps outlined thus far should result in a clear understanding of the

performance capabilities of the system. The performance of this system will be tested experimentally in the next chapter by comparing the measured noise level with that calculated in this chapter. In addition, conducting spheres of various diameters will be measured and compared to theoretically determined returns.

CHAPTER VI

EXPERIMENTAL RESULTS OF THE PULSED IF RADAR SYSTEM

To this point, the new system has been considered only in a theoretical way together with performance data on individual components. In this chapter, the results of this effort will be analyzed. Before any data is presented it is necessary to describe how the data is processed.

Typically, in the 2-18 GHz band, magnitude and phase data are measured every 10 MHz for a total of 1600 data points. Assuming the target is centered in the target zone, this raw data set is referred to as the "TARGET." The information in the "TARGET" return contains responses from both the intended target as well as clutter. To remove the clutter a second data set, "BACKGROUND," is recorded with no target present. A phasor subtraction is performed between "TARGET" and "BACKGROUND" as discussed in Chapter IV. The result, TARGET-BACKGROUND, is relatively free from clutter; however, the frequency response of the radar is not constant, and the system variations are present in the data. To remedy this, a six inch sphere is measured by the radar, and this data set is called the "SPHERE." The BACKGROUND data is then subtracted from SPHERE to again remove clutter. The data sets TARGET-BACKGROUND and SPHERE-BACKGROUND contain the same frequency variations caused by the radar, and their quotient is free from these variations. The calibrated data set $\left(\frac{\text{TARGET-BACKGROUND}}{\text{SPHERE-BACKGROUND}}\right)$ contains both

frequency variations due to the target as well as the sphere, so it is multiplied by a data set, "EXACT SPHERE," which is theoretically determined. This product not only removes the frequency variations due to the sphere, but also scales the result to the correct radar cross section values. The operation given as follows [2]:

$$\left(\frac{\text{TARGET-BACKGROUND}}{\text{SPHERE-BACKGROUND}}\right) \text{(EXACT SPHERE)} \qquad (6.1)$$

is performed at every measurement frequency.

A. 2-18 GHz DATA

Figures 6.1(a) and (b) show the frequency and time domain responses of the chamber with no target present. In this case the "TARGET" response is a background measurement, and no background subtraction is performed. This response is due to the clutter which enters the receive gate. Note that the average level increases near 2 GHz; this is due to the target pedestal having a larger RCS at lower frequencies as shown by Lai [3].

The next test is to subtract two consecutive background measurements. The results are shown in Figure 6.2 with the magnitude of Figure 6.1(a) overlayed. Generally, the amount of subtraction required to reach the system noise floor is approximately 40 dB, but near 2 GHz the difference is about 50 dB which is approximately the subtraction limit of this sytem. In order to achieve this level of subtraction, the system must be very stable, and before any measurements are made, the subtraction level must be verified to insure that the clutter will be removed down to the noise floor of the system. The noise level in

Figure 6.2(a) may be compared with those calculated in Figure 5.37. The calculated noise floor for the 2-6 GHz and 6-18 GHz bands are -84.8 dBsm and -71.7 dBsm, respectively. These numbers are reasonably close to the corresponding measured values. Note the difference in vertical scale between Figures 6.1(b) and Figure 6.2(b).

The horizontally polarized returns from 3.187 inch, 1.66 inch, 1.0 inch, .5 inch, .25 inch and .125 inch diameter spheres are shown in Figures 6.3 - 6.8. The corresponding returns for a vertically polarized field are shown in Figures 6.9 - 6.14. The exact sphere frequency domain response for each sphere return is shown overlaid for both polarizations. Generally, the measured magnitude values correspond well with the exact ones, and the measured time domain responses, shown above the exact response for each sphere, appear to be surprisingly close to the correct returns even for the smallest spheres. Referring to Figure 6-14(b) the time domain response is clear and sharp and well above the noise floor of the system. Note that the time domain response is a very sensitive and powerful tool in the study of electromagnetic scattering.

B. KA-BAND DATA

Similar plots were obtained for the Ka-band system. Referring to Figure 5.37, the noise level for this system should be located around -65.5 dBsm. Figure 6.15 shows the time and frequency domain returns for an unsubstracted background measurement. Figure 6.16 shows the result of subtracting two consecutive background measurements. The difference in magnitude between the two cases indicates that the 50 dB subtraction

limit is not closely approached; nevertheless, the noise floor in Figure 6.16(a) is very close to the -65.5 dBsm level determined from Figure 5.37. Comparing Figure 6.15(b) with Figure 6.16(b) shows that the clutter is effectively eliminated after a subtraction is performed. Again note the difference in vertical scale between the two figures.

Figures 6.17 - 6.22 show returns from the standard set of spheres. The exact sphere return in the frequency domain are overlaid on the measured returns, and as before the measured time domain response is shown above the exact response in each case. The results indicate that the Ka-band system is quite accurate and capable of measuring returns from low cross section targets. Once again note the well defined and distinctive time domain return of the one-eighth inch sphere in Figure 6.22(b).

The time domain responses for the system as a whole compare very well with the exact results. The t=0 position on the horizontal axis corresponds to the position of the center of the 6 inch sphere used during calibration. The vertical scale on each time domain plot is a relative magnitude, and an absolute amplitude should not be assigned to these values. They are produced by performing an inverse Fourier transform on the calibrated frequency domain data, and the value of the magnitude scale is primarily in comparison between targets. The time domain response is also very useful for diagnosing trouble within the radar and/or chamber. Since the time and frequency domain responses are related by the Fourier transform, they contain the same information, except it is presented in different forms. Scatterers which cannot be

distinguished in the frequency domain become apparent in the time domain, where their positions and relative amplitudes may be easily seen. It is useful to become comfortable with working with both domains as each gives different insight into the same measurement information.

The results presented in this chapter show that the radar is quite accurate, and it meets the sensitivity ratings determined in Chapter V. The sphere return plots in this chapter illustrate the usefulness of both the time and frequency domain responses in analyzing electromagnetic scatterers. For more elaborate targets complicated returns may be measured and transformed to the time domain to determine the location and magnitude of various scatterers; while the frequency domain measures the overall cross section of the target. These results illustrate that a digital computer in combination with an efficiently operating radar can be a powerful measurement and analysis tool.

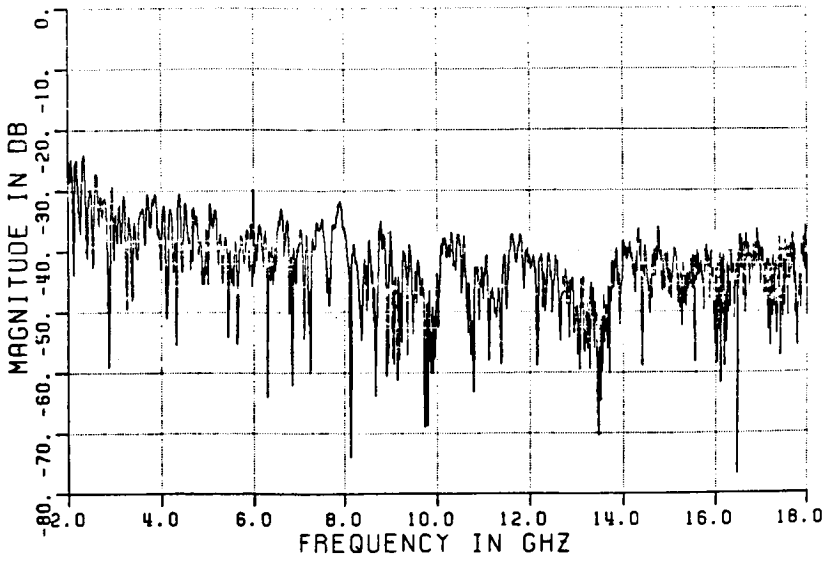

(a) frequency domain

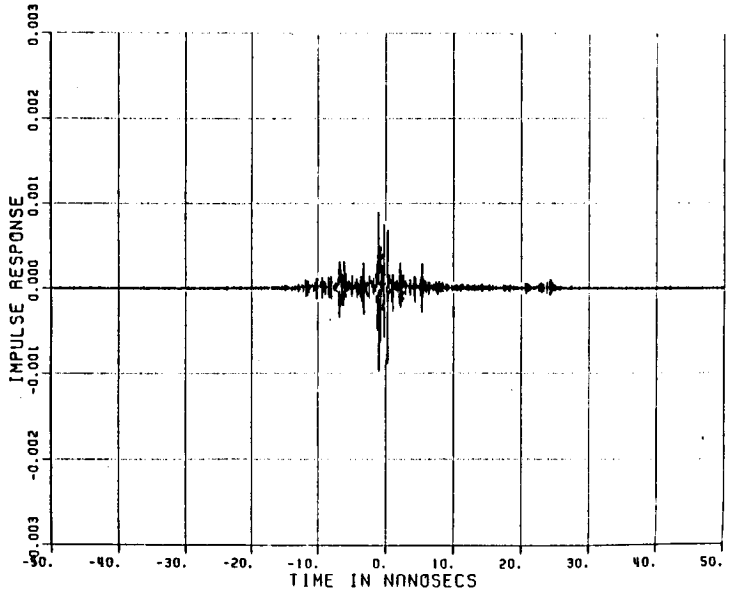

(b) time domain

Figure 6.1. Calibrated background measurement for the 2-18 GHz system.

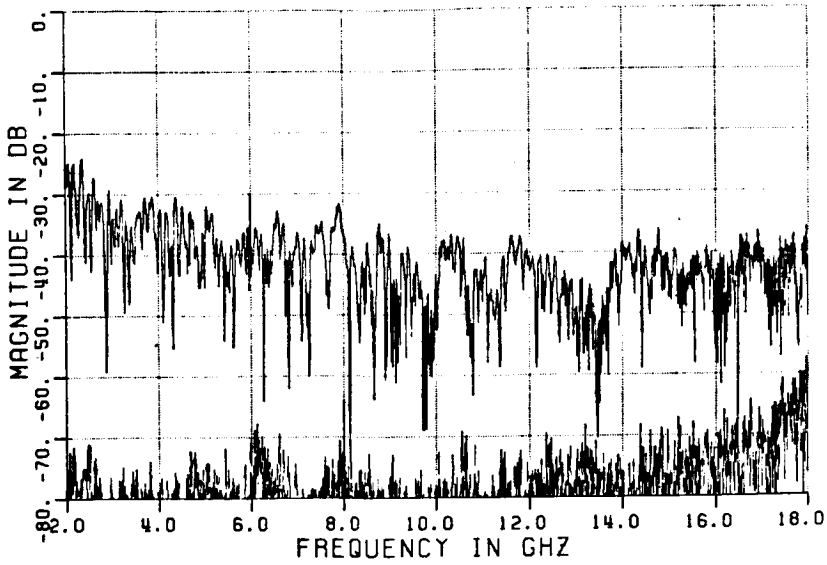

(a) frequency domain

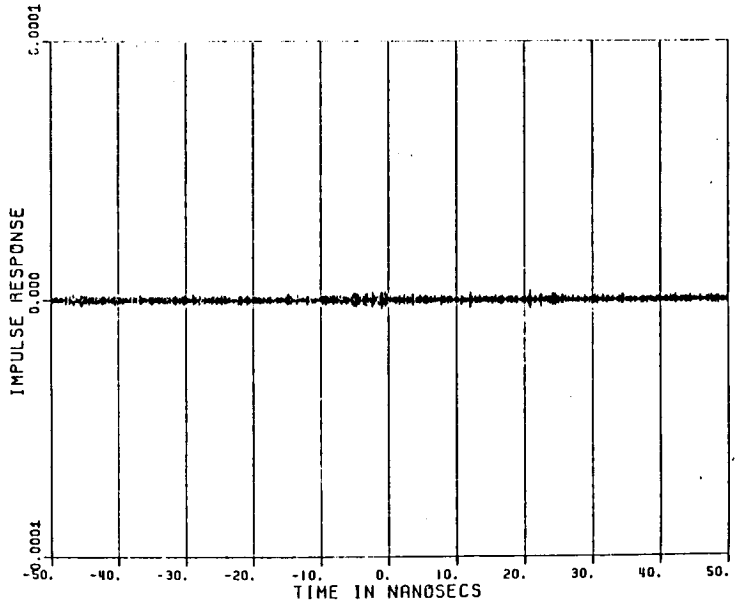

(b) time domain

Figure 6.2. Subtracted background response.

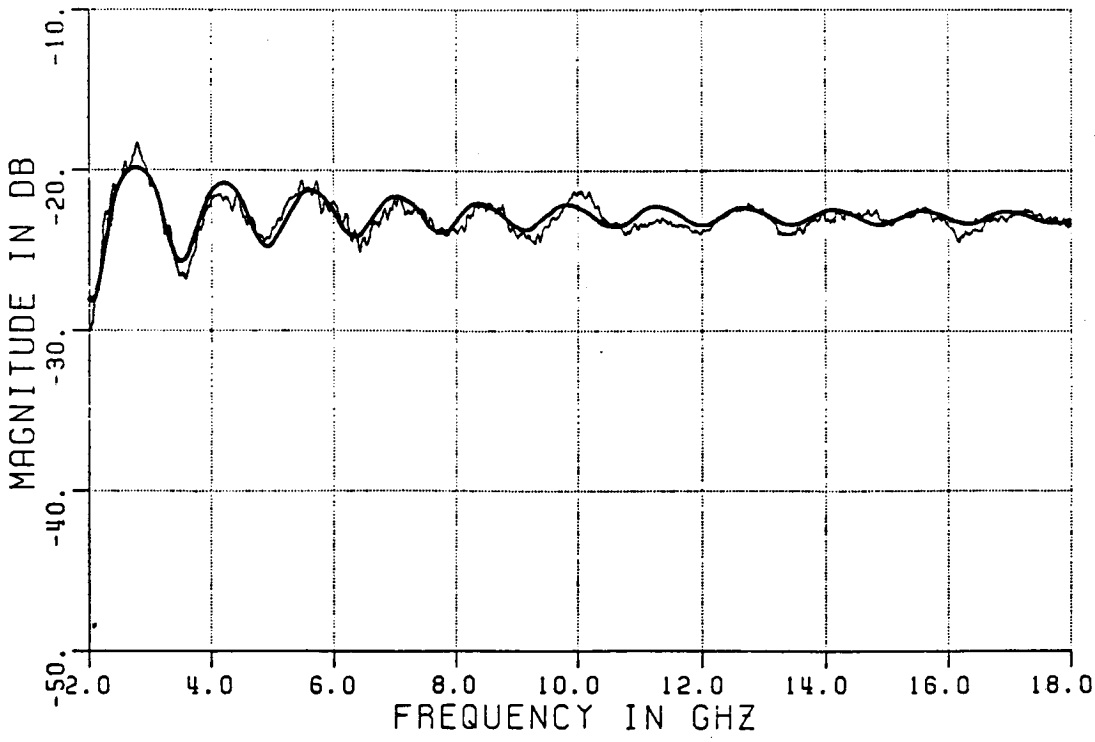

(a) frequency domain

Figure 6.3. 3.187 inch sphere response for a horizontally polarized field.

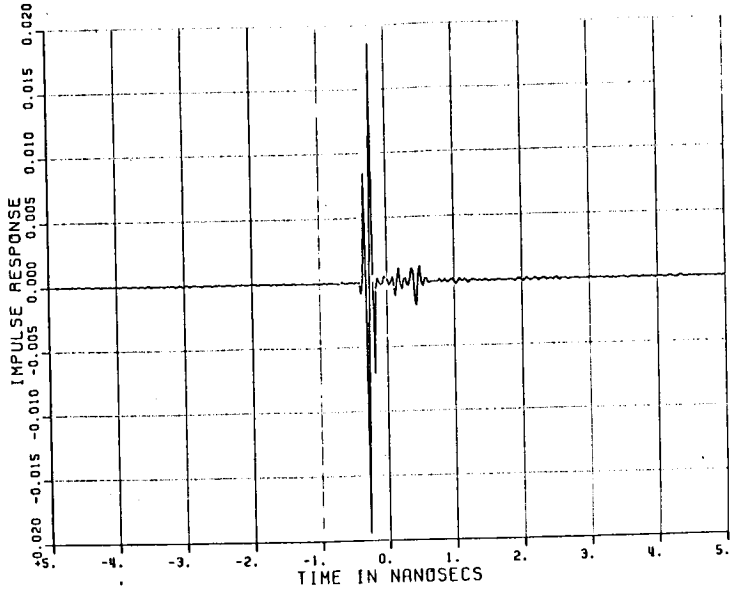

(b) measured time domain

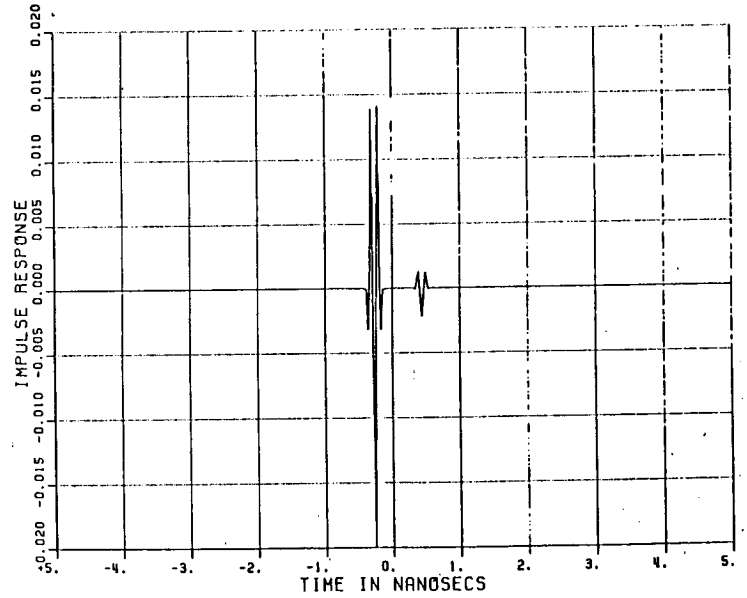

(c) exact time domain

Figure 6.3. Continued.

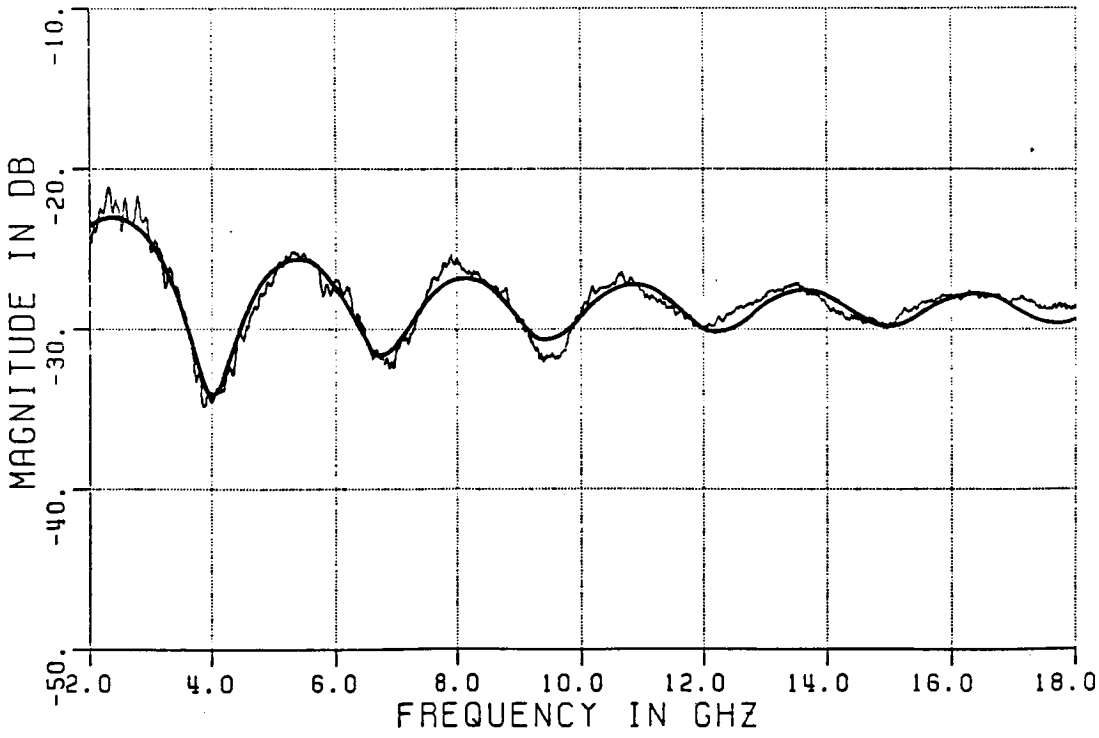

(a) frequency domain

Figure 6.4. 1.65 inch sphere response for a horizontally polarized field.

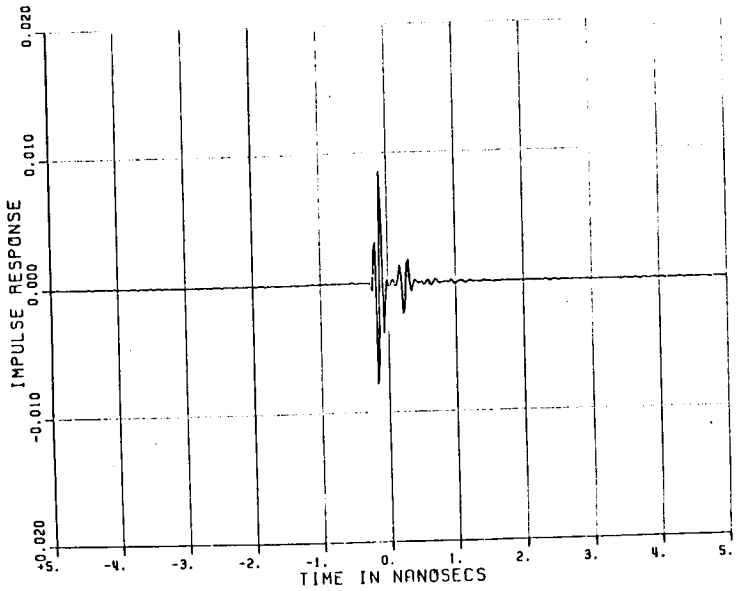

(b) measured time domain

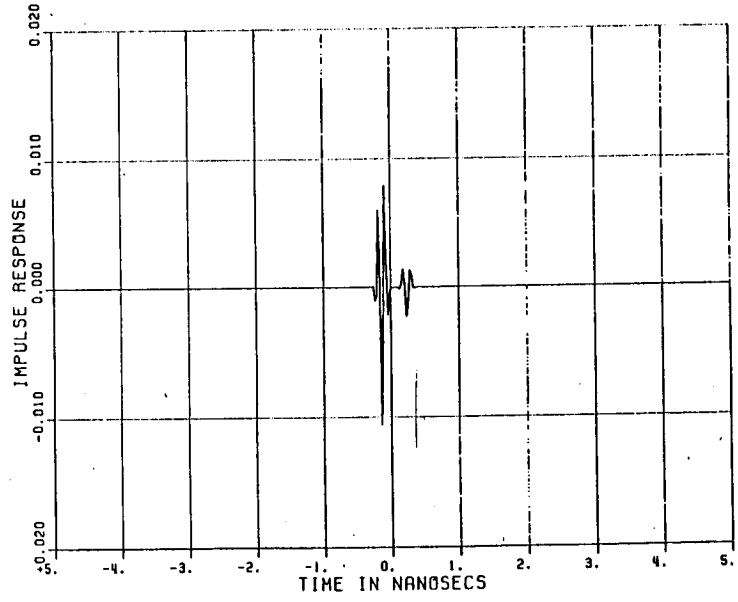

(c) exact time domain

Figure 6.4. Continued.

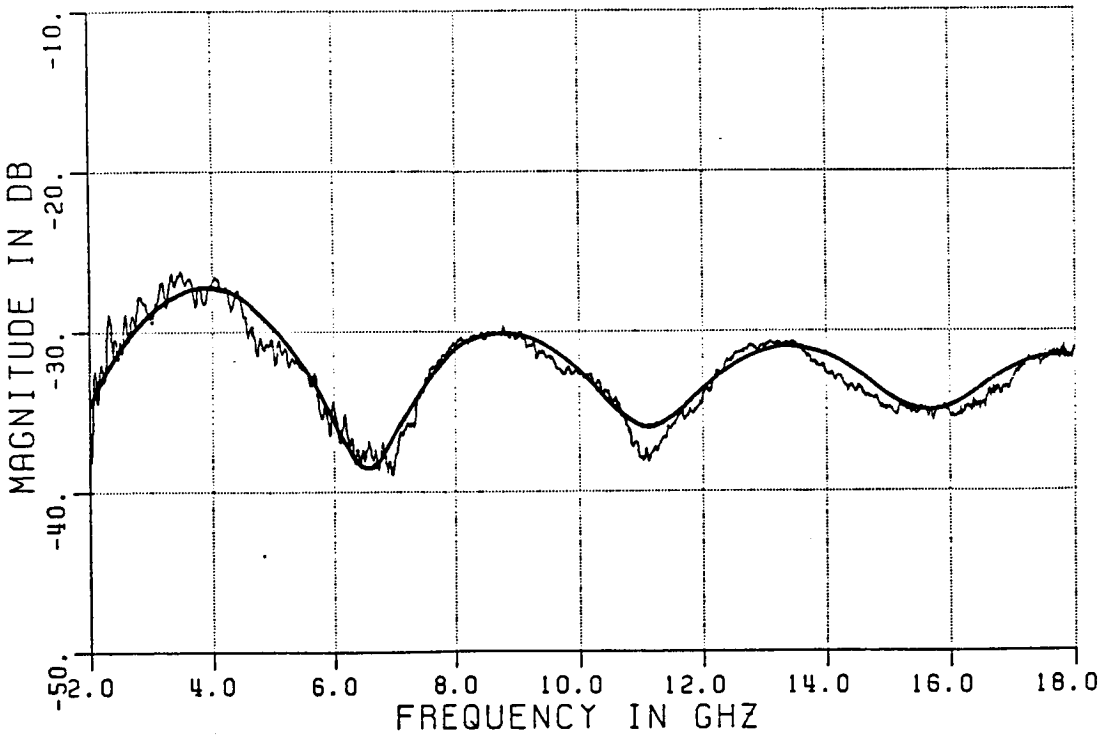

(a) frequency domain

Figure 6.5. 1 inch sphere response for a horizontally polarized field.

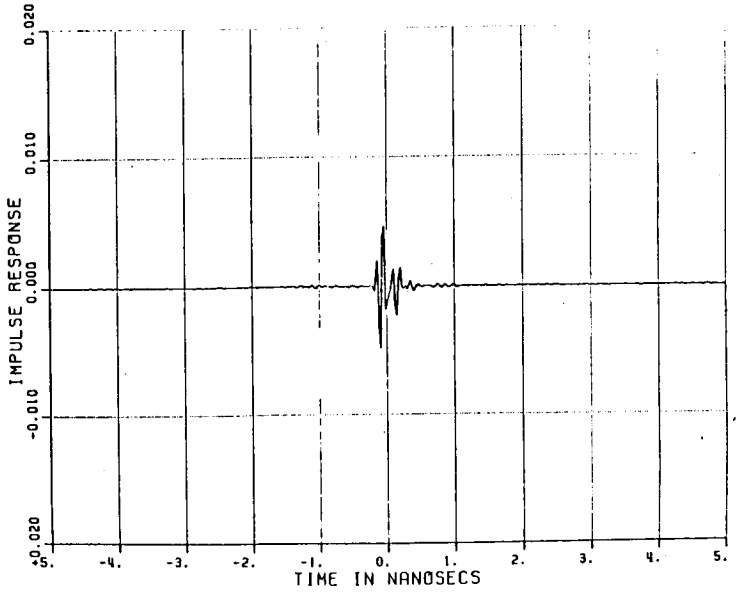

(b) measured time domain

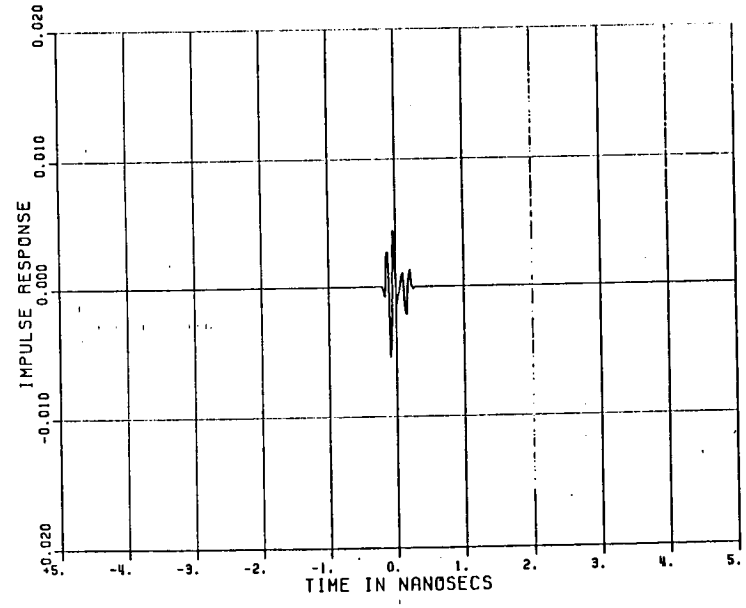

(c) exact time domain

Figure 6.5. Continued.

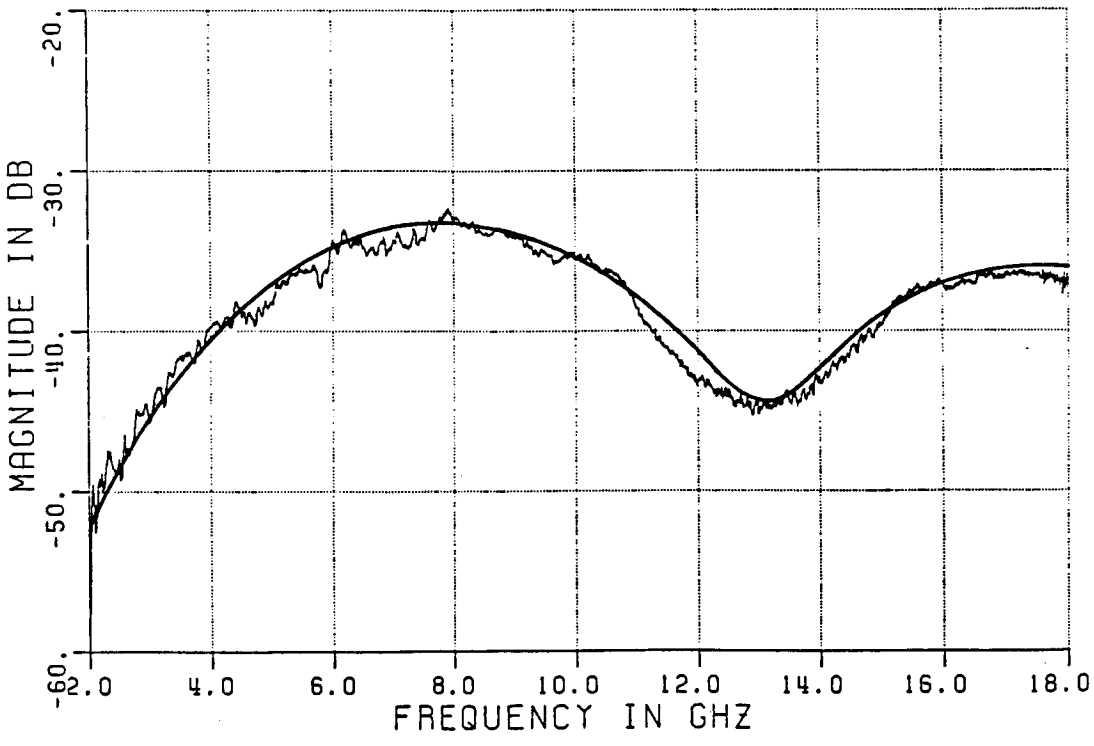

(a) frequency domain

Figure 6.6. 1/2 inch sphere response for a horizontally polarized field.

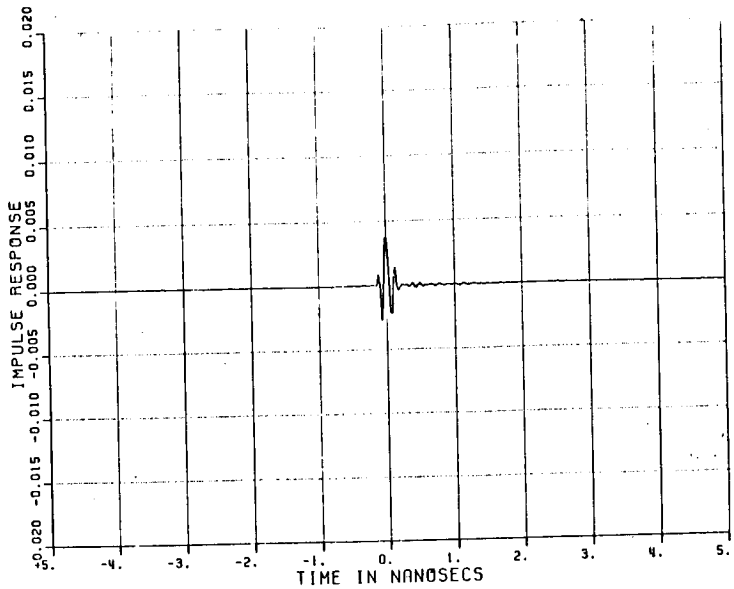

(b) measured time domain

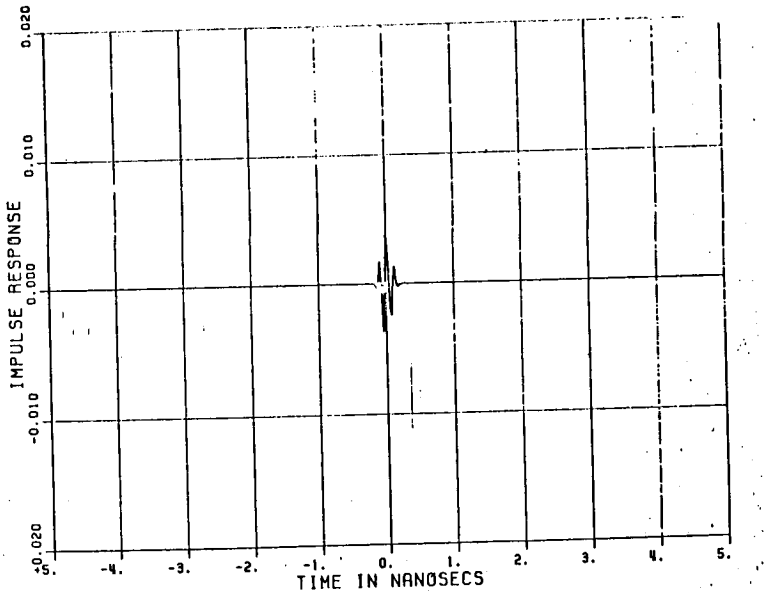

(c) exact time domain

Figure 6.6. Continued.

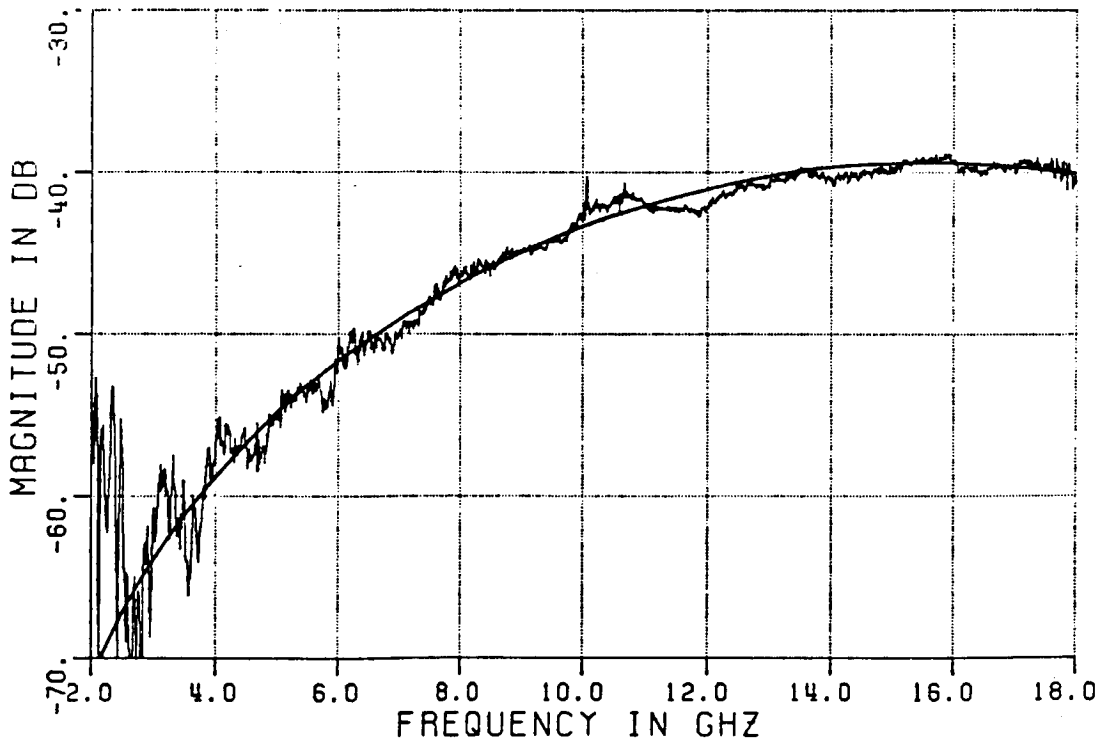

(a) frequency domain

Figure 6.7. 1/4 inch sphere response for a horizontally polarized field.

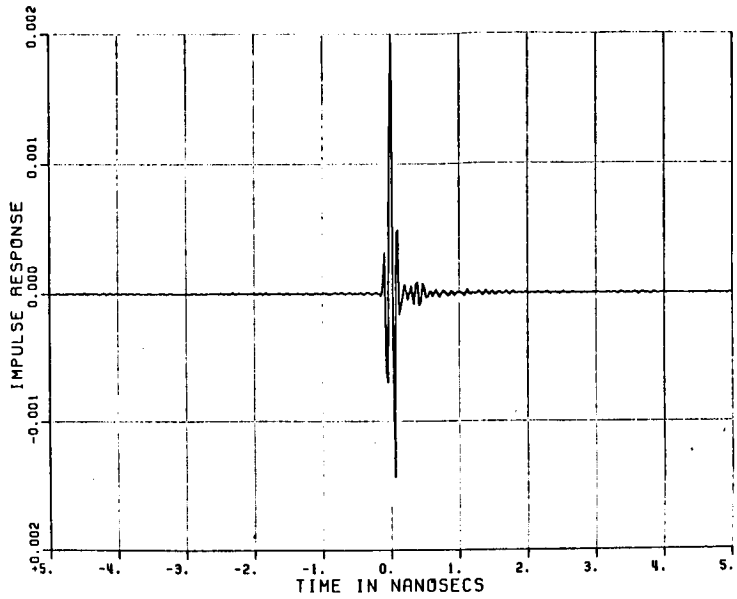

(b) measured time domain

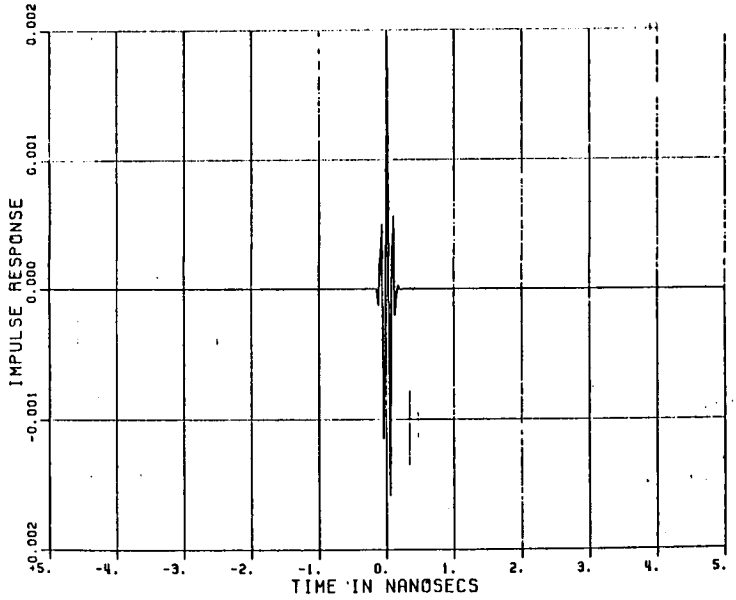

(c) exact time domain

Figure 6.7. Continued.

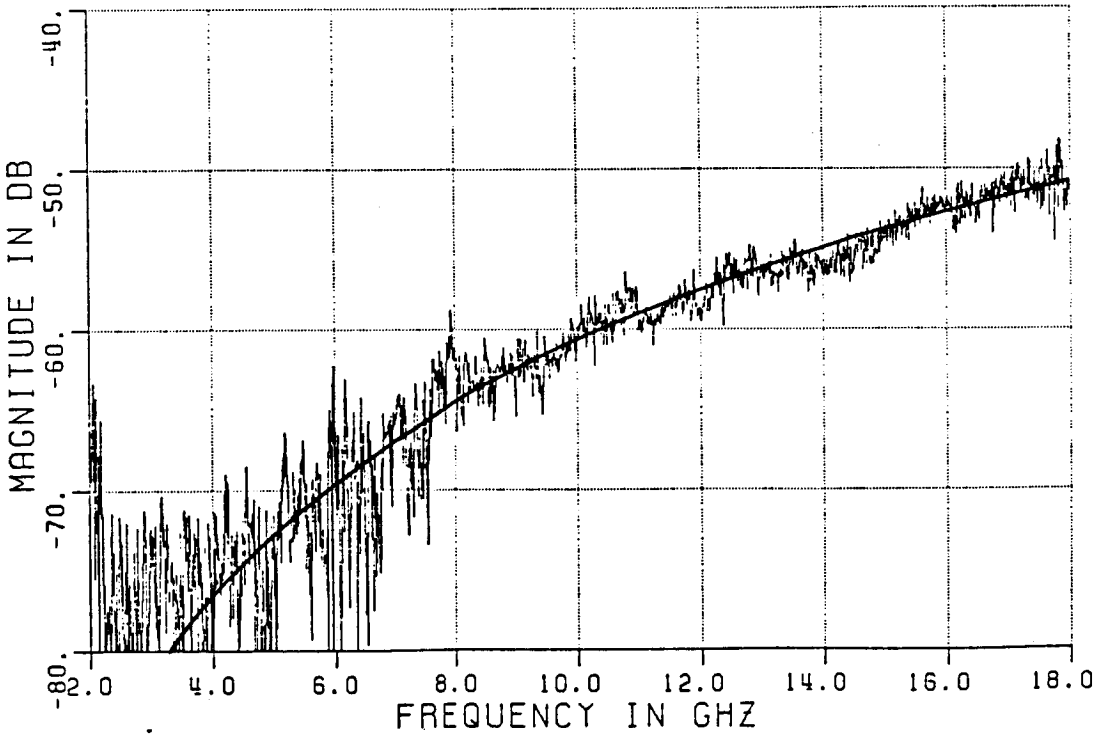

(a) frequency domain

Figure 6.8. 1/8 inch sphere response for a horizontally polarized field.

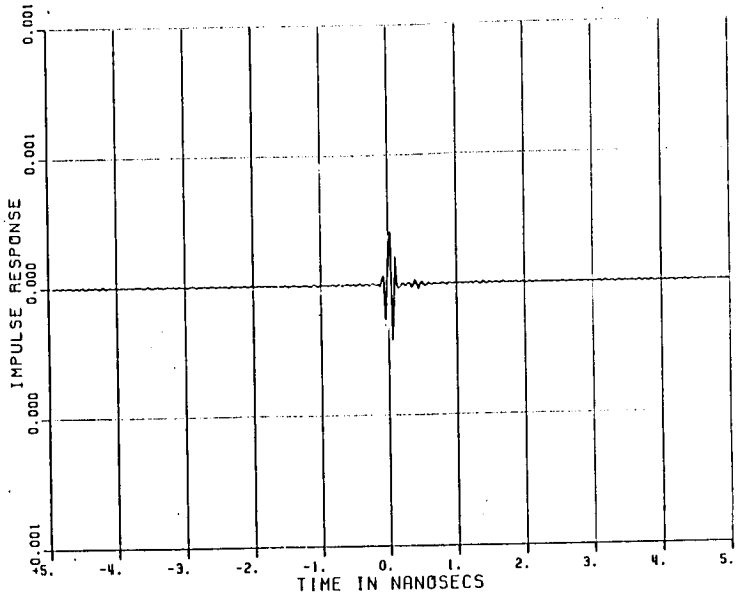

(b) measured time domain

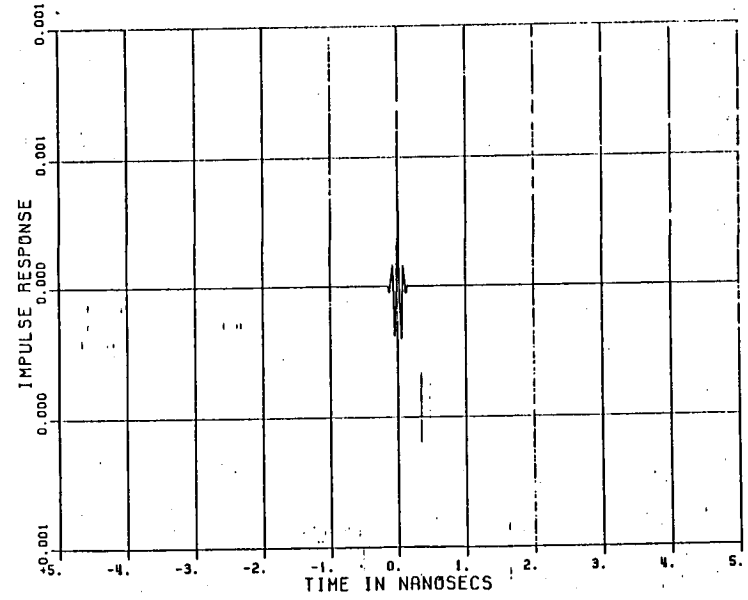

(c) exact time domain

Figure 6.8. Continued.

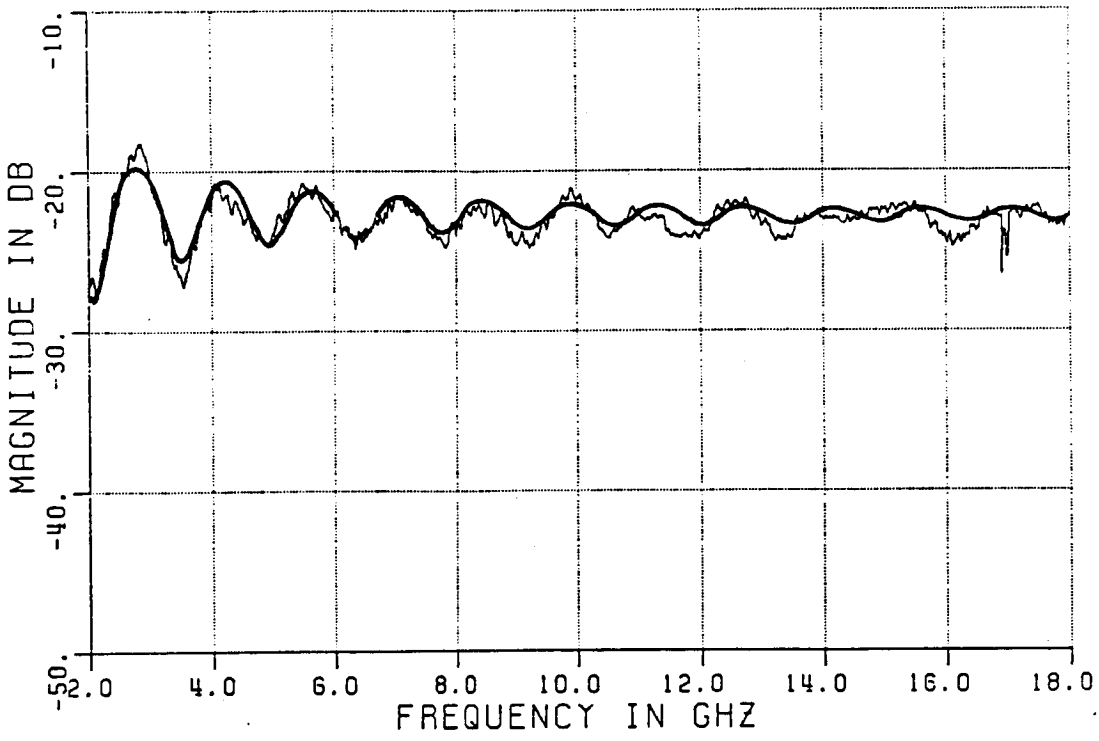

(a) frequency domain

Figure 6.9. 3.187 inch sphere response for a vertically polarized field.

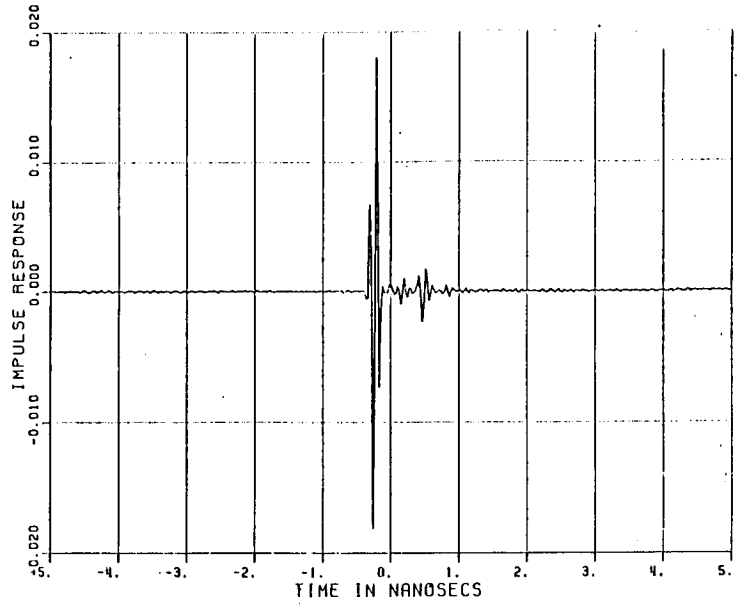

(b) measured time domain

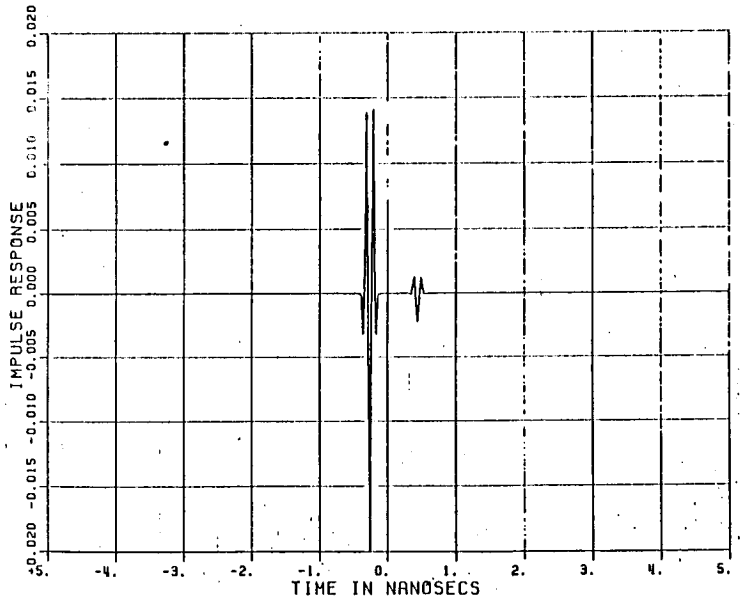

(c) exact time domain

Figure 6.9. Continued.

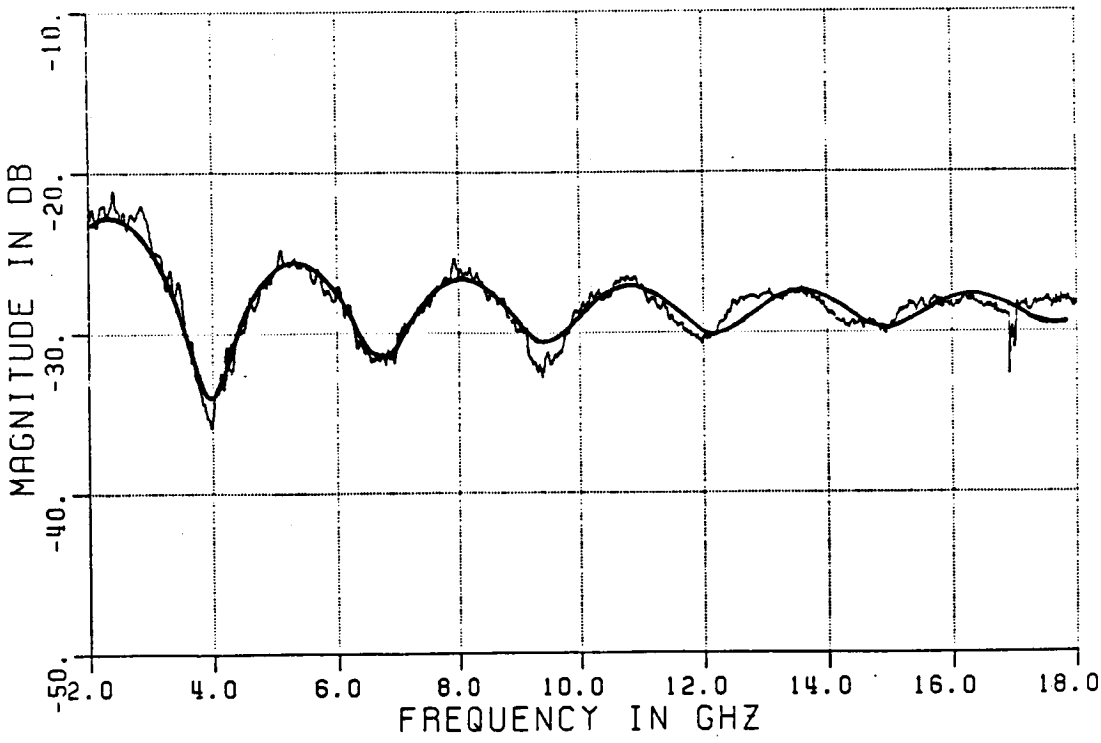

(a) frequency domain

Figure 6.10. 1.65 inch sphere response for a vertically polarized field.

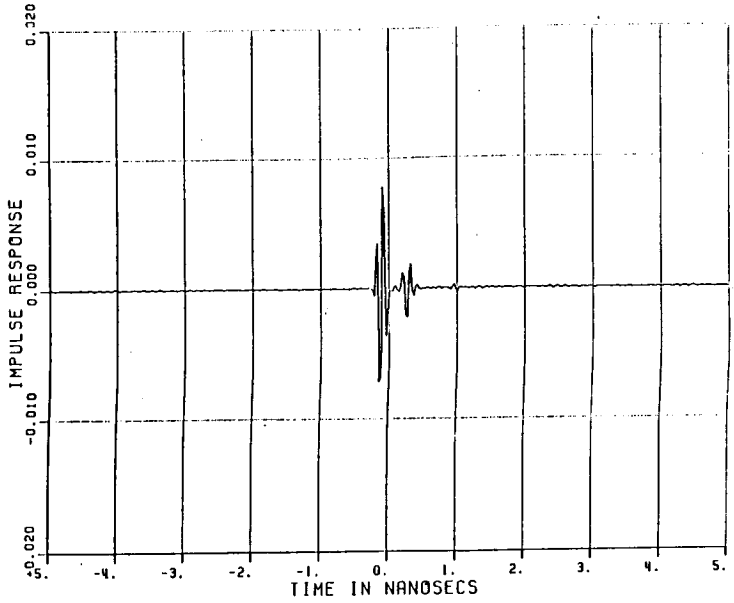

(b) measured time domain

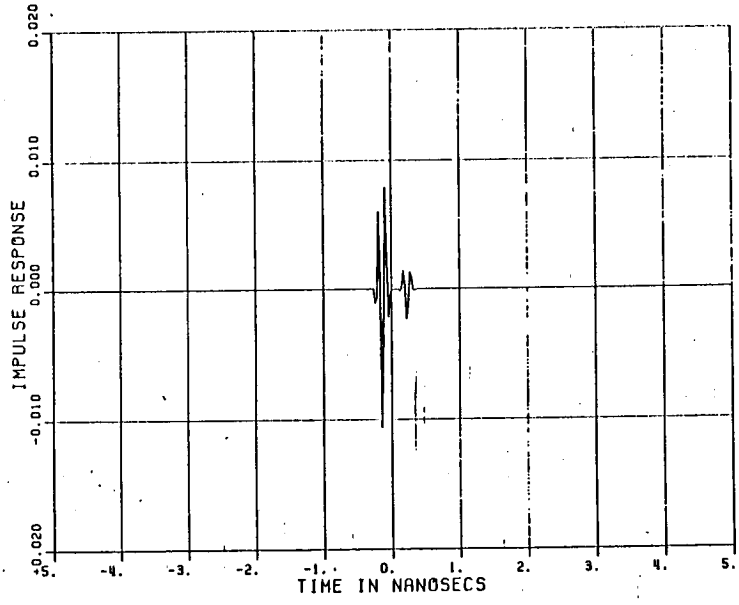

(c) exact time domain

Figure 6.10. Continued.

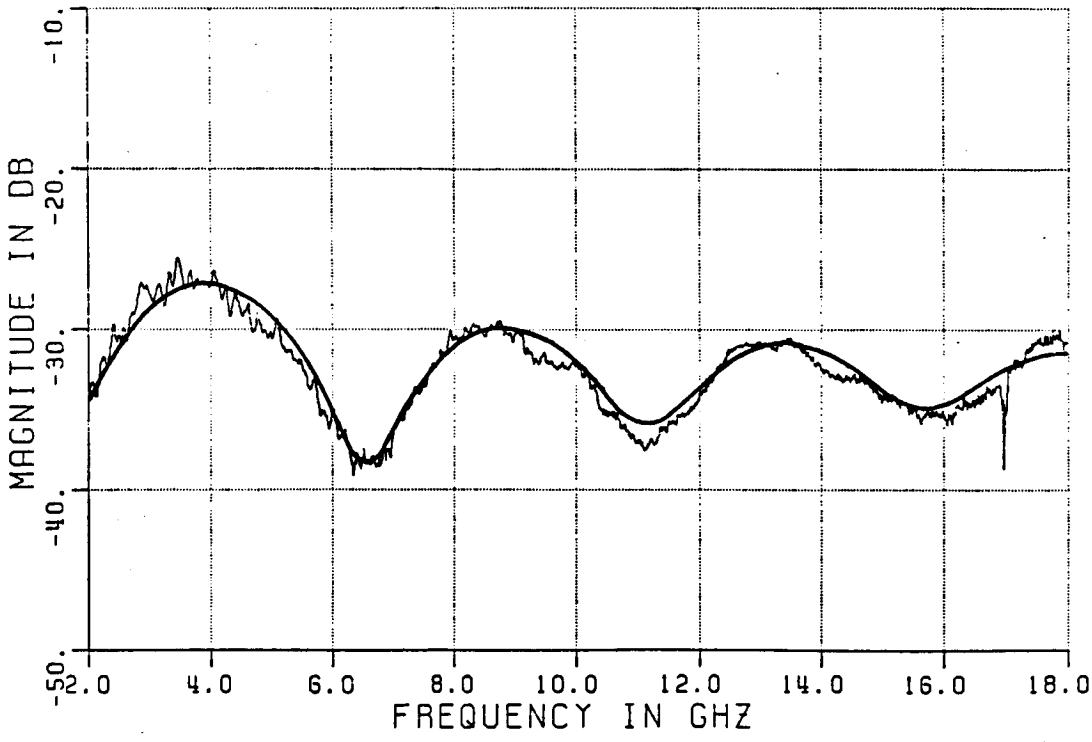

(a) frequency domain

Figure 6.11. 1 inch sphere response for a vertically polarized field.

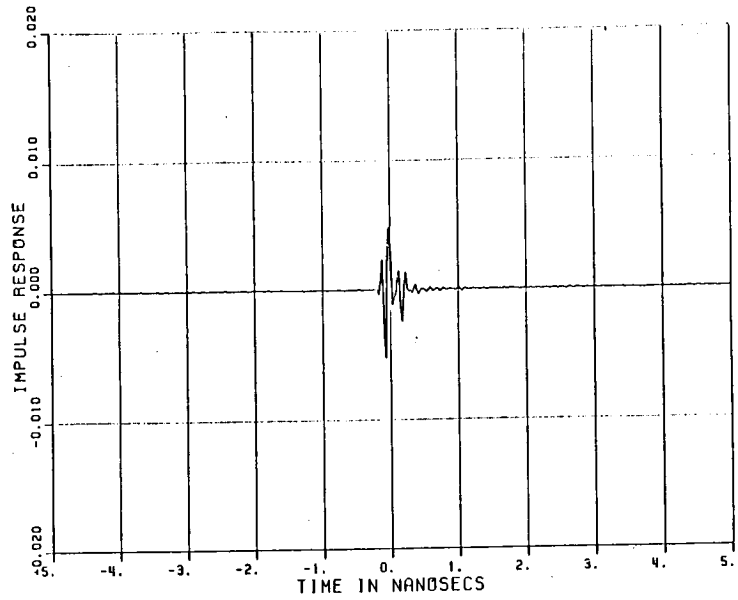

(b) measured time domain

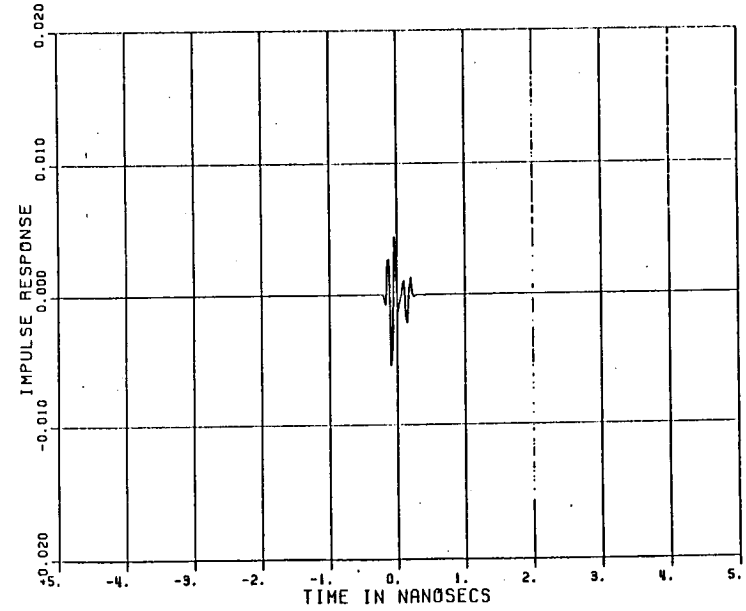

(c) exact time domain

Figure 6.11. Continued.

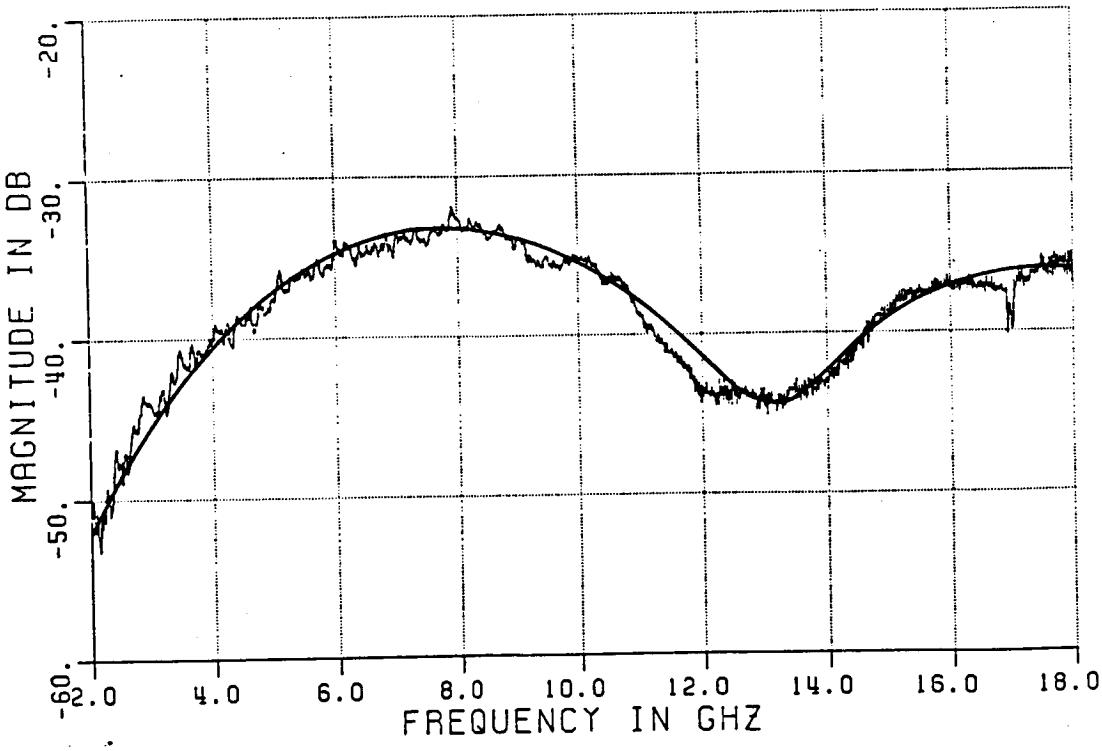

(a) frequency domain

Figure 6.12. 1/2 inch sphere response for a vertically polarized field.

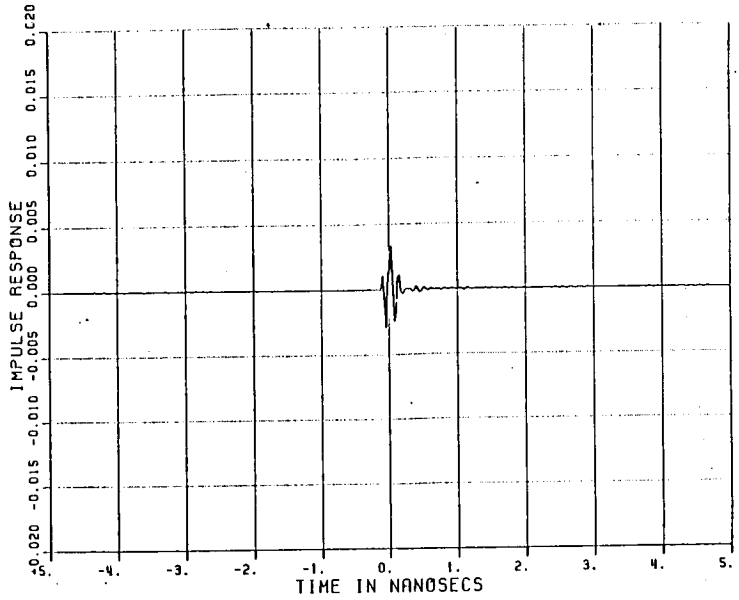

(b) measured time domain

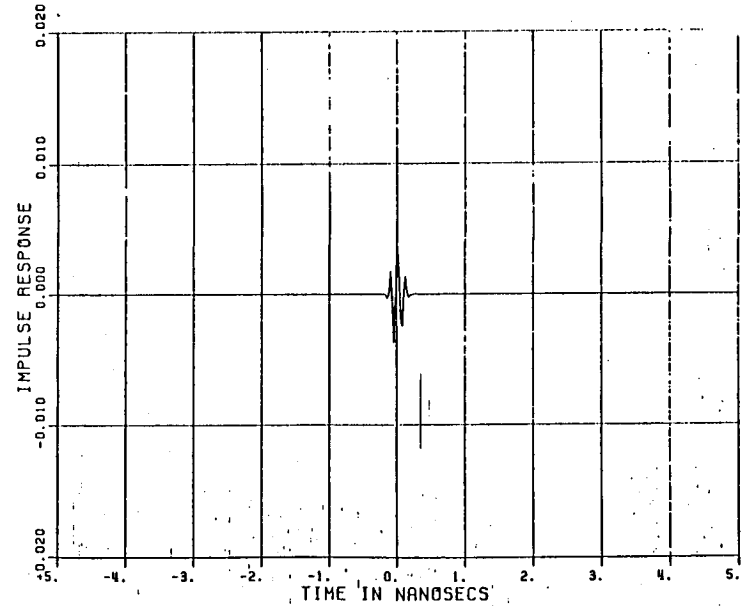

(c) exact time domain

Figure 6.12. Continued.

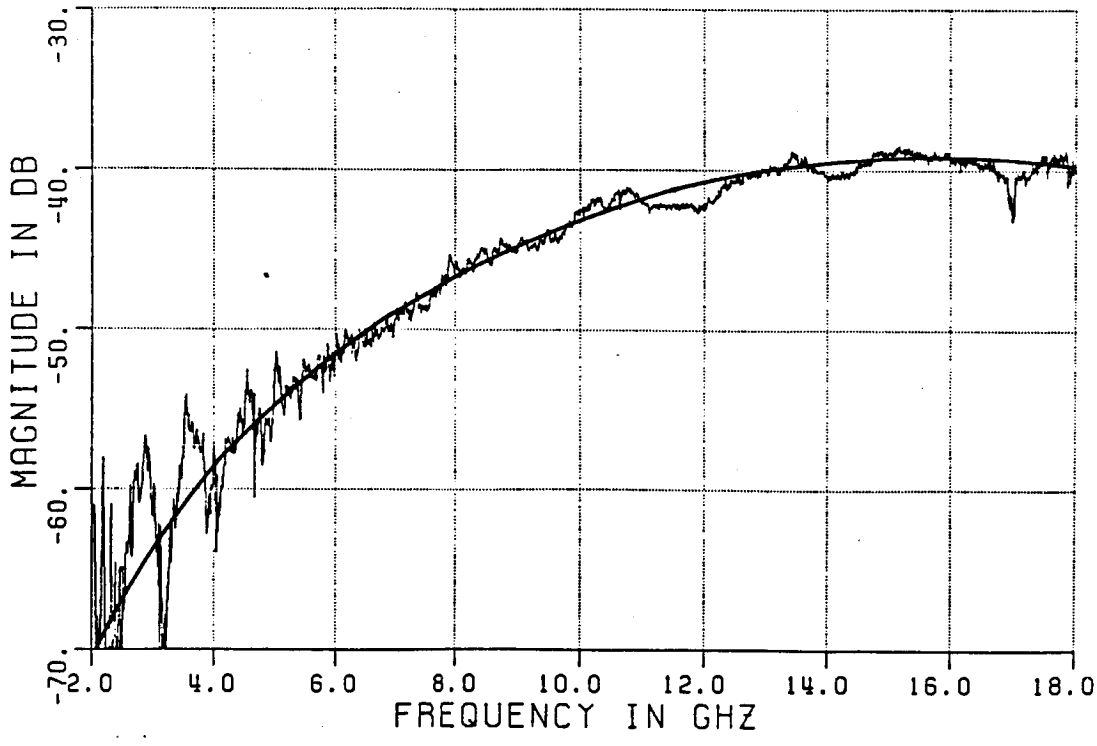

(a) frequency domain

Figure 6.13. 1/4 inch sphere response for a vertically polarized field.

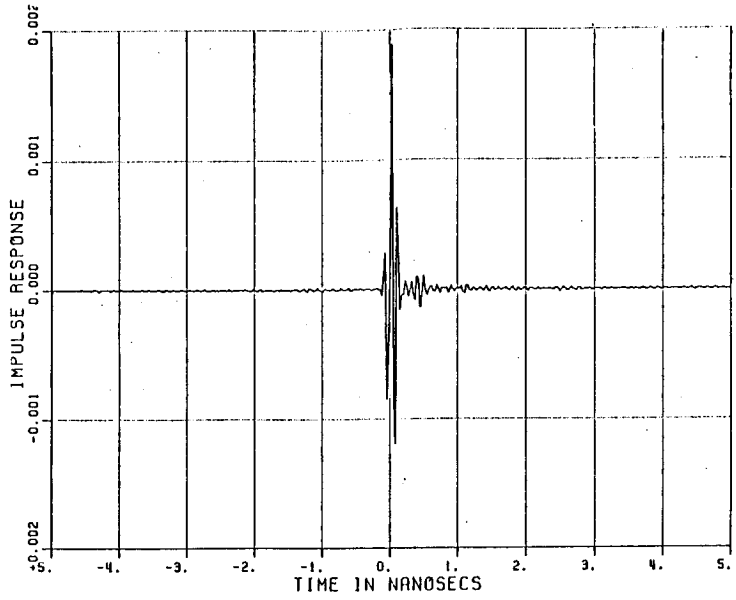

(b) measured time domain

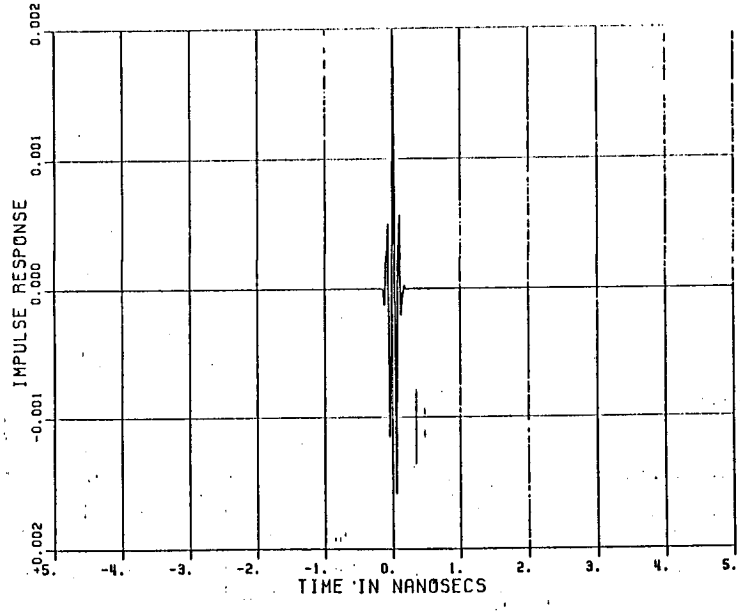

(c) exact time domain

Figure 6.13. Continued.

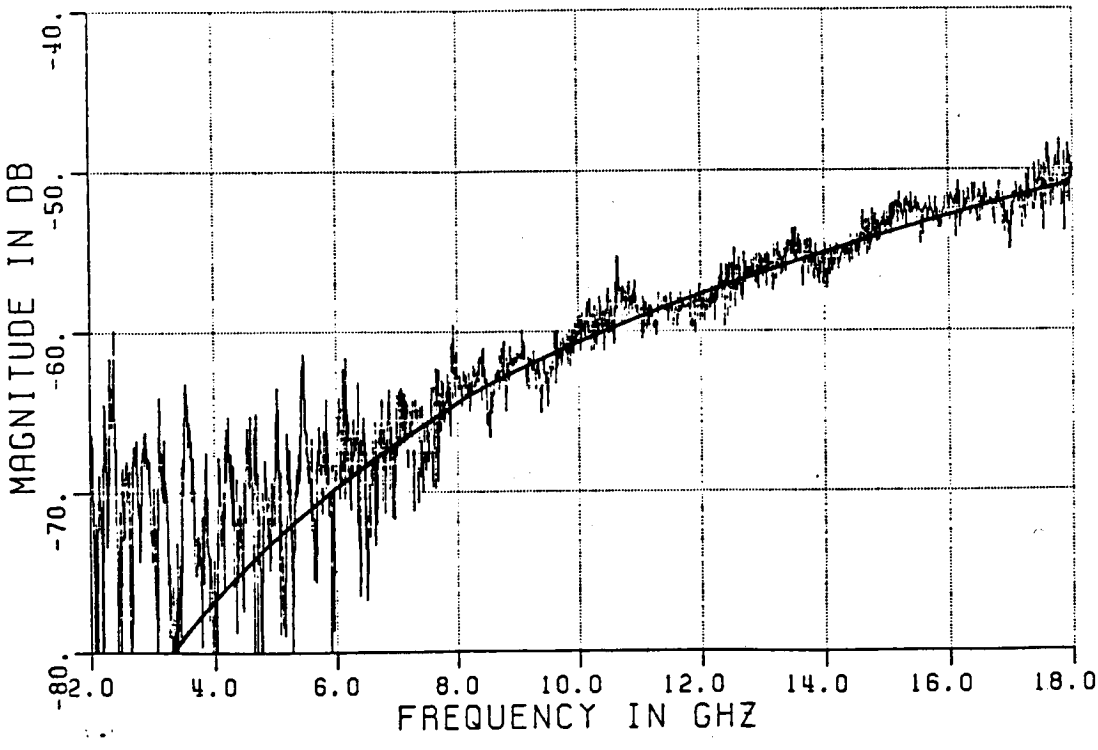

(a) frequency domain

Figure 6.14. 1/8 inch sphere response for a vertically polarized field.

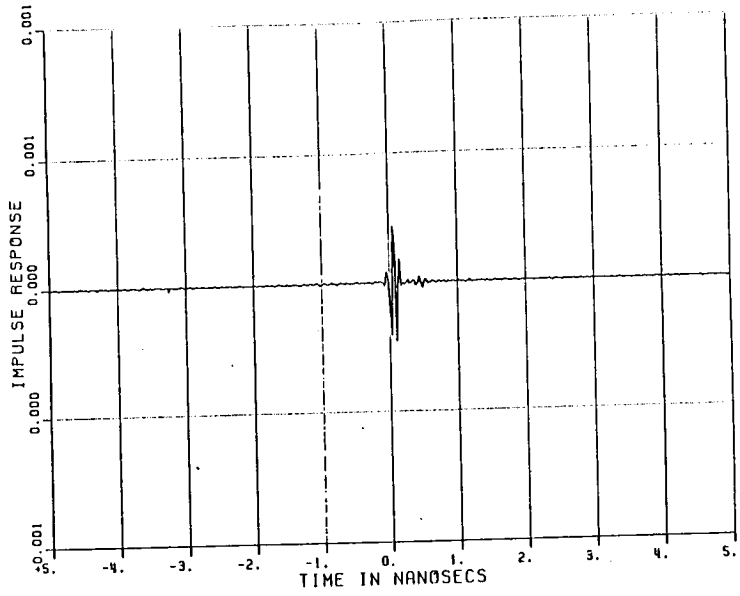

(b) measured time domain

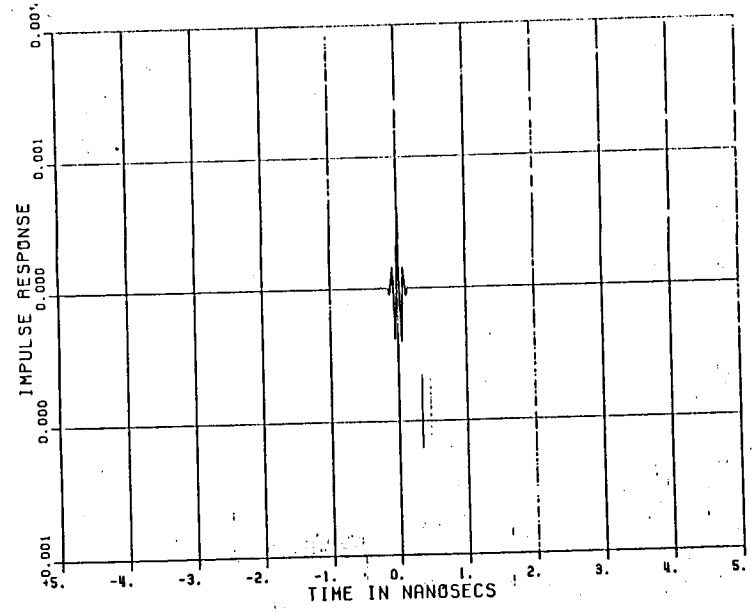

(c) exact time domain

Figure 6.14. Continued.

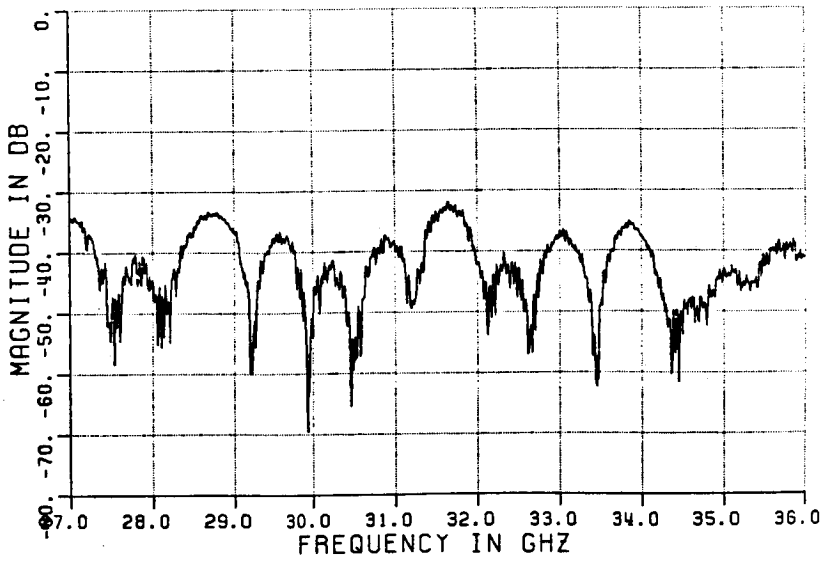

(a) frequency domain

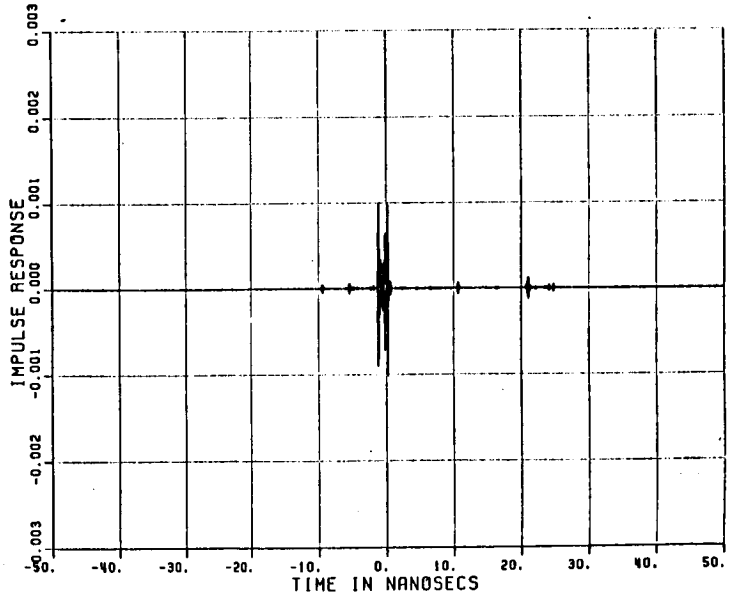

(b) time domain

Figure 6.15. Calibrated background measurement for the Ka-band system.

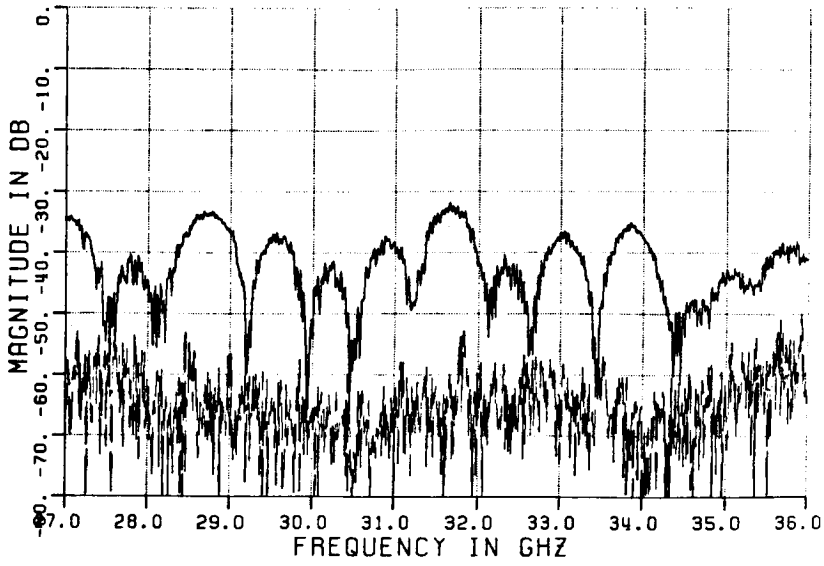

(a) frequency domain

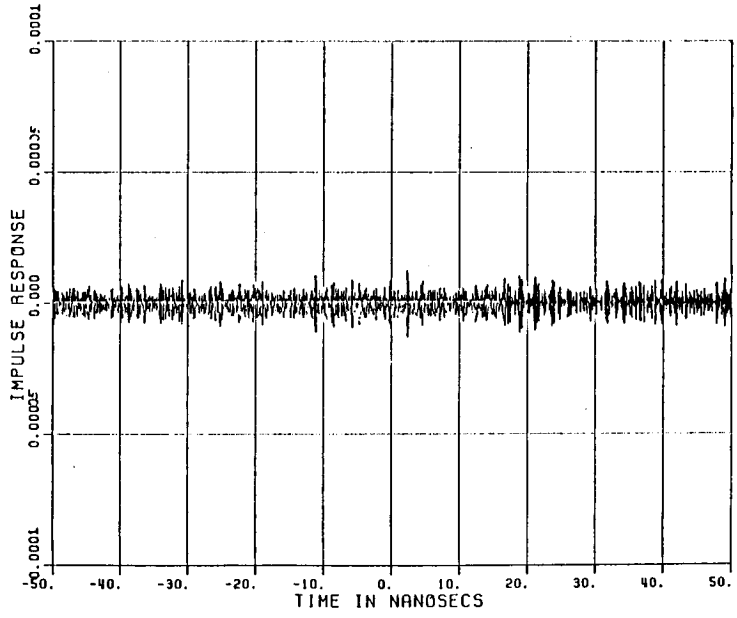

(b) time domain

Figure 6.16. Subtracted background level.

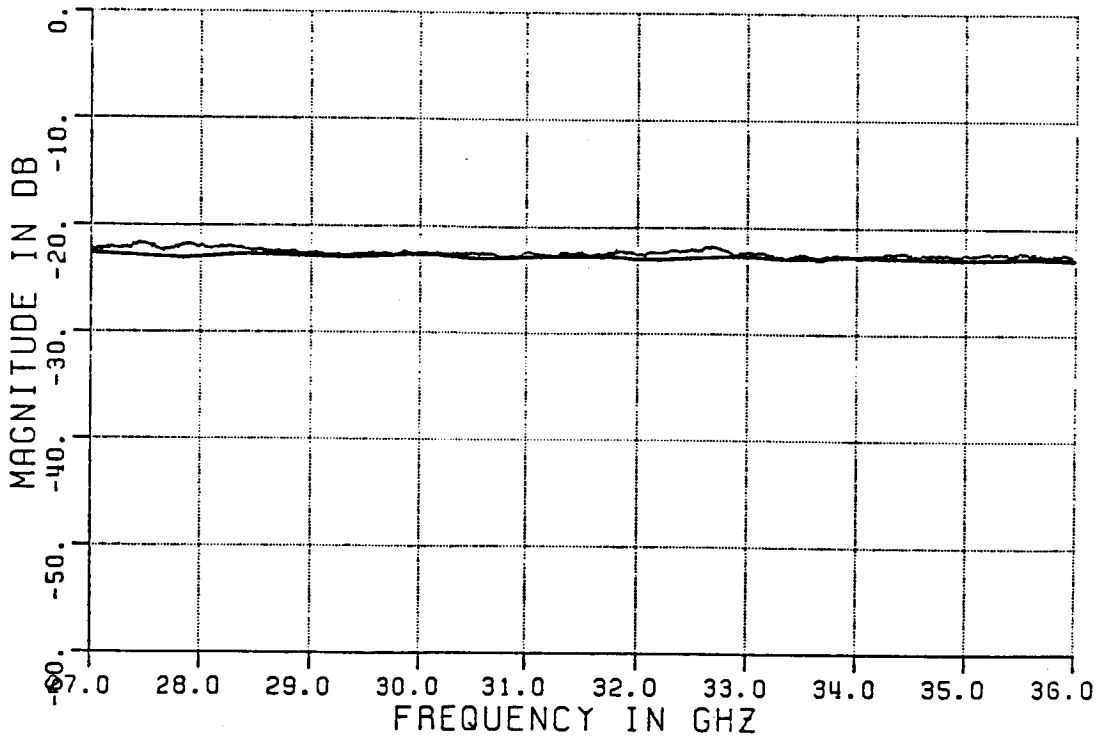

(a) frequency domain

Figure 6.17. 3.2 inch sphere response.

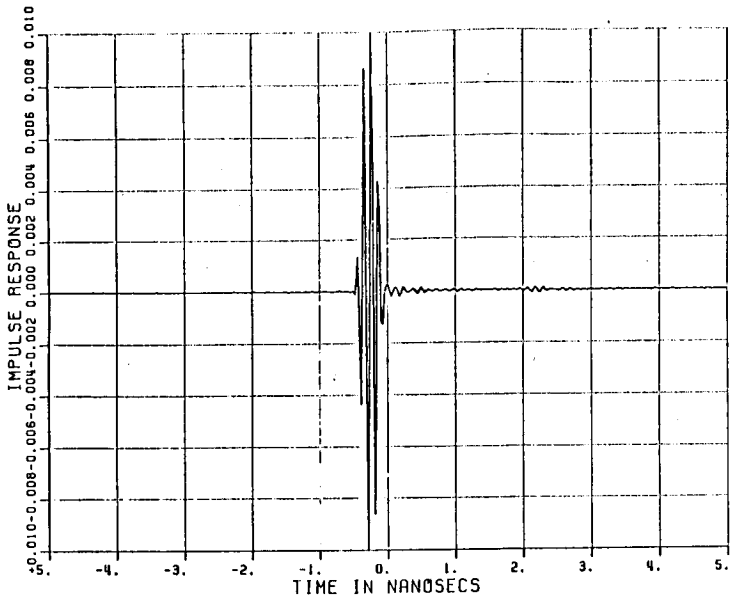

(b) measured time domain

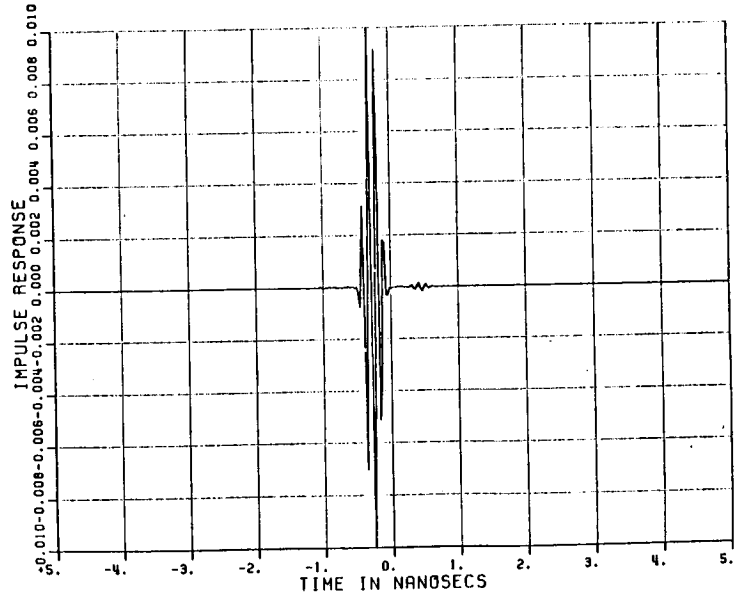

(c) exact time domain

Figure 6.17. Continued.

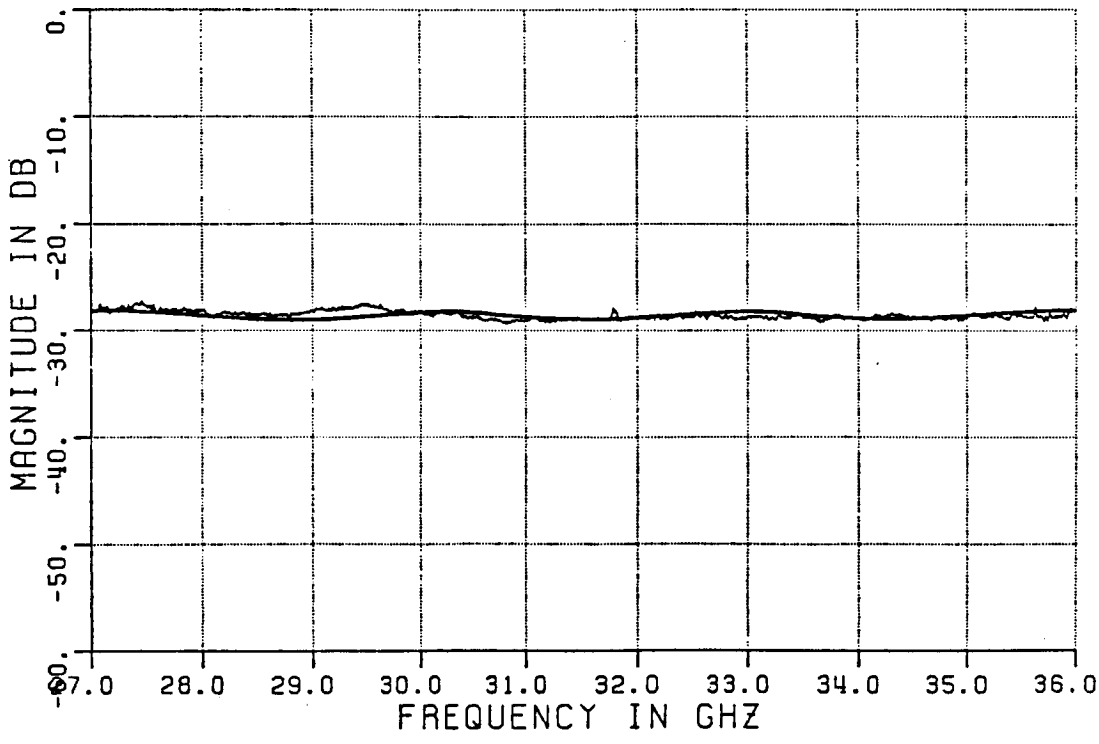

(a) frequency domain

Figure 6.18. 1.65 inch sphere response.

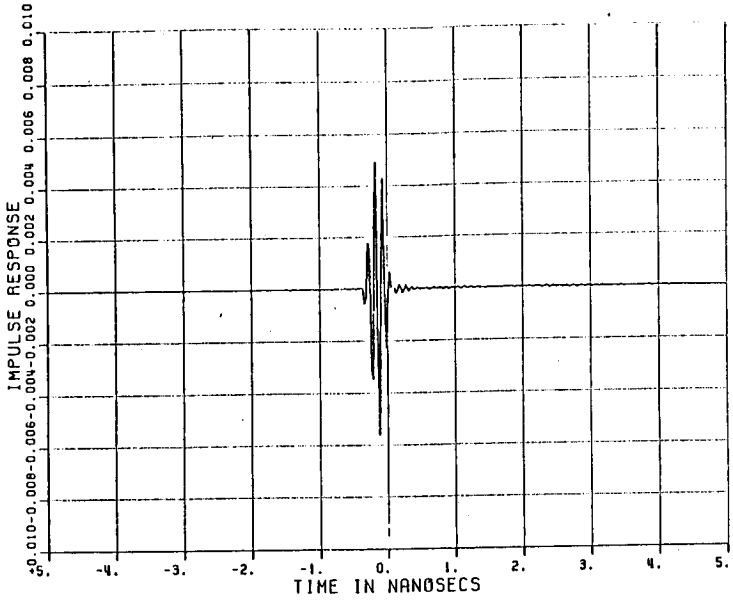

(b) measured time domain

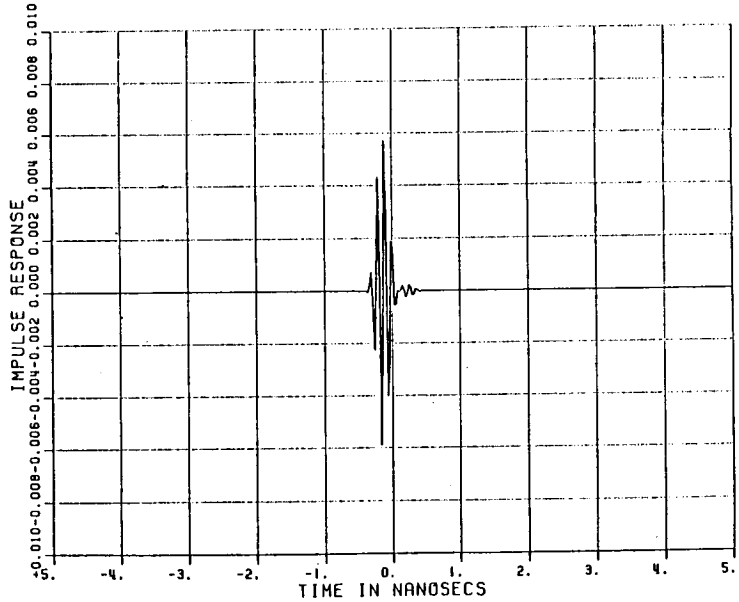

(c) exact time domain

Figure 6.18. Continued.

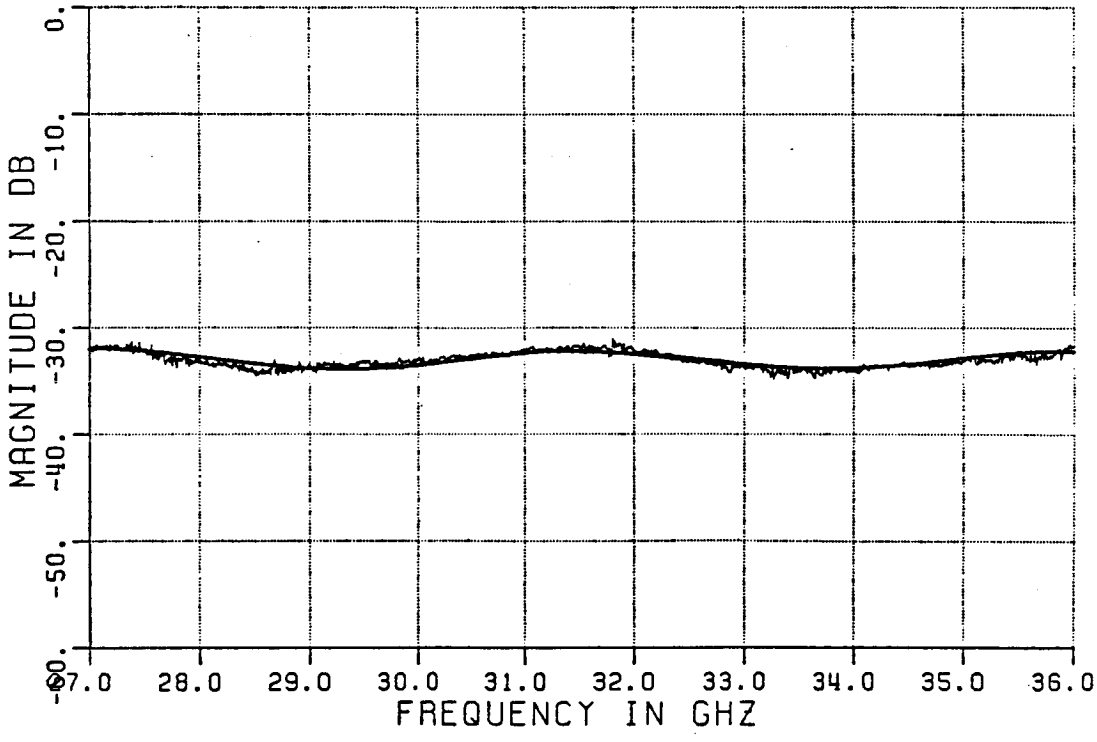

(a) frequency domain

Figure 6.19. 1 inch sphere response.

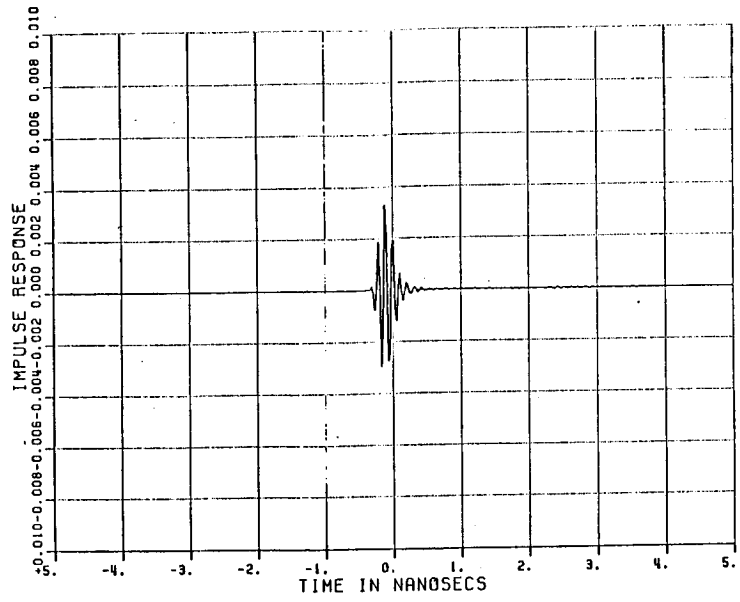

(b) measured time domain

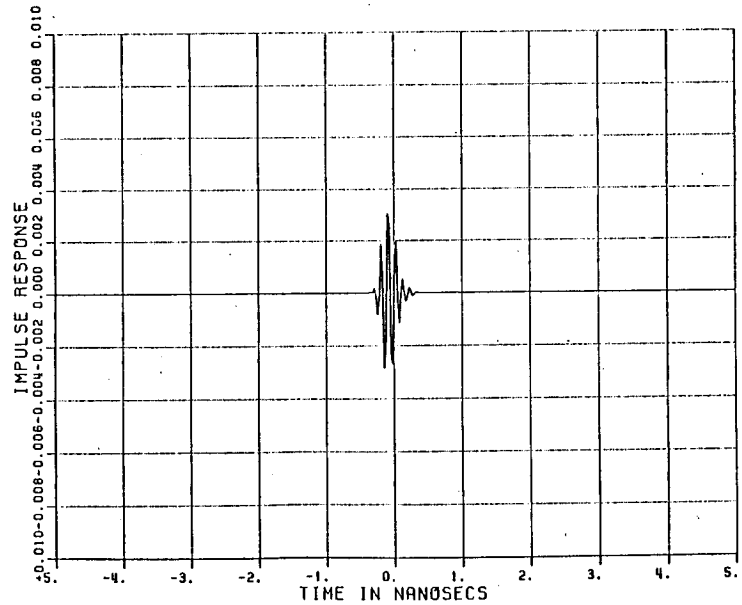

(c) exact time domain

Figure 6.19. Continued.

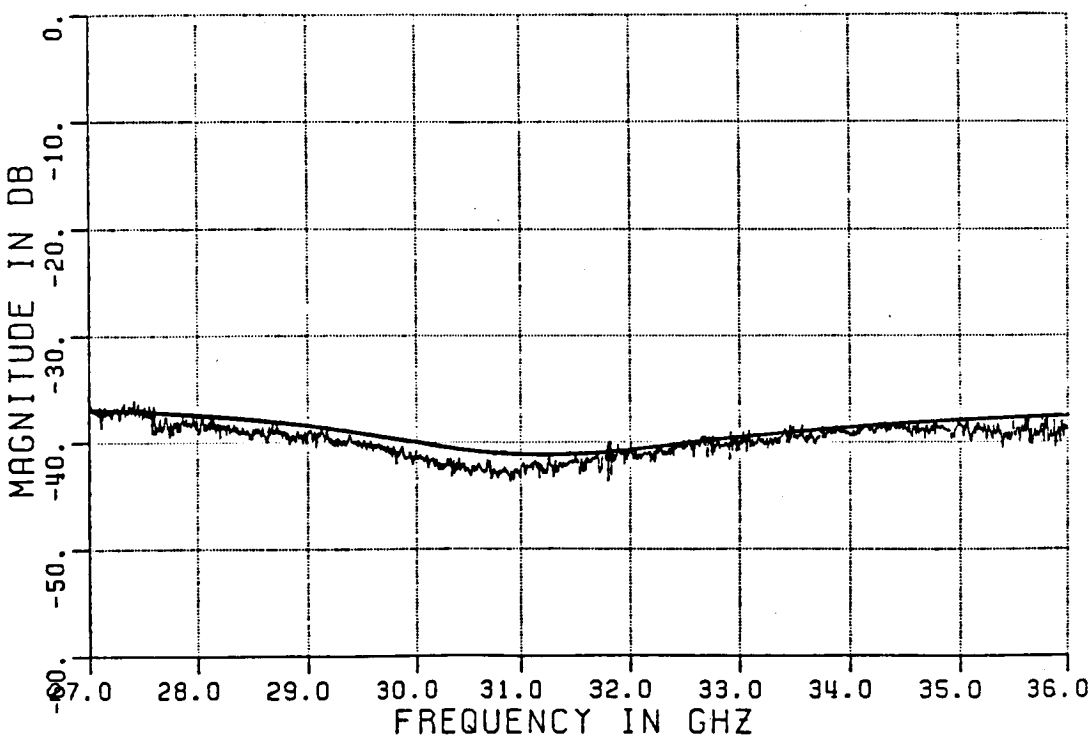

(a) frequency domain

Figure 6.20. 1/2 inch sphere response.

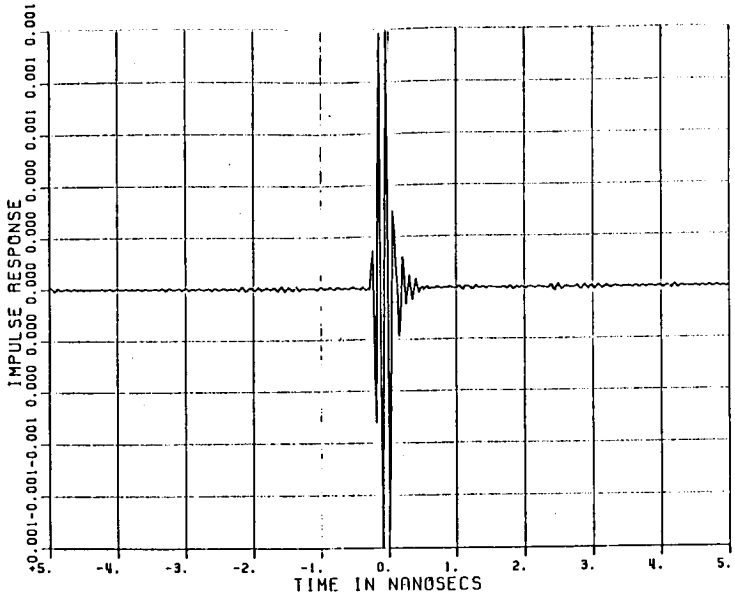

(b) measured time domain

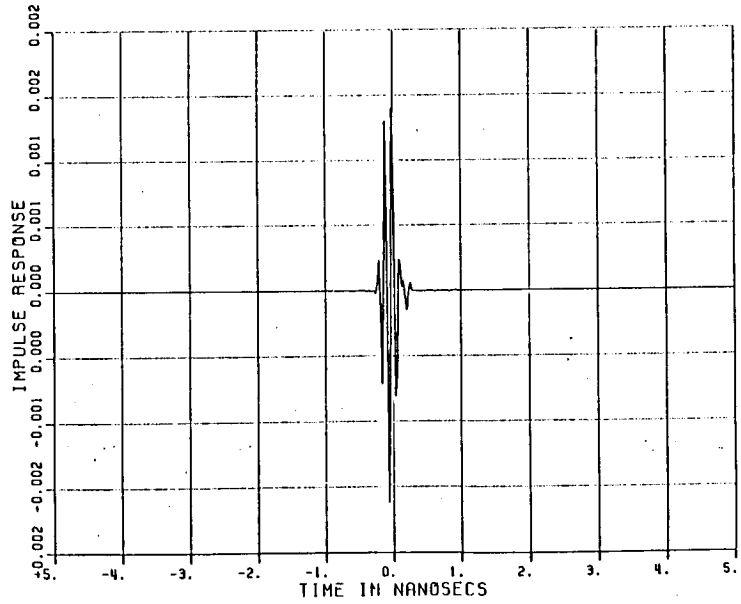

(c) exact time domain

Figure 6.20. Continued.

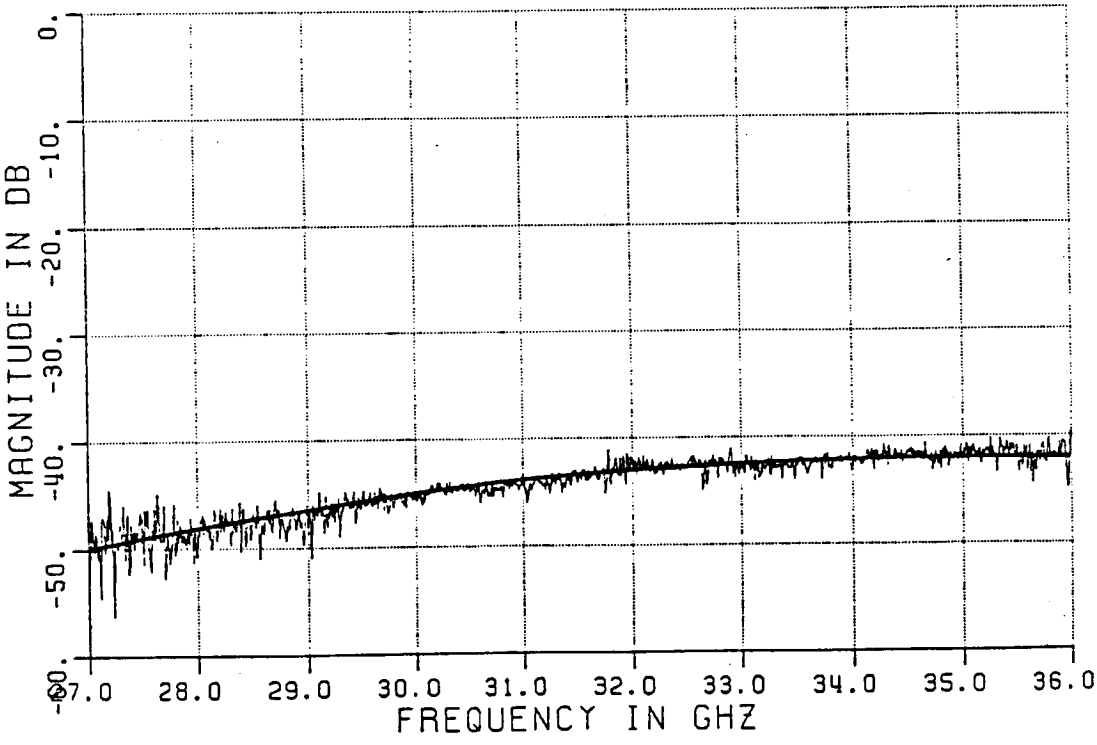

(a) frequency domain

Figure 6.21. 1/4 inch sphere response.

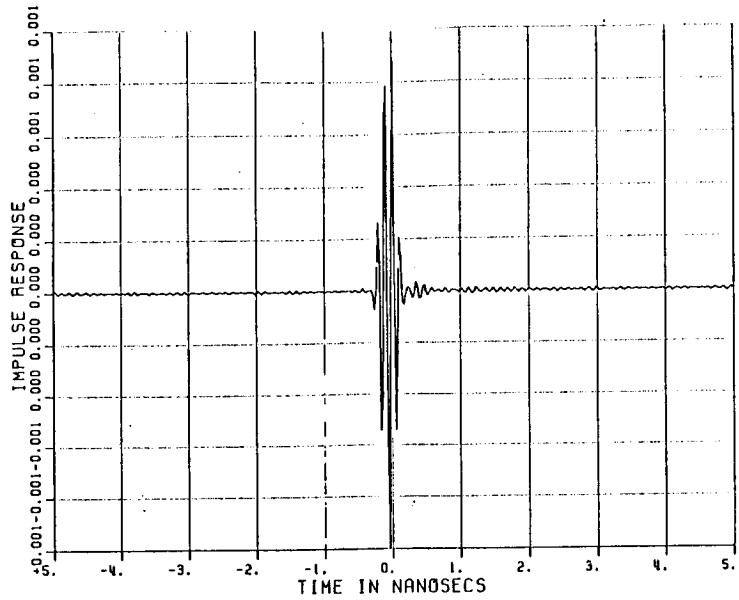

(b) measured time domain

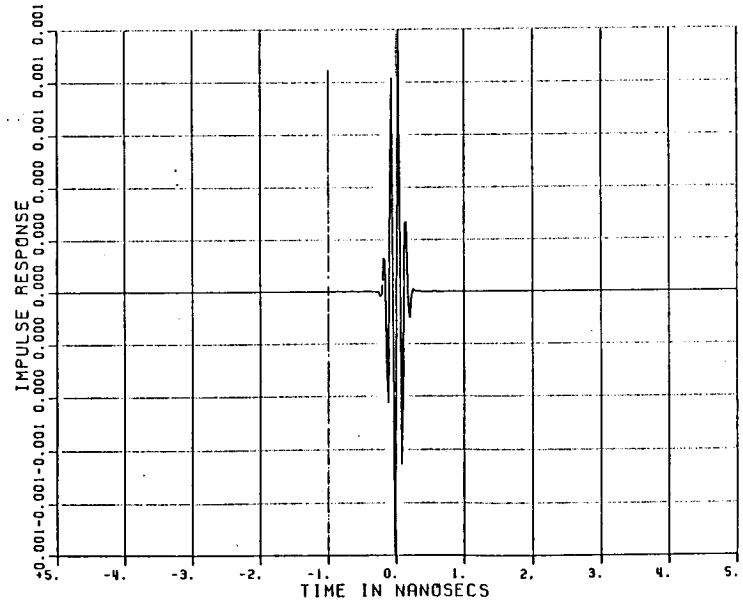

(c) exact time domain

Figure 6.21. Continued.

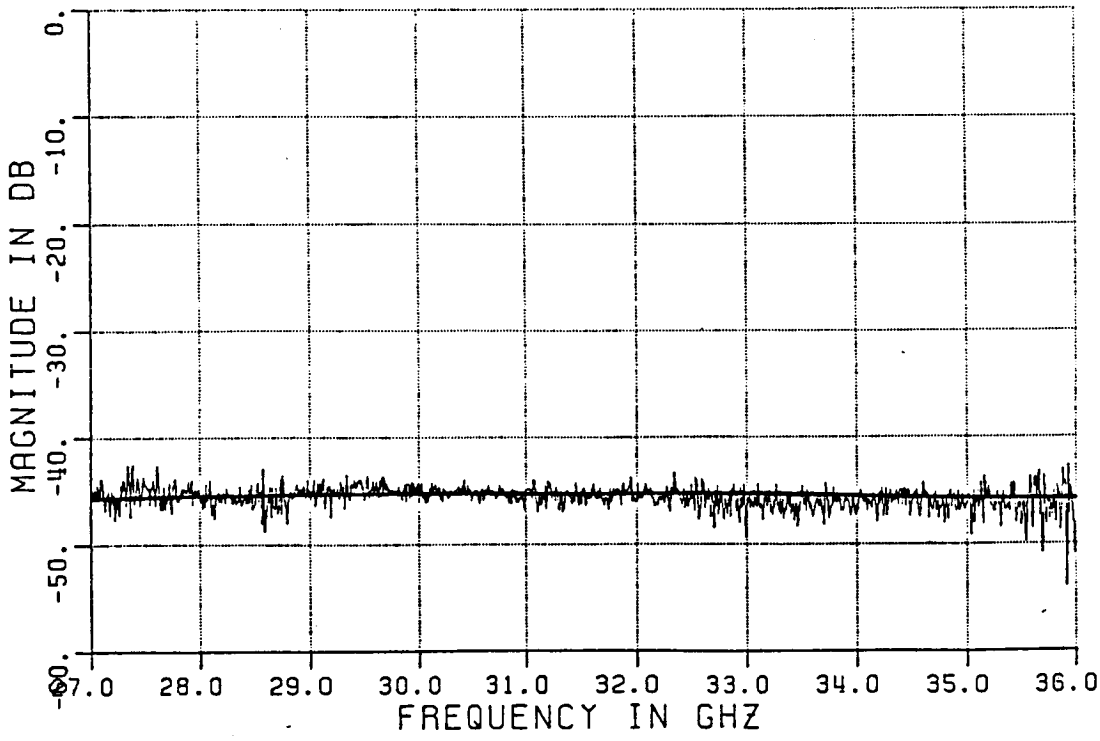

(a) frequency domain

Figure 6.22. 1/8 inch sphere response.

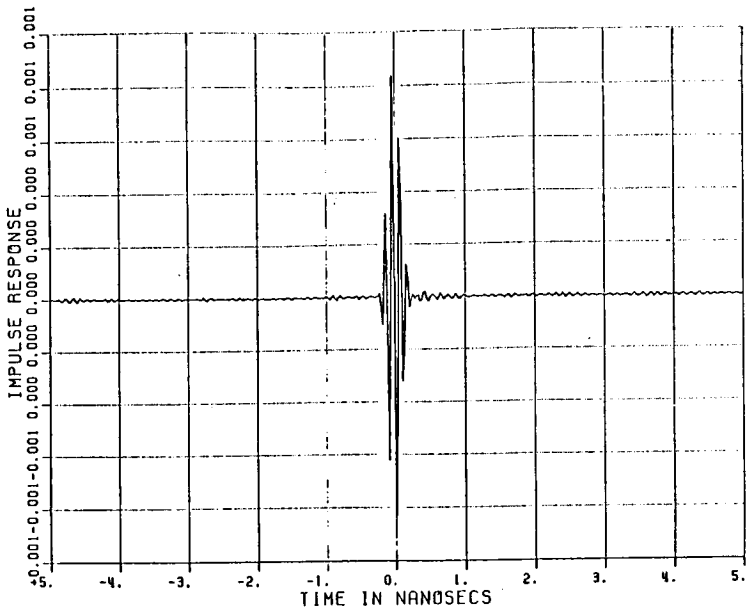

(b) measured time domain

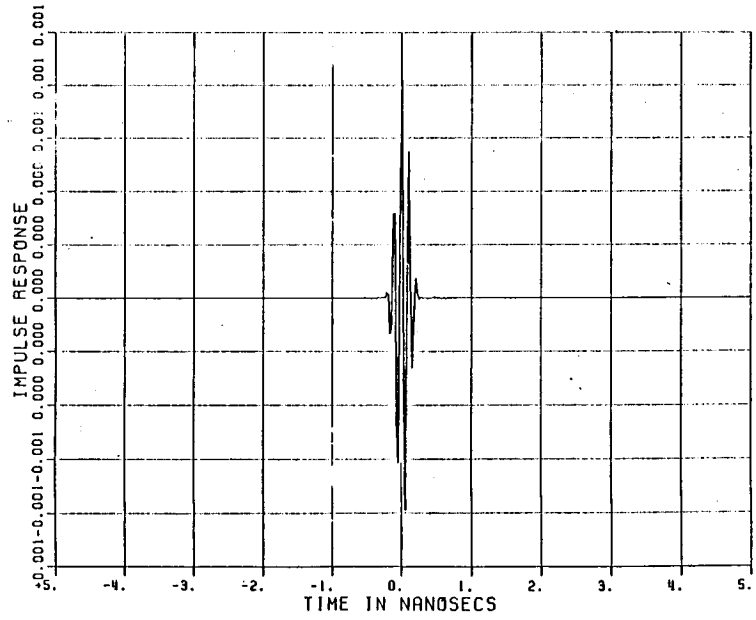

(c) exact time domain

Figure 6.22. Continued.

CHAPTER VII

CONCLUSION

A new pulsed/IF radar system is investigated from both a theoretical and experimental viewpoint, and in the process some useful analytic tools are developed. The key to the success of the system is that the receiver operates at a single frequency. It permits the use of components which have optimal performance at one frequency; no longer must wide band components be used which have unpredictable impedances. Another improvement is the reduction in redundancy from the use of a single receiver for all RF bands which permits a corresponding reduction in hardware costs.

Throughout this report, techniques which can be very useful in the analysis of signal and noise power levels in pulsed circuits have been explained. Both frequency and time domain representations are developed, and they are used interchangeably to explain the operation of this radar. The basic Fourier analysis is done in Chapter II so that the signal and noise calculations of the following chapters will be easier to understand.

Our old pulsed/RF radar was examined in Chapter III with the previously developed techniques. Shortcomings were discussed along with suggestions for optimizing the sensitivity of the system. Additional analysis concepts were developed in this chapter as they were required. The analysis of this old system served two purposes; first, to gain

confidence in analyzing pulsed radar systems and to promote careful record keeping; second, to determine how components behave in response to various target cross sections which led to a determination of the dynamic range.

In Chapter IV, the effects of transmit and receive pulse width on clutter terms were studied. Methods were derived for determining which returns from the compact range pass through the gate of the receiver. In analyzing pulsed returns from various parts of the range, timing diagrams became confusing, especially when a return only partially passes through the receive gate. For this reason timing diagrams were used only to develop more powerful techniques which transform pulse delays into target locations within the chamber. With this method evaluating relative return levels became a simple process without resorting to timing diagrams. Two transmit/receive timing schemes were analyzed for our compact range, and it was shown that clutter may be reduced by choosing a new timing scheme over that used in the old system.

Chapter V introduced the new pulsed/IF system with a single receiver for all RF bands. Detailed drawings of the system as well as typical insertion loss parameters for most components were given along with signal and noise power calculations, using the analysis techniques developed in the previous chapters along with the improved timing scheme of Chapter IV. The calculated dynamic range was compared with that of the old system, and the sensitivity of the new system was found to be better, which met one of our design goals.

The new Ka-band system is much simpler than the old system, since it is composed of only the most essential hardware. This is important because Ka-band components are particularly expensive. The same style of design may be used when adding new RF bands as long as the RF is converted to the receiver's IF.

The experimental data of Chapter VI agreed well with theory. The measured noise floor of the new system was very close to the level calculated in Chapter V, and the accuracy tests, using conducting spheres, show that the system is quite precise. Overall, the following design goals have been met: a single receiver was designed, built and tested to work optimally at one frequency, an improvement in system sensitivity was achieved, and the ability to change bands by changing a minimal amount of hardware was verified.

Other improvements currently under way include a new receiver which is being built to replace the SA receiver. It will be much simpler in design and permit the frequency bands to be scanned much more quickly. In addition, software is being written which will permit the automatic calibration and transformation of data without the cumbersome manipulation of data files as in the present system. These are a few of the projects underway to improve the performance of the compact range instrumentation.

APPENDIX A

FREQUENCY DOMAIN DERIVATION OF PULSE POWER

It may be instructive to consider a frequency domain approach to the power loss associated with pulsing a CW signal and extracting a corresponding Fourier component.

Parseval's theorem states that the time-averaged power contained in a signal is equal to the sum of all the Fourier components squared [4] such that

$$P_{ave} = \frac{1}{T} \int_{T} f^2(t)dt = \sum_{n=-\infty}^{\infty} |F_n|^2 \quad . \tag{A.1}$$

Fn is given in (2.14) for the pulse with unit amplitude and duty cycle, d, by

$$F_n = d \ \text{sinc} \ (n\pi d) \ . \tag{A.2}$$

The average power contained in the pulse may be calculated as follows:

$$P_{ave} = \sum_{n=-\infty}^{\infty} d^2 \text{sinc}^2(n\pi d) \tag{A.3}$$

$$P_{ave} = d^2 \left[1 + 2 \sum_{n=1}^{\infty} \text{sinc}^2 \ (n\pi d) \right] \tag{A.4}$$

$$P_{ave} = d^2 \left[1 + \frac{2}{\pi^2 d^2} \sum_{n=1}^{\infty} \frac{\sin^2 \ (n\pi d)}{n^2} \right] \tag{A.5}$$

$$P_{ave} = \left[d^2 + \frac{1}{\pi^2} \sum_{n=1}^{\infty} \left(\frac{1}{n^2} - \frac{\cos(2n\pi d)}{n^2} \right) \right] \tag{A.6}$$

These summations have been calculated and are given in [5] by

$$\sum_{n=1}^{\infty} \frac{1}{n^2} = \frac{\pi^2}{6} \tag{A.7}$$

$$\sum_{n=1}^{\infty} \frac{\cos(2n\pi d)}{n^2} = \frac{\pi^2}{6} - \pi^2 d + \pi^2 d^2 \tag{A.8}$$

$$P_{ave} = \left[d^2 + \frac{1}{\pi^2} \left(\frac{\pi^2}{6} - \frac{\pi^2}{6} + \pi^2 d - \pi^2 d^2 \right) \right] \tag{A.9}$$

or

$$P_{ave} = d \quad . \tag{A.10}$$

This confirms the result that the average power contained in a pulse is reduced by a factor of its duty cycle.

Filtering out the unwanted harmonics permits only F_o to pass, and it causes a power reduction from the average power calculated above. The reduction is

$$\frac{|F_o|^2}{P_{ave}} = \frac{d^2}{d} = d \quad . \tag{A.11}$$

Thus, the power contained in F_o is reduced from P_{ave} by another factor of d, and the ratio of the power contained in F_o to the power in the original CW signal is equal to d^2. Consequently, the total signal power loss is given by

$$\text{signal loss in dB} = 20 \log(d) \quad . \tag{A.12}$$

REFERENCES

[1] R.T. Whitacre, "The OSU Pulsed/CW Radar for Compact Range Radar Cross Section Measurements," M.Sc. Thesis, The Ohio State University, Department of Electrical Engineering, Columbus, Ohio, 1985.

[2] E.K. Walton and J.D. Young, "The Ohio State University Compact Radar Cross-Section Measurement Range," IEEE Trans. on Antennas and Propagation, Vol. AP-32, No. 11, November 1984.

[3] K.Y. Lai, "A GTD Analysis of Ogive Pedestal," M.Sc. Thesis, The Ohio State University, Department of Electrical Engineering, Columbus, Ohio, 1986.

[4] R.J. Mayhan, Discrete-Time and Continuous-Time Linear Systems, Addison-Wesley, Reading, Massachusetts (1984), pp. 417-419.

[5] J.S. Gradshteyn and I.M. Ryzhik, Table of Integrals Series and Products, Academic Press, Orlando, Florida (1980).

50272-101

REPORT DOCUMENTATION PAGE	1. REPORT NO.	2.	3. Recipient's Accession No.

4. Title and Subtitle

A VERY WIDE FREQUENCY BAND PULSED/IF RADAR SYSTEM

5. Report Date: March 1988

6.

7. Author(s): D.N. Jones and W.D. Burnside

8. Performing Organization Rept. No.: 716148-28

9. Performing Organization Name and Address
The Ohio State University ElectroScience Laboratory
1320 Kinnear Road
Columbus, Ohio 43212

10. Project/Task/Work Unit No.

11. Contract(C) or Grant(G) No.
(C)
(G) NSG 1613

12. Sponsoring Organization Name and Address
National Aeronautics and Space Administration
Langley Research Center
Hampton, Virginia 23665

13. Type of Report & Period Covered: Technical

14.

15. Supplementary Notes
This report was also submitted as a Master's Thesis, Winter 1987.

16. Abstract (Limit: 200 words)

A pulsed/IF radar for compact range radar cross section measurements has been developed which converts RF returns to a fixed IF, so that amplification and gating may be performed at one frequency. This permits the use of components which have optimal performance at this frequency which results in a corresponding improvement in performance. Sensitivity and dynamic range are calculated for this system and compared with our old radar, and the effect of pulse width on clutter level is also studied. Sensitivity and accuracy tests are included to verify the performance of the radar.

17. Document Analysis a. Descriptors

b. Identifiers/Open-Ended Terms

c. COSATI Field/Group

18. Availability Statement	19. Security Class (This Report): Unclassified	21. No. of Pages: 155
	20. Security Class (This Page): Unclassified	22. Price

(See ANSI-Z39.18) See Instructions on Reverse OPTIONAL FORM 272 (4-77) (Formerly NTIS-35) Department of Commerce